NASA
Technical
Paper
2183

November 1983

Simulator Study of Flight Characteristics of a Large Twin-Fuselage Cargo Transport Airplane During Approach and Landing

William D. Grantham,
Perry L. Deal,
Gerald L. Keyser, Jr.,
and Paul M. Smith

NASA

NASA
Technical
Paper
2183

1983

Simulator Study of Flight Characteristics of a Large Twin-Fuselage Cargo Transport Airplane During Approach and Landing

William D. Grantham,
Perry L. Deal, and
Gerald L. Keyser, Jr.
Langley Research Center
Hampton, Virginia

Paul M. Smith
Kentron International, Inc.
Hampton, Virginia

NASA
National Aeronautics
and Space Administration

Scientific and Technical
Information Branch

SUMMARY

A six-degree-of-freedom, ground-based simulator study has been conducted to evaluate the low-speed flight characteristics of a twin-fuselage cargo transport airplane and to compare these characteristics with those of a large, single-fuselage (reference) transport configuration which was similar to the Lockheed C-5A airplane. The twin-fuselage turbojet concept simulated in this study had a landing weight of approximately 1.3 million pounds and was designed to carry 284 tons of payload 3500 n.mi. at a Mach number of 0.8 and a cruise altitude of 32 000 ft. The primary piloting task was the approach and landing.

The results of this study indicated that the twin-fuselage cargo transport airplane had unacceptable low-speed handling qualities with no augmentation. In order to achieve "acceptable" handling qualities, considerable augmentation was required, and although the augmented airplane could be landed under adverse conditions, the roll performance of the aircraft had to be improved appreciably before the handling qualities were rated as being "satisfactory."

The roll performance parameter $t_{\phi=30}$ (time required to bank 30°) was examined extensively during this simulation study, and an attempt was made to determine the maximum value of $t_{\phi=30}$ that the pilots would accept as being satisfactory for various simulated piloting tasks. For such large and unusually configured aircraft as the subject twin-fuselage concept, the ground-based simulation results indicated that a value of $t_{\phi=30}$ less than 6 sec should result in acceptable roll response characteristics, and when $t_{\phi=30}$ is less than 3.8 sec, satisfactory roll response should be attainable. In order to accomplish this roll performance on the simulated twin-fuselage concept, the fuselages had to be relocated from 50 percent of the wing semispan to 20 percent of the wing semispan and, as the fuselages were moved inboard, the aileron span was increased such that the basic aileron effectiveness coefficients were increased by a factor of 2.17.

Because the pilots were located significantly far from the roll axis on the simulated twin-fuselage configurations (various fuselage locations), it was evident that there could be relatively high levels of normal acceleration generated during certain phases of flight. These simulator results indicated that the response of the twin-fuselage configurations to atmospheric turbulence would not be expected to be any worse than the response of present-day transports. However, indications were that, in general, higher accelerations were experienced at the pilot station when correcting for landing approach lateral offsets than for corrections due to turbulence.

The results of the present study, in general, agree reasonably well with the handling qualities criteria used for comparison, except for the roll-acceleration and roll-rate capability requirements. Also, the augmented twin-fuselage concept compares favorably with the reference (single-body) transport, except for these roll capability parameters.

INTRODUCTION

Airplanes have continued to grow to the point where a gross weight of a million pounds is a near reality for large transport aircraft presently in service (Boeing 747 and Lockheed C-5A). Studies of still larger aircraft (up to 3 million pounds) have suggested that reducing the wing loading to approximately one-half that of current large aircraft increases the volume within the wing more rapidly than the volume required for fuel or payload and, therefore, eliminates the requirement for a fuselage. An interesting consequence of such a design approach is the elimination of the fuselage drag and the reduction in wing-bending loads realized by distributing the airplane weight along the wing span - thereby providing improvement in both the payload ratio and fuel efficiency relative to smaller conventional designs.

A disadvantage of the all-wing (span loader) design is the very large size required by the low wing loading to accommodate a given payload. As a possible means of avoiding this disadvantage, an alternate design approach - the multibody - is currently under study. Such designs utilize two or more discrete bodies to contain the payload which are so located along the wing span to realize substantial bending-moment relief and, therefore, "maintain" much of the wing-weight advantage of the all-wing span loader. In comparison with single-body aircraft of the same payload capacity, it is believed possible to use the volume of the smaller bodies more efficiently and thereby compensate for the inherent wetted-area and weight disadvantages of providing the same total volume in two or more bodies rather than a single body. Also, the multibody arrangement is compatible with use of wing lift flaps and conventional tail arrangements for trim and control; therefore, wing loadings equal to those of current large aircraft seem practical.

The multibody designs presently under study differ from current large aircraft in at least two features that can be expected to have important effects on handling qualities, especially during the approach and landing phase. First, there is the higher gross weight (more than double that of the C-5A) and the related increased dimensions of such items as the wing span, landing gear track, and cockpit location. Second, the magnitude of the inertias and the inertia distribution are considerably different from those of conventional design and can be expected to have a significant impact on control requirements during landing approach.

Piloted simulation studies appeared to offer the best means for obtaining a preliminary evaluation of the expected handling qualities of such diverse airplane concepts and to assess the adequacy of current handling qualities requirements. Therefore, this paper evaluates the low-speed flight characteristics of one such multibody (twin-fuselage) jet transport airplane using a six-degree-of-freedom, ground-based simulator.

The primary objectives of this simulation study were to evaluate the low-speed handling characteristics of the subject twin-fuselage transport and to obtain sufficient information to provide guidance for future research requirements. Other major objectives were

1. Compare the low-speed dynamic stability and control characteristics of the subject twin-fuselage cargo transport to those of a large "reference" transport configuration. (The reference aircraft was similar to the Lockheed C-5A.)

2. Determine the minimum control power required for satisfactory maneuvering capabilities.

3. Develop any augmentation systems necessary to produce satisfactory handling qualities.

4. Attain some insight as to the ride qualities of this large, unusually configured airplane.

5. Evaluate the effects of various atmospheric conditions on the ability of the pilot to make a satisfactory approach and landing.

6. Attain some insight as to the minimum size (width) runway required to land this large, unusually configured aircraft.

SYMBOLS AND ABBREVIATIONS

Measurements and calculations were made in U.S. Customary Units, and all calculations are based on the aircraft body axes. Dots over symbols denote differentiation with respect to time.

a_n normal acceleration, g units

a_y lateral acceleration, g units

C_{L_α} lift-curve slope per unit angle of attack, per radian

C_l rolling-moment coefficient

C_{l_β} rolling-moment coefficient due to sideslip, per degree

C_m pitching-moment coefficient

C_{m_α} pitching-moment coefficient per unit angle of attack, per radian

C_n yawing-moment coefficient

C_X longitudinal-force coefficient

C_Y side-force coefficient

C_Z vertical-force coefficient

$\bar{c}$ mean aerodynamic chord, ft

g acceleration due to gravity, ft/sec^2

h altitude, ft

I_X, I_Y, I_Z moments of inertia about X, Y, and Z body axes, respectively, $slug\text{-}ft^2$

I_{XZ} product of inertia, $slug\text{-}ft^2$

K_A autothrottle gain, degrees per knot

K_a aileron control effectiveness multiplier

K_p roll-rate gain, $\frac{\text{deg}}{\text{deg/sec}}$

$K_{p,c}$ commanded roll-rate gain, $\frac{\text{deg/sec}}{\text{deg}}$

$K_{p,I}$ roll-rate-integrator gain, deg/deg

$K_{p,Y}$ roll-rate gain in the yaw axis, $\frac{\text{deg}}{\text{deg/sec}}$

K_q pitch-rate gain, $\frac{\text{deg}}{\text{deg/sec}}$

$K_{q,c}$ commanded pitch-rate gain, $\frac{\text{deg/sec}}{\text{in.}}$

$K_{q,I}$ pitch-rate-integrator gain, $\frac{\text{deg/sec}}{\text{deg/sec}}$

K_V autothrottle velocity gain, deg/deg

$K_{V,I}$ autothrottle velocity-integrator gain, 1/sec

K_{WL} wing-leveler gain, deg/deg

K_{δ_p} pedal-to-rudder gearing, deg/in.

K_θ pitch-attitude gain, deg/deg

$K_{\theta,A}$ autothrottle pitch-attitude gain, deg/deg

$K_{\theta,H}$ pitch-attitude-hold gain, $\frac{\text{deg/sec}}{\text{deg/sec}}$

$K_{\phi,2}$ roll-attitude-hold gain, deg/deg

$K_{\phi,TC}$ roll-attitude-hold filter gain, 1/sec

$K_{\phi,R}$ roll-coordination gain, deg/deg

L_α lift per unit angle of attack per unit momentum $(\bar{q}S/mV)C_{L_\alpha}$, per second

m airplane mass, slugs

n/α steady-state normal acceleration change per unit change in angle of attack for an incremental horizontal-tail deflection at constant airspeed, g units/rad

P_d period of Dutch roll oscillation, sec

P_{ph}	period of longitudinal phugoid oscillation, sec
P_{sp}	period of longitudinal short-period oscillation, sec
p,q,r	rolling, pitching, and yawing angular velocities, respectively, deg/sec or rad/sec
p_1,p_2	roll rates at first and second peaks, respectively, deg/sec or rad/sec
$\bar{q}$	dynamic pressure, lbf/ft^2
S	reference wing area, ft^2
s	Laplace operator
T	thrust, lbf
t_c	pitch time constant, sec
t_2	time to double amplitude, sec
t_{s2}	time for spiral mode to double amplitude, sec
$t_{\phi=30}$	time to achieve 30° bank angle, sec
t_1	intersection of the pitch-rate-response maximum-slope tangent line and the zero amplitude line, effective time delay, sec
t_2	intersection of the pitch-rate-response maximum-slope tangent line and the steady-state pitch-rate line, sec
Δt	effective rise time parameter, $t_2 - t_1$, sec
V	indicated airspeed, knots or ft/sec
V_s	stall speed, knots
W	airplane weight, lbf
x'	longitudinal distance from point at which glide slope intercepts runway, ft
$\bar{x}$	longitudinal distance from aircraft center of gravity to pilot station, ft
y	lateral distance from centerline of runway, ft
$\dot{y}$	lateral velocity during landing, ft/sec
y'	lateral dispersion margin, distance from outside of main gear bogie to a point 5 ft from edge of runway with aircraft axis of symmetry on runway centerline, ft
$\bar{y}$	lateral distance from aircraft center of gravity to pilot station, positive when pilot located to right of center of gravity, ft

$\bar{z}$	vertical distance from aircraft center of gravity to pilot station, positive when pilot located below center of gravity, ft
α	angle of attack, deg
β	angle of sideslip, deg
γ	flight-path angle, deg
Δ	increment
δ_a	aileron deflection, positive for right roll command, deg
δ_c	column deflection, in.
δ_e	elevator deflection, deg
δ_f	trailing-edge flap deflection, deg
δ_h	horizontal tail deflection, deg
δ_p	pedal deflection, in.
δ_r	rudder deflection, deg
δ_w	wheel deflection, deg
ε_{zh}	glide-slope error, ft
ζ_d	Dutch roll mode damping ratio
ζ_{ph}	longitudinal phugoid mode damping ratio
ζ_{sp}	longitudinal short-period mode damping ratio
ζ_ϕ	damping ratio of numerator quadratic ϕ/δ_a transfer function
η_b	position of bodies along wing as a fraction of semispan
θ	pitch attitude, deg
θ_o	initial trim (reference) pitch attitude
$\Delta\dot{\theta}_1$	magnitude of first pitch-rate overshoot, deg/sec
$\Delta\dot{\theta}_2$	magnitude of first pitch-rate undershoot, deg/sec
$\Delta\dot{\theta}_2/\Delta\dot{\theta}_1$	transient peak ratio
κ	ratio of commanded roll performance to applicable roll performance requirement
σ	standard deviation
τ_R	roll mode time constant, sec

ϕ angle of roll, deg

ψ heading angle, deg

ψ_β phase angle expressed as a lag for a cosine representation of Dutch roll oscillation in sideslip, deg

ω_d undamped natural frequency of Dutch roll mode, rad/sec

ω_{ph} undamped natural frequency of phugoid mode, rad/sec

ω_{sp} longitudinal short-period undamped natural frequency, rad/sec

ω_ϕ undamped natural frequency appearing in numerator quadratic of ϕ/δ_a transfer function, rad/sec

Subscripts:

app approach

av average

cg center of gravity

ge ground effect

H hold

ℓ landing

ℓg landing gear

max maximum

osc oscillatory

ps pilot station

rms root mean square

rs roll spiral

ss steady state

td touchdown

Abbreviations:

CTOL conventional take-off and landing

DQ(PIL) pilot commanded pitch rate

FAA Federal Aviation Administration

IFR instrument flight rules

ILS	instrument landing system
MTBT	multibody transport
PLA	power lever angle
PR	pilot rating
RAH	roll-attitude-hold mode on
REF	reference
rms	root mean square
SAS	stability augmentation system
SCAS	stability and control augmentation system
SCR	supersonic cruise research
SJT	subsonic jet transport
VFR	visual flight rules
VMS	Langley Visual/Motion Simulator
WL	wing-leveler mode on

DESCRIPTION OF SIMULATED AIRPLANES

Two distinctly different airplane concepts were simulated during the present study. Three-view sketches of the two concepts are presented in figures 1 and 2, the representative landing mass and dimensional characteristics and the control surface deflection and deflection rate limits for these aircraft are presented in table I, and the aerodynamic data used in the study are presented in tables II and III.

Twin-Fuselage Airplane

The twin-fuselage turbojet transport concept simulated in this study was developed by the Lockheed-Georgia Company (under a NASA contract) to carry 284 tons of payload 3500 n.mi. at a Mach number of 0.8 and a cruise altitude of 32 000 ft. The three-view sketch presented in figure 1 illustrates the basic location of the fuselages as being at 50 percent of the wing semispan. This configuration was a preliminary version of the "optimized" twin-fuselage concepts reported in reference 1. The airplane is powered by four large, advanced-turbofan engines providing a static takeoff thrust-to-weight ratio of 0.162. An example of the estimated engine thrust response characteristics used in the simulation is presented in figure 3.

The effects of changing the spanwise location of the fuselages were evaluated, and the resulting variations in roll and yaw inertias are presented in figure 4(a). As the fuselages were moved inboard, it was assumed that the aileron span could be increased as a direct function of the fuselage relocation. The estimates of the

increased roll control derivatives were made using the methods presented in reference 2 and are indicated as multipliers (K_a) in figure 4(b), where K_a is varied from 1.0 to 2.17. However, as the fuselages were moved inboard and the aileron span increased for a given trailing-edge flap deflection, there was an associated loss of lift due to the loss of trailing-edge flap span. The lift increment was gained back by drooping the ailerons 20° and increasing the trailing-edge flap chord, the chord increase being a function of the fuselage position on the wing. The simulated representative landing mass and dimensional characteristics are presented in table I(a), and the aerodynamic data are presented in table II.

Reference Airplane

A single-fuselage turbojet cargo transport, similar to the Lockheed C-5A airplane, was simulated during this study to provide a reference base from which the subject twin-fuselage concept could be evaluated. This reference airplane was powered by four turbojet engines providing a static take-off thrust-to-weight ratio of 0.213. A three-view sketch of the airplane is presented in figure 2, the simulated representative landing mass and dimensional characteristics are presented in table I(b), and the aerodynamic data are presented in table III.

DESCRIPTION OF SIMULATION EQUIPMENT

The simulation study of the two airplane concepts was made using the general-purpose cockpit of the Langley Visual/Motion Simulator (VMS). This is a ground-based motion simulator with six degrees of freedom. For this study it had a transport-type cockpit which was equipped with conventional flight and engine-thrust controls and with a flight-instrument display representative of those found in current transport airplanes. (See fig. 5.) Instruments that indicated angle of attack, angle of sideslip, and flap angle were also provided. A conventional cross-pointer-type flight-director instrument was used, the command bars (cross pointers) being modeled to be compatible with the proposed microwave landing systems.

The control forces on the wheel, column, and rudder pedals were provided by a hydraulic system coupled with an analog computer. The system allows for the usual variable-feel characteristics of stiffness, damping, coulomb friction, breakout forces, detents, and inertia.

The airport-scene display used an "out-the-window" virtual image system of the beam-splitter, reflective-mirror type. (See fig. 6.)

The motion performance characteristics of the VMS system possess time lags of less than 60 msec. A nonstandard washout system, utilizing nonlinear coordinated adaptive motion, was used to present the motion-cue commands to the motion base. (See ref. 3.)

A runway "model" was programmed that had a maximum width of 267 ft, a total length of 11 500 ft, roughness characteristics, and a slope from the center to the edge representing a runway crown. Only a dry runway was considered in this study.

The only aural cues provided were engine noises and landing-gear extension and retraction noises.

TESTS AND PROCEDURES

Two research pilots participated in the simulation program; each flew all simulated configurations and tasks, and each used standard flight-test procedures in the evaluation of the handling and ride qualities. The primary piloting task was the approach and landing. The tests consisted of IFR and simulated VFR landing approaches for various configurations - with crosswinds, turbulence, wind shear, glide-slope and localizer offsets, and engine failure as added complicating factors. The ILS approach was initiated with the airplane in the power-approach condition (power for level flight), at an altitude below the glide slope, and on course but offset from the localizer. The pilot's task was to capture the localizer and glide slope and to maintain them as closely as possible while under simulated IFR conditions. At an altitude of approximately 300 ft, the aircraft "broke out" of the simulated overcast; whereupon the pilot converted to VFR conditions and attempted to land the airplane visually (with limited reference to the flight instruments).

This study, using the aforementioned evaluation procedures, evaluated handling and ride qualities by analysis of recorded aircraft-motion time histories, calculation of various flying qualities parameters, and pilot comments on the flying qualities of the simulated twin-body cargo transport and the effects of various stability and control augmentation systems on these characteristics. The more significant results are reviewed in the following sections.

RESULTS AND DISCUSSION

The results of this study are discussed in terms of the previously stated objectives, and the pilot ratings listed for the various conditions evaluated are an average of the ratings from both pilots who flew that particular condition. See table IV for the pilot rating system used for handling qualities and table V for the turbulence effect rating scale. Also, the results discussed pertain to the data obtained on the twin-fuselage configuration with the fuselages located at 50 percent of the wing semispan ($\eta_b = 0.5$) unless otherwise noted.

No Stability Augmentation

The average pilot rating assigned to the longitudinal handling qualities of the unaugmented airplane was 5, the primary objections being (1) low apparent pitch damping, (2) sluggish initial pitch response, and (3) unusually large pitch-attitude excursions associated with changes in flaps.

A pilot rating of 10 was assigned to the lateral directional handling qualities of the unaugmented airplane. The major objections were (1) very sluggish roll response, (2) unacceptably large sideslip excursions in turns, and (3) a large amount of adverse yaw.

Longitudinal characteristics.- The static longitudinal stability of the subject twin-fuselage transport airplane was considered by the pilots to be adequate. (The aircraft had a static margin of 5 percent.) Also, this configuration was flown on the stable side (front side) of the thrust-required curve - the variation of thrust required with velocity $\partial(T/W)/\partial V$ was approximately 0.0003 per knot.

The dynamic stability characteristics of this twin-fuselage configuration, for the approach and landing flight conditions, are indicated in table VI(a). Also, the

short-period undamped natural frequency ω_{sp} and damping ratio ζ_{sp} of the simulated twin-fuselage transport are indicated in figure 7 and compared with some present-day jet transports. As shown in table VI(a), $\zeta_{sp} \approx 1.2$, a value normally considered an indication of good pitch damping - or possibly even overdamping. (A short-period damping ratio on the order of 0.7 is said to be a good level.) However, as stated previously, the pilots commented that the damping in pitch appeared to be low for this configuration.

Figure 8 presents two of the most widely used longitudinal handling qualities criteria. Figure 8(a) shows the short-period frequency requirement of reference 4. As can be seen, the results predicted by the criterion agree with the results obtained during the present simulation study: acceptable, but not satisfactory short-period dynamics. Figure 8(b) shows the Shomber-Gertsen longitudinal handling qualities criterion of reference 5. This criterion relates the ability of the pilot to change flight path with normal acceleraton to the factor L_α. By using this parameter and by recognizing that the pilot's mode of control is not constant for all flight regimes, a criterion for satisfactory short-period characteristics was developed (ref. 5) that correlates well with current airplane experience as well as with the results obtained during the present twin-fuselage transport simulation program. It can be seen from these two criteria that it is the low magnitude of ω_{sp} that causes the twin-fuselage configuration from being "located" in the satisfactory regions.

The relatively low value of ω_{sp} was brought about by the combination of high pitch inertia ($I_Y = 95 \times 10^6$ slug-ft^2) and the low level of static stability ($C_{m_\alpha} = -0.267$). Although it is not immediately obvious, the pitch damping of the unaugmented twin-fuselage transport appeared to be low to the pilots because of the low magnitude of the short-period natural frequency. For example, figure 9 presents time-history responses to various column inputs. Figure 9(a) shows the pitch-rate response to a column step input with zero overshoot in the pitch rate, indicating deadbeat (very high) damping. However, the response to a column pulse (fig. 9(b)) might appear to the pilot as being lightly damped. The long pitch-rate time constant ($t_c = 1.3$ sec) would appear to the pilot as sluggish initial response, and the integral of the pitch rate following control release (shaded area) would appear to the pilot as an undesired overshoot in pitch attitude and, hence, low pitch damping. It can be concluded therefore that it is not the magnitude of the damping-in-pitch parameter $2\zeta_{sp}\omega_{sp}$, which is 1.58/sec, that makes the configuration response appear to be lightly damped, but rather the magnitude of ω_{sp}. For example, if ζ_{sp} were 0.7 (which is a good level) and $2\zeta_{sp}\omega_{sp}$ were still 1.58/sec, ω_{sp} would be 1.13; then, from figure 8, the short-period dynamic characteristics of the configuration ($L_\alpha/\omega_{sp} = 0.389$) would be predicted as being satisfactory.

The pilots commented that the initial pitch response to column inputs was sluggish. This sluggish response, caused by the high pitch inertia, is illustrated in figure 10, which presents the pitch-rate response to a column step input calculated from two-degree-of-freedom equations of motion with airspeed constrained. Using the pitch-rate response criteria of reference 6, figure 10 indicates that the reason the pilots rated the pitch response as being sluggish was the magnitude of the "rise time parameter." The reference 6 criterion dictates that the pitch-rate rise time parameter Δt of the simulated twin-fuselage configuration must be less than 0.91 sec for satisfactory response and less than 2.93 sec for acceptable response. As noted in table VII and figure 10, the pitch-rate rise time parameter for the unaugmented twin-fuselage transport (table VII(a)) was 1.58 sec, which predicts acceptable, but not satisfactory, pitch-rate response characteristics; this agrees

with the pilots' rating of 5 determined on the simulator. The pitch control power was rated acceptable insofar as the longitudinal control power requirements for the approach and landing tasks are concerned. This is in agreement with the control power requirements criterion of reference 7, as shown in figure 11.

Lateral-directional characteristics.- As stated previously, the pilots assigned a rating of 10 to the lateral-directional handling qualities of the unaugmented airplane. One primary factor that contributed to the poor pilot rating for the lateral-directional characteristics was the large adverse sideslip experienced during rolling maneuvers, and this characteristic is indicated in figure 12. For a step wheel input, it is desirable to have (1) a rapid roll-rate response that reaches a reasonably steady-state value with a minimum of oscillation, (2) essentially zero sideslip produced by the roll control input, and (3) an immediate response in heading. However, it is evident from figure 12 that for a lateral control step input for this unaugmented configuration, a large amount of adverse sideslip is experienced that washes out the roll rate $\dot{\phi}$ in a short time and causes appreciable adverse yaw ($-\psi$). In addition, table VII(a) indicates that it takes approximately 12 sec to bank 30° on this unaugmented airplane in the landing configuration and that the requirement of reference 4 is $t_{\phi=30} \leq 4$ sec, even for acceptable handling qualities. This sluggish roll response, in combination with the large adverse sideslip, made it impossible for the pilot to make safe landings consistently on this unaugmented airplane; thus, the lateral-directional characteristics of this configuration were rated as being uncontrollable (PR = 10). It was therefore apparent that considerable stability and control augmentation would be required to achieve satisfactory handling qualities for the approach and landing piloting task.

Augmented Airplane

Based on the results obtained for the unaugmented configuration, the objective for the design of the stability and control augmentation system (SCAS) was that the system should provide satisfactory handling qualities (PR $\leq$ 3.5) at all flight conditions evaluated during the study. A block diagram of the SCAS design obtained is shown in figure 13. The selected gains for the roll and yaw axes SCAS are indicated in table VIII.

Longitudinally, a high-gain pitch-rate command/attitude-hold system was chosen because (1) the system provided good short-period characteristics and rapid response to pilot inputs and (2) the attitude-hold feature minimized disturbances due to turbulence or variations in flaps and/or thrust.

Laterally, a roll-rate command/attitude-hold system was employed in an attempt to provide a rapid roll mode and quick uniform response to pilot inputs; the attitude-hold feature resulted in a desirable neutrally stable spiral mode while counteracting disturbances due to turbulence. In addition, a wings-leveler feature was provided which automatically leveled the wings ($\phi = 0$) whenever the bank angle was less than 2° and the wheel was centered. This feature relieved the pilot of the task of "hunting" for zero bank angle and was particularly useful when rolling out of a turn to a desired heading. (See fig. 13(b) for lateral control system.)

Directionally, roll-rate and roll-attitude feedbacks were used to provide turn coordination and improved Dutch roll characteristics. (See fig. 13(c).)

An autothrottle that maintained the selected airspeed throughout the landing approach was also used as part of the normal operational augmentation. (See fig. 14

for block diagram of the autothrottle design.) Since the simulated engine dynamics (e.g., fig. 3) produced very good thrust response, the autothrottle generally maintained the desired airspeed within ±3 knots and considerably reduced the pilot workload on the landing approach.

Longitudinal characteristics.- The longitudinal SCAS (fig. 13(a)) provided pitch rate proportional to column deflection and produced the desired characteristics of rapid, well-damped responses to pilot inputs, as well as inherent attitude stability. Figure 15 shows the improvement in pitch-rate response provided by the SCAS and compares the pitch response of the twin-fuselage transport with the simulated reference airplane. As can be seen, the SCAS improved the pitch-rate response of the twin-fuselage configuration appreciably in that the pitch time constant was decreased by 50 percent (t_c decreased from 1.30 sec to 0.65 sec) and the steady-state pitch rate commanded by a given column input was increased by 16 percent. It may also be noted that the pitch-rate response of the augmented twin-fuselage configuration compares favorably with the augmented reference airplane. With the augmentation system operative, the average pilot rating for the longitudinal handling qualities during the ILS approach was improved from PR = 5 to PR = 2.

Figure 16 compares these configurations with the short-period handling qualities criteria of references 4 and 5; and as can be seen, the twin-fuselage configuration agrees quite well with both criteria and the augmented configuration is in the satisfactory region.

The low-speed pitch-rate response criterion shown in figure 17, and reported in reference 8, was based on the Shomber-Gertsen criterion of reference 5. Indications are that the twin-fuselage configuration does not meet the pitch-rate response requirements of this criterion, even when the airplane is highly augmented. (Also note that the simulated reference airplane does not meet this criterion.) However, when the pitch-rate response of the augmented twin-fuselage configuration is compared with the criteria of reference 6, it can be seen from figure 18 and table VII(b) that the predicted characteristics were at satisfactory levels - in agreement with the pilots' assessment of the configuration.

Lateral-directional characteristics.- A block diagram of the lateral-directional SCAS is presented in figure 13. Laterally, a rate command system provided roll rate proportional to wheel position (fig. 13(b)), and the directional system consisted of two turn coordination features (fig. 13(c)). Table VI(a) shows that the Dutch roll characteristics were improved considerably, ω_ϕ/ω_d was increased from 0.676 to 0.993 (which indicates that the Dutch roll oscillation should be much less easily excited for roll control inputs), and the damping parameter $\zeta_d\omega_d$ was increased from 0.004 rad/sec to 0.060 rad/sec. The improvement in the roll response and damping is indicated by the reduction of τ_R from 2.15 sec to 1.33 sec.

Figure 19 shows the improvement in the roll-rate response provided by the SCAS. By elimination of the large adverse sideslip, the roll rate attained for a given amount of wheel deflection was increased appreciably, and the heading response was immediate (no lag). A comparison of the lateral-directional response to a wheel step for the augmented twin-fuselage airplane and the simulated reference airplane indicates that the initial roll-rate response of the twin-fuselage airplane is slower than the $\dot{\phi}$ response of the reference aircraft but that the "final" $\dot{\phi}$ response is faster for the twin-fuselage configuration. Indications are that the sideslip (β) and heading ($\dot{\psi}$) response of the two configurations are similar. (See fig. 19.)

With the SCAS operative, the average pilot rating for the lateral-directional handling qualities on the ILS approach, in calm air, was improved from PR = 10 to PR = 5. The primary objection of the pilots to the lateral-directional characteristics of the augmented twin-fuselage configuration was the "low roll response."

The roll-rate response characteristics presented in tables VI(b) and VII(b) indicate that (1) the effective time delay would be expected to be at a satisfactory level since $t_1 < 0.283$ sec, (2) the roll mode time constant would be expected to be at a satisfactory level since $\tau_R < 1.4$ sec, and (3) the time required to bank 30° would be expected to be at an unacceptable level since $t_{\phi=30} > 6$ sec. However, as stated previously, the roll response of the augmented configuration was rated as acceptable but not satisfactory (PR = 5). Therefore, the parameter $t_{\phi=30}$ was examined quite thoroughly during the subject simulation study, and the results are presented in the form of pilot opinion of the maximum tolerable values of $t_{\phi=30}$ for various simulated piloting tasks.

Evaluation of Roll Performance Requirements

The roll requirements of reference 4 for large, heavy, low-to-medium maneuverability airplanes - the airplane class applied to the twin-fuselage configuration simulated in the present study, although it is much larger than "normal" class III aircraft - are as follows for satisfactory performance:

1. The roll mode time constant τ_R shall be no greater than 1.4 sec;

2. The yaw and roll control power shall be adequate to develop at least 10° of sideslip in the power-approach flight condition, with not more than 75 percent of the available roll control power;

3. It shall be possible to land with normal pilot skill and technique in 90° crosswinds of velocities up to 30 knots; and

4. The time required to bank the airplane 30° shall not exceed 2.5 sec.

As can be seen from table VI(a), the roll mode time constant τ_R was 1.33 sec for the augmented twin-fuselage transport concept. This level meets the requirement of reference 4 for satisfactory performance.

Figure 20 indicates the crosswind trim capability of the twin-fuselage configuration, and it can be seen that (1) the yaw and roll control power is adequate to develop more than a 10° sideslip with 75 percent of the roll control power available, and (2) the roll and yaw control power is sufficient to trim the aircraft in 90° crosswinds of velocities up to 30 knots. Therefore, the roll control power is sufficient to meet both of these reference 4 requirements.

In addition to these requirements, however, reference 4 dictates that the time required to bank the airplane 30° shall not exceed 2.5 sec. As can be seen from table VII(a), the time required for the augmented twin-fuselage airplane to bank 30° was 7.8 sec, in the landing configuration, which is more than 3 times the amount of time allowed for satisfactory roll performance. In fact, reference 4 implies that if the parameter $t_{\phi=30}$ is greater than 6 sec, it is doubtful that the aircraft could consistently be landed safely. However, as stated previously, the simulated twin-fuselage airplane with the SCAS operative, which requires 7.8 sec to bank 30°, was

assigned an average pilot rating of 5 (acceptable, but not satisfactory) for the approach and landing task in calm air. (It should be mentioned that the simulated reference transport had a value of $t_{\phi=30}$ greater than 3 sec, and it is considered to be a good flying machine.) Furthermore, figure 21 indicates that when simulated landing approaches were performed in 90° crosswinds, the pilots felt that they could perform safe landings on the twin-fuselage airplane in crosswinds up to 30 knots and rated the roll performance as being acceptable (PR $\leq$ 6.5) for landing in crosswinds as high as approximately 25 knots. It was obvious from these results (fig. 21) that although the twin-fuselage airplane could be landed under adverse conditions, the roll performance of the aircraft would have to be improved appreciably before being rated as satisfactory (PR $\leq$ 3.5).

Figure 22 presents the average pilot rating assigned to the twin-fuselage transport concept for various locations of the fuselage along the wing span and relates these fuselage locations to the parameter $t_{\phi=30}$. (Note SCAS gain changes for various fuselage locations in table VIII.) The piloting task was the approach and landing in calm atmospheric conditions, and the indicated times required to bank 30° are for the "landing" configuration and speed: $\delta_f = 50°$ and $V_\ell = 126$ knots. These results indicate that when the fuselages are moved from $\eta_b = 0.5$ to $\eta_b = 0.2$ (which correspond to fuselage separation distances of 202 ft and 80.8 ft, respectively), the time required to bank 30° is decreased from 7.8 sec to 6.1 sec, and the pilots' evaluation of their ability to land the airplane in calm air varied from PR = 5 (acceptable, but unsatisfactory) for the $\eta_b = 0.5$ configuration to PR = 3.5 (marginally satisfactory) for the $\eta_b = 0.2$ configuration. Also, table VI(b) indicates that the roll mode time constant τ_R was decreased from 1.33 sec to 0.71 sec; table VII(b) indicates that the effective time delay in the roll-rate response t_1 remained at a satisfactory level ($t_1 < 0.283$ sec) for all fuselage locations simulated.

Figure 4(a) shows that when the fuselages were moved inboard from $\eta_b = 0.5$ to $\eta_b = 0.2$, the roll inertia I_X was decreased by more than 60 percent (345×10^6 to 129×10^6 slug-ft^2). Therefore, an attempt was made to determine the maximum tolerable time required to bank the aircraft 30° in adverse landing conditions; these results are summarized in table IX and figure 23.

The landing tasks simulated included (1) an artificial ceiling of 300 ft, (2) a 200-ft lateral offset from the extended centerline of the runway (localizer beam), (3) a steady 90° crosswind of 15 knots; (4) a 16-knot, 90° horizontal crosswind shear for the last 200 ft of altitude, and (5) various combinations of these four. The landing tasks were simulated with the fuselages located at $\eta_b = 0.5$ to $\eta_b = 0.2$, in 0.1 increments. Also, as the fuselages were moved inboard, it was assumed that the aileron span could be increased as a direct function of the fuselage relocation.

From table IX, it may be noted that the twin-fuselage airplane in the $\eta_b = 0.2$ configuration was consistently rated by the pilots as being better (could accomplish the task more easily) than the reference (single-body) airplane. For most landing tasks, the twin-fuselage airplane in the $\eta_b = 0.3$ configuration was also rated better than the reference airplane, although the roll response ($t_{\phi=30}$) was not nearly as fast for either of the twin-fuselage configurations, regardless of whether the aileron span was increased (increased roll control). The reference airplane used in this simulation study was said to represent a transport similar to the Lockheed C-5A. Since the C-5A is known to be a "good flying machine," the data presented in table IX imply that the pilots would accept values of $t_{\phi=30}$ much greater than 3 sec on very large cargo transports of the future.

The simulation results presented in figure 23 indicate that for such large and unusually configured aircraft as the subject twin-fuselage concept, a value of $t_{\phi=30} < 6$ sec should result in acceptable roll response characteristics, and when $t_{\phi=30} < 3.8$ sec, satisfactory roll response should be attainable.

Airplane Touchdown Variables

In an attempt to gain some insight as to the minimum runway width required for operation with large multibody cargo transports, 79 simulated landings involving instrument flight were analyzed with a breakout altitude of 300 ft, with and without 200-ft lateral offsets, and with and without a steady 15-knot crosswind or wind shear of 16 knots (8 knots per 100 feet of altitude). The results are presented in table X and figure 24.

Figure 24 presents the longitudinal and lateral dispersions of the touchdown points (where the zero index on the longitudinal scale represents the point at which the glide slope intercepts the runway) and indicates that the longitudinal and lateral dispersions were ±740.60 ft and ±31.88 ft, respectively, for 95 percent of the simulated landings (2σ). The maximum allowable longitudinal and lateral dispersions in touchdown position are given in reference 9, on a 2σ basis, as being ±750 ft and ±27 ft, respectively. Therefore, upon comparing the data presented in figure 24 with these criteria, it can be seen that the longitudinal touchdown dispersions for these simulated landings were acceptable (±740.60 ft compared to ±750 ft), but the lateral dispersion points would be considered marginal (±31.88 ft compared to ±27 ft). All landings were performed using a visually simulated runway 11 500 ft long and 267 ft wide. For the twin-fuselage configuration with $\eta_b = 0.5$, the outside dimension of the main landing-gear wheels was 213.6 ft, leaving, therefore, only 26.7 ft to the edge of the 267-ft-wide runway when the aircraft center of gravity was on the runway centerline. Reference 9 suggests that when using computer analysis (simulation) for landing, the outboard landing gear should be no closer than 5 ft from the lateral limits of a 150-ft-wide runway; if this 5-ft "requirement" is assumed for the present simulation study, that leaves a lateral dispersion margin of 21.7 ft. Of the 13 landings performed with the $\eta_b = 0.5$ configuration, three exceeded the 21.7-ft lateral dispersion limit, thus violating the 5-ft requirement. However, all other landings with the other simulated configurations (various values of η_b) were acceptable, thus meeting the 5-ft requirement.

Table X indicates that the bank-angle (ϕ_{td}) and crab-angle (ψ_{td}) requirements of reference 10 for an acceptable touchdown were met, but the sink-rate ($-\dot{h}_{td}$) and lateral-drift-velocity ($\dot{y}_{td}$) limits were slightly exceeded on a 2σ basis. However, it should be mentioned that the sink-rate limit of 5 ft/sec was suggested as a limit for passenger comfort, and since the 2σ maximum sink rate of 5.93 ft/sec is well below the structural design limits, the sink rates for the simulated cargo transport (table X) would be considered acceptable. Similarly, the 2σ maximum lateral drift velocity ($\dot{y}_{td}$) of 8.61 ft/sec could be considered acceptable if the aircraft were designed with the castering-type crosswind landing gear. (It is generally believed that future airplanes of this size will have crosswind landing gear.)

Ride Qualities

Flight in rough air was evaluated by using a turbulence model based on the Dryden spectral form. The root-mean-square value of the longitudinal, lateral, and

vertical gust-velocity components was 6 ft/sec; this level was described by the pilots as being representative of heavy turbulence.

The pilots commented that the rating for the approach task on the augmented twin-fuselage transport was degraded by one-half when the landing approach was made in the simulated heavy turbulence because of the increased workload required to maintain ILS tracking. (PR increased from 5 for calm air to 5.5 in heavy turbulence.) Utilizing the turbulence effect rating scale indicated in table V, the twin-fuselage airplane was assigned a rating of D.

The rms values of the vertical and lateral accelerations at the pilot station of the simulated twin-fuselage transport were calculated during ILS approaches made in simulated heavy turbulence, and these values were compared with the ride quality criterion of reference 11. This criterion relates the rms values of Δa_n and a_y to the rms values of the gust intensity (level of turbulence). The response of the simulated twin-fuselage cargo transport configuration to the FAA heavy turbulence level compares favorably with the aforementioned criterion, although the rms normal acceleration response as measured at the pilot station, for $\eta_b = 0.5$, approaches the 0.11g limit (0.103g). (See fig. 25 and refs. 11 and 12.) Because the pilots are located significantly far from the roll axis on the simulated twin-fuselage configurations studied, it is evident that there could be relatively high levels of normal acceleration generated during certain phases of flight.

Vibrational accelerations measured on the passenger cabin floor of two jet transports during a total of 13 flights are summarized in reference 13. The flights were made in normal weather conditions and included taxiing, take-off, ascent, cruise, descent, and landing. Ride vibration measurements obtained indicated that for the smooth-cruise condition there were rms accelerations of 0.008g and peak accelerations of less than 0.03g in the vertical direction. Other flight conditions showed rms accelerations up to the touchdown level of 0.12g and peak accelerations up to the touchdown level of 0.67g in the vertical direction. The maximum in-flight measurements occurred during the descent mode with an rms acceleration of 0.09g and a a peak acceleration of 0.53g. Table XI presents the average rms and peak accelerations for seven flight phases and their respective standard deviations. The two airplanes used in the tests are known to be quite comfortable, both from individual passenger reaction and from wide passenger acceptance. This observation, from reference 13, served to emphasize the importance of such features as duration, spectrum, and amplitude distribution, as well as rms and peak accelerations, in determining the subjective response to a given vibration environment. Analysis of the twin-fuselage cargo transport in the simulated landing configurations has shown that peak normal accelerations at the pilot station of up to 0.24g were achieved, but in light of the aforementioned findings of reference 13, this level would be said to be acceptable.

Previous studies using CTOL jet transport aircraft have shown that the rms acceleration measurements in the lateral direction for various flight phases have been generally considerably lower than those measured in the vertical direction. Stephens, in reference 14, analyzed the data from reference 13 and established boundaries which he considered to be representative of a good-riding, acceptable air-transportation system and which may therefore serve as a reference base for examination of other systems. The acceptable boundaries were established at $(a_y)_{rms}/(\Delta a_n)_{rms}$ from 0.125 to 0.288. Figure 26 presents the twin-fuselage-configuration landing-task results and shows the data to be close to the upper limit of acceptability with an average $(a_y)_{rms}/(\Delta a_n)_{rms}$ of 0.265. Note that the results for flight in heavy turbulence are significantly better, thus indicating that more roll control was required to correct for landing approach lateral offsets from the

runway centerline than for corrections due to turbulence. Table XII presents the average peak accelerations and their respective standard deviations, based on a small sampling of landing approaches, for the four twin-fuselage configurations studied. When comparing the normal acceleration results with the findings of reference 13 and the lateral acceleration at the cockpit during rolling maneuvers with the criterion of reference 6, the "ride qualities" of the simulated twin-fuselage configurations would be considered to be acceptable.

Figure 27 presents the lateral and normal acceleration time histories resulting from a 3.8° wheel step input. (This wheel input was selected from the average of the rms levels measured during the landing-task studies.) These data clearly illustrate the normal acceleration spike at the pilot station due to the roll acceleration contribution. It may also be noted from figure 27 that the lateral acceleration at the pilot station is more positive (less negative) than that measured at the airplane center of gravity. The following equation represents an approximation of the lateral acceleration at the pilot station:

$$(a_y)_{ps} \approx (a_y)_{cg} + \frac{\dot{r}\bar{x} - (p^2 + r^2)\bar{y} - \dot{p}\bar{z}}{g}$$

For a positive wheel input, $(a_y)_{cg}$ is negative and $\dot{p}$, p, r, and $\dot{r}$ are positive. Therefore, with the pilot located at positive $\bar{x}$ and negative $\bar{y}$ and $\bar{z}$, the lateral acceleration at the pilot station $(a_y)_{ps}$ is less negative than the lateral acceleration at the airplane center of gravity $(a_y)_{cg}$.

Engine Failure

Lateral-directional control with a critical engine (outboard) failed has always been a prime consideration in the rudder design for multiengine airplanes. Control of asymmetries due to engine failure can be easily analyzed from static conditions by calculating the steady-state sideslip angle, bank angle, and control deflections for a straight flight path over the ground. The transient responses immediately following an engine failure, however, present problems involving pilot reaction time, the manner in which controls are applied, and, of course, the altitude and configuration of the airplane at the time of the failure. During the subject study, attempts were made to simulate the wave-off capabilities as well as continued approaches and landings after an outboard engine failure on the twin-fuselage transport airplane.

The manner in which an engine was failed during this study was that which would be considered the most severe; that is, the engine was failed instantaneously. Also, the configuration flown in each instance incorporated what was considered to be the best stability and control augmentation system (SCAS) evaluated in this study and an autothrottle.

Wave-off capability after engine failure.- The requirement used for evaluating the wave-off capability of the simulated twin-fuselage transport airplane after engine failure was determined on the basis of the airworthiness standards of reference 15: in the approach configuration corresponding to the normal all-engines-operating procedure, the steady gradient of climb may not be less than 2.7 percent (1.547°), with the critical engine inoperative and the remaining engines at the available take-off power or thrust.

The wave-off capability of the augmented twin-fuselage airplane in the approach configuration (δ_f = 30°; gear down; V_{app} = 138 knots) met the aforementioned requirement in that a 2.7-percent climb gradient could be achieved with an outboard engine inoperative. However, it should be mentioned that even when the landing gear was retracted, approximately 93 percent of the available thrust, 58 percent of the available rudder deflection, 13 percent of the available aileron deflection, and 75 percent of the available stabilizer deflection were required to achieve this climb gradient and maintain rectilinear flight. Also, the increase in pilot workload caused by the necessity to retrim after an engine failure degraded the pilot rating for the wave-off task to 6. (A pilot rating of 5 was assigned to this η_b = 0.5 configuration with no engine failure.)

Continued approach and landing after engine failure.- Attempts were made to simulate a continued approach and landing following the loss of an outboard engine. The configuration flown incorporated the previously discussed stability and control augmentation systems (pitch-rate command/attitude-hold, roll-rate command/attitude-hold, and various turn coordination features) and autothrottle. A typical approach, for which the number 1 engine was failed at an altitude of 1000 ft, is presented in figure 28. The most interesting points indicated are the excursions from the localizer and glide slope following the engine failure. As can be seen, the maximum lateral displacement from the localizer beam (y) was approximately 150 ft, and the maximum vertical displacement from the glide slope beam (ε_{zh}) was less than 15 ft.

The pilots commented that the loss of a critical engine during an ILS approach posed no problems (insofar as tracking localizer and glide slope) but that the requirement of using rudder for trimming sideslip was bothersome. For the continued approach task after an outboard engine failure, the pilots assigned a rating of 5.5 to the subject twin-fuselage transport airplane with the fuselages located at 50 percent of the wing semispan (η_b = 0.5). (For the η_b = 0.5 configuration, the outboard engines are located at 71 percent of the wing semispan; see table I(a) and fig. 1.) It should be noted that this η_b = 0.5 configuration was assigned a pilot rating of 5 when no failures occurred - primarily because of the low roll response capability.

Effects of Center-of-Gravity Location

As stated previously, the longitudinal handling qualities evaluations for the landing-approach task at the basic center-of-gravity position ($0.25\bar{c}$) resulted in a pilot rating of 5 with no augmentation and a pilot rating of 2 with the SCAS and autothrottle operative. To evaluate the effects of center-of-gravity location on the low-speed handling qualities, the airplane was flown with increasing levels of negative static margin. The technique used to determine the most tolerable aft center-of-gravity location was to determine the center-of-gravity position at which the pilots evaluated the low-speed, longitudinal handling qualities as being satisfactory with the SCAS operative, PR $\leq$ 3.5, and also as being acceptable with no augmentation (PR $\leq$ 6.5). Figure 29 indicates that for a center-of-gravity location of $0.46\bar{c}$, the pilots rated the landing approach task as being marginally acceptable (PR = 6.5) with no augmentation and satisfactory (PR = 3) with SCAS operative. Therefore, from considerations of low-speed longitudinal handling qualities, the aft center-of-gravity limit on the subject twin-fuselage cargo transport airplane was said to be $0.46\bar{c}$ (16-percent negative static margin).

Dynamic Stability Requirements and Criteria

For several years the aircraft industry has been aware that many of the existing stability and control requirements of aircraft are outdated because of the expansion of flight envelopes, the increases in airplane size, and the utilization of complex stability and control augmentation systems. Although research is presently being conducted in an effort to remedy this situation, to date essentially no clearly defined stability requirements and criteria have been established for aircraft similar to those of very large conventional or multibody cargo transports. Therefore, in an effort to aid in the future establishment of new stability requirements, the low-speed handling qualities parameters of a large reference transport and several multibody transport configurations are compared with some existing handling qualities criteria.

Two of the most widely used longitudinal handling qualities criteria are presented in figure 16. Figure 16(a) shows the short-period frequency requirements of reference 4 and, as stated previously, the results predicted by the criterion agree with the results obtained during the present simulation studies. Figure 16(b) shows the Shomber-Gertsen longitudinal handling qualities criterion of reference 5; this criterion relates the ability of the pilot to change flight path with normal acceleration to the factor L_{α}. By using this parameter and by recognizing that the pilot's mode of control is not constant for all flight regimes, a criterion for satisfactory low-speed, short-period characteristics was developed (ref. 5) that correlates well with current airplane experience and is consistent with the results presented in figure 16(a) obtained during the present low-speed twin-fuselage transport simulation program.

The low-speed pitch-rate response criterion presented in figure 17, and reported in reference 8, was based on the Shomber-Gertsen criterion of reference 5. After a short time, there is excellent agreement between the results obtained during the present study and this low-speed pitch response criterion, especially for the twin-fuselage concept with pitch-rate-command augmentation. However, in terms of effective time delay and transient peak ratio, as defined in reference 6, these aircraft exhibit level 1 (satisfactory) characteristics; and in terms of rise time parameter (ref. 6), the augmented reference airplane and unaugmented twin-fuselage airplane have level 2 (acceptable but unsatisfactory) characteristics, and the augmented twin-fuselage airplane has level 1 characteristics. (See fig. 18 and tables VII(a) and (b).) These results suggest that the lower boundary of the reference 8 pitch-rate response criterion (fig. 17) should be modified for this class of large transports.

The roll-acceleration and roll-rate capability criteria for transport aircraft are presented in figures 30 and 31, respectively, and reported in references 16 and 17. The various configurations evaluated during the present simulation study are indicated in these figures and would not be considered to be in agreement with results predicted by these criteria.

The bank-angle oscillation, roll-rate oscillation, and sideslip excursion limitations criteria of reference 16 are presented in figures 32, 33, and 34, respectively. They relate the phase angle of the Dutch roll component of sideslip (ϕ_{β}) to the measure of the ratio of the oscillating component to the average component of bank angle and roll rate, and to the maximum sideslip excursion. The various configurations evaluated during the present simulation study are indicated in these figures, and it can be seen that the simulated characteristics agree well with the aforementioned criteria.

In general, it is concluded that the results of the present simulation study agree reasonably well with the handling qualities criteria used for comparison in this paper, except for the roll-acceleration and roll-rate capability criteria of references 16 and 17. Also, it may be noted that the augmented twin-fuselage concept compared favorably with the reference (single-body) transport, except for the roll-acceleration and roll-rate capability parameters.

CONCLUDING REMARKS

A six-degree-of-freedom, ground-based simulator study has been conducted to evaluate the low-speed flight characteristics of a twin-fuselage cargo transport airplane and to compare these characteristics with those of a large, single-fuselage (reference) transport configuration. The primary piloting task was the approach and landing. This paper has attempted to summarize the results of the study which support the following major conclusions.

The average pilot rating assigned to the longitudinal handling qualities of the unaugmented twin-fuselage airplane was 5 (acceptable, but unsatisfactory), the primary objections being (1) low apparent pitch damping, (2) sluggish initial pitch response, and (3) unusually large pitch-attitude excursions associated with changes in flaps.

A pilot rating of 10 (uncontrollable) was assigned to the lateral-directional handling qualities of the unaugmented airplane. The major objections were (1) very sluggish roll response, (2) unacceptably large sideslip excursions in turns, and (3) a large amount of adverse yaw. Therefore, the overall low-speed handling qualities of the unaugmented twin-fuselage cargo transport concept would be said to be unacceptable.

The longitudinal stability and control augmentation system, consisting of a high-gain pitch-rate command/attitude-hold system and an autothrottle, developed for this twin-fuselage transport airplane provided good short-period characteristics and rapid response to pilot inputs and the attitude-hold feature minimized disturbances due to turbulence or variations in flaps and/or thrust. With this augmentation operative, the average pilot rating for the longitudinal handling qualities on the instrument approach was improved from 5 (acceptable, but unsatisfactory) to 2 (satisfactory).

Laterally, a roll-rate command/attitude-hold augmentation system was employed in an attempt to provide a rapid roll mode and quick uniform response to pilot inputs; the attitude-hold feature resulted in a desirable neutrally stable spiral mode while counteracting disturbances due to turbulence. Directionally, roll-rate and roll-attitude feedbacks were used to provide turn coordination and improved Dutch roll characteristics. With this augmentation system operative, the average pilot rating for the lateral-directional handling qualities on the instrument approach, in calm air, was improved from a 10 (uncontrollable) to a 5 (acceptable). The primary objection of the pilots to the low-speed flight characteristics of the augmented twin-fuselage configuration was the "low roll response."

When simulated landing approaches were performed in 90° crosswinds, the pilots felt that they could perform safe landings on the twin-fuselage airplane in crosswinds up to 30 knots and rated the roll performance as being acceptable (pilot ratings less than 6.5) for landing in crosswinds as high as approximately 25 knots. It was obvious, however, that although the twin-fuselage airplane could be landed

under adverse conditions, the roll performance of the aircraft would have to be improved appreciably before being rated as satisfactory.

The roll performance parameter $t_{\phi=30}$ (time required to bank the aircraft 30°) was examined quite thoroughly during the subject simulation study, and an attempt was made to determine the maximum value of $t_{\phi=30}$ the pilots would accept as being satisfactory for various simulated piloting tasks. These ground-based simulation results indicated that for such large and unusually configured aircraft as the subject twin-fuselage concept, a value of $t_{\phi=30}$ less than 6 sec should result in acceptable roll response characteristics, and when $t_{\phi=30}$ is less than 3.8 sec, satisfactory roll response should be attainable. In order to accomplish this roll performance on the simulated twin-fuselage concept, the fuselages had to be relocated from 50 percent of the wing semispan to 20 percent of the wing semispan, and as the fuselages were moved inboard, the aileron span was increased such that the "basic" aileron effectiveness coefficients were increased by a factor of 2.17.

In an attempt to gain insight as to the minimum runway size required for operation with large multibody cargo transports, 79 simulated landings involving instrument flight were analyzed with a breakout altitude of 300 ft, with and without 200-ft lateral offsets, and with and without a steady 15-knot crosswind or wind shear of 16 knots (8 knots per 100-feet altitude). The results indicated that the longitudinal and lateral touchdown dispersions were ±740.60 ft and ±31.88 ft, respectively, for 95 percent of the simulated landings (2σ). Upon comparing these results with existing touchdown-position criteria for conventional transports, it can be said that the longitudinal touchdown dispersions for the simulated landings were acceptable (±740.60 ft compared to allowable ±750 ft) but the lateral dispersion points would be considered marginal (±31.88 ft compared to allowable ±27 ft).

Because the pilots are located significantly far from the roll axis on the simulated twin-fuselage configurations (various fuselage locations) studied, it was evident that there could be relatively high levels of normal acceleration generated during certain phases of flight. The results of this simulation study indicate that the response of these configurations to atmospheric turbulence would not be expected to be any worse than the response of present-day transports. However, the pilots commented that the pilot rating for the instrument approach on the augmented twin-fuselage concept was degraded by one-half when the landing approach was made in the simulated heavy turbulence because of the increased workload required to maintain glide slope and localizer tracking. Also, utilizing the turbulence effect rating scale, the twin-fuselage airplane was assigned a rating of D (moderate deterioration of task performance). These simulator results also indicated, however, that higher accelerations, in general, were experienced at the pilot station when correcting for landing-approach lateral offsets from the extended runway centerline than for corrections due to turbulence.

The wave-off capabilities, as well as continued approaches and landing, were simulated after the failure of an outboard (critical) engine. The wave-off capability of the augmented twin-fuselage airplane in the approach configuration met the Federal Aviation Administration requirement in that a 2.7-percent climb gradient could be achieved with a critical engine inoperative. Also, the pilots commented that the loss of a critical engine during an instrument approach posed no problems (insofar as tracking localizer and glide slope) but that the requirement of using rudder for trimming sideslip was bothersome.

In an effort to evaluate the effects of center-of-gravity location on the low-speed handling qualities, the twin-fuselage airplane was flown with increasing levels of negative static margin. It was determined that the aft center-of-gravity limit (from a handling qualities standpoint) on the subject cargo transport airplane was 46 percent of the wing mean aerodynamic chord, which represents a negative static margin of 16 percent.

In general, it was concluded that the results of the present simulation study agree reasonably well with the handling qualities criteria used for comparison in this paper, except for the roll-acceleration and roll-rate capability requirements. It was also noted that the augmented twin-fuselage concept compared favorably with the reference (single-body) transport except for these roll capability parameters. It is further concluded, however, that additional low-speed research is required in order to develop a data base and to formulate handling qualities and ride qualities criteria for highly augmented and/or unusually configured aircraft of the future.

Langley Research Center
National Aeronautics and Space Administration
Hampton, VA 23665
August 4, 1983

REFERENCES

1. Moore, J. W.; Craven, E. P.; Farmer, B. T.; Honrath, J. F.; Stephans, R. E.; and Meyer, R. T.: Multibody Aircraft Study - Volume I. NASA CR-165829, 1982.

2. USAF Stability and Control Datcom. Contracts AF33(616)-6460 and F33615-76-C-3061, McDonnell Douglas Corp., Oct. 1960. (Revised Apr. 1978.)

3. Martin, D. J., Jr.: A Digital Program for Motion Washout on Langley's Six-Degree-of-Freedom Motion Simulator. NASA CR-145219, 1977.

4. Military Specification - Flying Qualities of Piloted Airplanes. MIL-F-8785C, Nov. 5, 1980. (Supersedes MIL-F-8785B, Aug. 7, 1969.)

5. Shomber, H. A.; and Gertsen, W. M.: Longitudinal Handling Qualities Criteria: An Evaluation. AIAA Paper No. 65-780, Nov. 1965.

6. Chalk, C. R.: Recommendations for SCR Flying Qualities Design Criteria. NASA CR-159236, 1980.

7. Stability and Control, Flight Control, Hydraulic Systems and Related Structures Criteria. Doc. No. D6-6800-5, Boeing Co., Jan. 1970.

8. Sudderth, Robert W.; Bohn, Jeff G.; Caniff, Martin A.; and Bennett, Gregory R.: Development of Longitudinal Handling Qualities Criteria for Large Advanced Supersonic Aircraft. NASA CR-137635, 1975.

9. Automatic Landing Systems (ALS). AC No. 20-57A, FAA, Jan. 12, 1971.

10. Johnson, Walter A.; and Hoh, Roger H.: Determination of ILS Category II Decision Height Window Requirements. NASA CR-2024, 1972.

11. Low-Wing-Loading STOL Transport Ride Smoothing Feasibility Study. D3-8514-2 (Contract NAS1-10410), Boeing Co., Feb. 8, 1971. (Available as NASA CR-111819.)

12. Grantham, William D.; Nguyen, Luat T.; Deal, Perry L.; Neubauer, M. J., Jr.; Smith, Paul M.; and Gregory, Frederick D.: Ground-Based and In-Flight Simulator Studies of Low-Speed Handling Characteristics of Two Supersonic Cruise Transport Concepts. NASA TP-1240, 1978.

13. Catherines, John J.; Mixson, John S.; and Scholl, Harland F.: Vibrations Measured in the Passenger Cabins of Two Jet Transport Aircraft. NASA TN D-7923, 1975.

14. Stephens, David G.: Developments in Ride Quality Criteria. Noise Contr. Eng., vol. 12, no. 1, Jan.-Feb. 1979, pp. 6-14.

15. Airworthiness Standards: Transport Category Airplanes. FAR Pt. 25, FAA, June 1974.

16. Chalk, C. R.; Neal, T. P.; Harris, T. M.; Pritchard, F. E.; and Woodcock, R. J.: Background Information and User Guide for MIL-F-8785B(ASG), "Military Specification - Flying Qualities of Piloted Airplanes." AFFDL-TR-69-72, U.S. Air Force, Aug. 1969. (Available from DTIC as AD 860 856.)

17. Aerospace Recommended Practice: Design Objectives for Flying Qualities of Civil Transport Aircraft. ARP 842B, Soc. Automot. Eng., Aug. 1, 1964. Revised Nov. 30, 1970.

TABLE I.- MASS AND DIMENSIONAL CHARACTERISTICS OF SIMULATED TRANSPORT AIRPLANES

(a) Twin-fuselage cargo transport; $\eta_b = 0.5$

Weight, lbf	1 287 500
Reference wing area, ft^2	12 980
Wing span, ft	404.00
Wing leading-edge sweep, deg	26
Reference mean aerodynamic chord, ft	44.62
Center-of-gravity location, percent $\bar{c}$	25
Static margin, percent	5
I_X, slug-ft^2	345 000 000
I_Y, slug-ft^2	95 000 000
I_Z, slug-ft^2	431 000 000
I_{XZ}, slug-ft^2	6 500 000
Maximum control surface deflections:	
δ_f, deg	0 to 50
δ_h, deg	5 to -15.5
δ_e, deg	±25
δ_a, deg	±40
δ_r, deg	±35
Maximum control surface deflection rates:	
$\dot{\delta}_f$, deg/sec	±15
$\dot{\delta}_h$, deg/sec	±0.5
$\dot{\delta}_e$, deg/sec	±25
$\dot{\delta}_a$, deg/sec	±40
$\dot{\delta}_r$, deg/sec	±35
Horizontal tail:	
Gross horizontal-tail area, ft^2	2200
Mean aerodynamic chord, ft	15.86
Distance from center of gravity to horizontal-tail $0.25\bar{c}$, ft	114.47
Vertical tail:	
Exposed vertical-tail area, ft^2	2646
Mean aerodynamic chord, ft	32.52
Distance from center of gravity to vertical-tail $0.25\bar{c}$, ft	92.42
Engines:	
Lateral distance from center of gravity to engine centerline	
Outboard, ft	143.00
Inboard, ft	101.00
Vertical distance from center of gravity to engine centerline	
Outboard, ft	4.00
Inboard, ft	-12.00

TABLE I.- Concluded

(b) Reference transport

Weight, lbf	579 000
Reference wing area, ft^2	6200
Wing span, ft	219.20
Wing leading-edge sweep, deg	28
Reference mean aerodynamic chord, ft	30.93
Center-of-gravity location, percent $\bar{c}$	35
Static margin, percent	10.77
I_X, slug-ft^2	34 900 000
I_Y, slug-ft^2	40 400 000
I_Z, slug-ft^2	60 100 000
I_{XZ}, slug-ft^2	60 600
Maximum control surface deflections:	
δ_f, deg	25 to 40
δ_h, deg	2 to -16.5
δ_e, deg	15 to -25
δ_a, deg	±40
δ_r, deg	±35
Maximum control surface deflection rates:	
$\dot{\delta}_f$, deg/sec	±15
$\dot{\delta}_h$, deg/sec	±0.5
$\dot{\delta}_e$, deg/sec	±25
$\dot{\delta}_a$, deg/sec	±40
$\dot{\delta}_r$, deg/sec	±35
Horizontal tail:	
Gross horizontal-tail area, ft^2	965.82
Mean aerodynamic chord, ft	15.29
Distance from center of gravity to horizontal-tail $0.25\bar{c}$, ft	125.87
Vertical tail:	
Exposed vertical-tail area, ft^2	961.07
Mean aerodynamic chord, ft	27.95
Distance from center of gravity to vertical-tail $0.25\bar{c}$, ft	110.15
Engines:	
Lateral distance from center of gravity to engine centerline	
Outboard, ft	61.9
Inboard, ft	39.8
Vertical distance from center of gravity to engine centerline	
Outboard, ft	3.3
Inboard, ft	3.3

TABLE II.- AERODYNAMIC DATA USED IN SIMULATION OF TWIN-FUSELAGE AIRPLANE CONCEPT

α, deg	$C_{m_{\delta_h}}$, deg^{-1}	C_X	C_Z	C_m	C_X	C_Z	C_m
		$\delta_f = 30°$			$\delta_f = 50°$		
-8	-0.0350	-0.1354	-0.4507	-0.3153	-0.2627	-0.7991	-0.4195
-4	↓	-.1432	-.8293	-.3339	-.2538	-1.1852	-.4381
0		-.1064	-1.2093	-.3526	-.1995	-1.5721	-.4568
4		-.0254	-1.5870	-.3712	-.1001	-1.9560	-.4754
8		.1006	-1.9586	-.3899	.0461	-2.3326	-.4940
12		.2707	-2.3201	-.4085	.2333	-2.6989	-.5127
16		.4860	-2.6672	-.4271	.4565	-3.0530	-.5313

α, deg	$C_{X_{\delta_e}}$, deg^{-1}	$C_{Z_{\delta_e}}$, deg^{-1}	$C_{m_{\delta_e}}$, deg^{-1}	$\Delta C_{X_{\ell g}}$	$\Delta C_{Z_{\ell g}}$	$\Delta C_{m_{\ell g}}$
-8	-0.00081	-0.00574	-0.01501	-0.01158	0.00163	-0.00423
-4	-.00040	-.00579	↓	-.01017	.00071	-.00371
0	0	-.00580		-.01002	0	-.00366
4	.00040	-.00579		-.00960	-.00067	-.00350
8	.00081	-.00574		-.00804	-.00113	-.00294
12	.00121	-.00567		-.00510	-.00108	-.00186
16	.00160	-.00558		0	0	0

α, deg	Numerical values at h/b^* of -								
	0.0454	0.10	0.15	0.20	0.30	0.40	0.60	0.80	1.00
	$C_{X_{ge}}$								
-8	0.00639	0.00397	0.00214	0.00143	0.00071	0.00041	0.00017	0.00006	0
-4	.01108	.00689	.00372	.00248	.00123	.00072	.00030	.00010	↓
0	.02316	.01440	.00777	.00519	.00258	.00150	.00063	.00020	
4	.04258	.02647	.01428	.00954	.00474	.00276	.00116	.00036	
8	.06922	.04304	.02322	.01551	.00771	.00448	.00188	.00059	
12	.10292	.06399	.03453	.02306	.01146	.00667	.00280	.00087	
16	.14340	.08916	.04811	.03213	.01598	.00929	.00390	.00121	
	$C_{Z_{ge}}$								
-8	-0.12095	-0.07520	-0.04057	-0.02710	-0.01347	-0.00783	-0.00329	-0.00102	0
-4	-.17352	-.10788	-.05821	-.03888	-.01933	-.01124	0.00472	-.00146	↓
0	-.22575	-.14036	-.07574	-.05059	-.02515	-.01462	-.00614	-.00190	
4	-.27688	-.17215	-.09289	-.06205	-.03084	-.01793	-.00753	-.00233	
8	-.32615	-.20278	-.10942	-.07309	-.03633	-.02112	-.00887	-.00274	
12	-.37279	-.23179	-.12506	-.08354	-.04152	-.02414	-.01014	-.00314	
16	-.41606	-.25870	-.13959	-.09323	-.04635	-.02694	-.01131	-.00350	
	$C_{m_{ge}}$								
-8	-0.01010	-0.00628	-0.00339	-0.00226	-0.00112	-0.00065	-0.00027	-0.00009	0
-4	-.01463	-.00910	-.00491	-.00328	-.00163	-.00095	-.00040	-.00012	↓
0	-.01917	-.01192	-.00643	-.00430	-.00214	-.00124	-.00052	-.00016	
4	-.02371	-.01474	-.00795	-.00531	-.00264	-.00154	-.00064	-.00020	
8	-.02825	-.01756	-.00948	-.00633	-.00315	-.00183	-.00077	-.00020	
12	-.03278	-.02038	-.01100	-.00735	-.00365	-.00212	-.00089	-.00028	
16	-.03732	-.02320	-.01252	-.00836	-.00416	-.00242	-.00102	-.00031	

*b denotes wing span in feet.

TABLE II.- Concluded

α, deg	$C_{Y_{\delta_a}}$, deg^{-1}	$C_{l_{\delta_a}}$, deg^{-1}	$C_{n_{\delta_a}}$, deg^{-1}	$C_{Y_{\delta_r}}$, deg^{-1}	$C_{l_{\delta_r}}$, deg^{-1}	$C_{n_{\delta_r}}$, deg^{-1}	C_{Y_β}, deg^{-1}	C_{l_β}, deg^{-1}	C_{n_β}, deg^{-1}
-8	0	0.00116	-0.00016	0.00470	0.00009	-0.00102	-0.01340	-0.00276	0.00191
-4	↓	.00117	-.00008	↓	.00016	-.00101	↓	-.00289	.00171
0		.00117	0		.00023	-.00100		-.00300	.00150
4		.00117	.00008		.00030	-.00098		-.00309	.00129
8		.00116	.00016		.00037	-.00096		-.00318	.00106
12		.00115	.00024		.00043	-.00093		-.00324	.00084
16		.00113	.00032		.00050	-.00090		-.00329	.00061

α, deg	C_{m_q}, rad^{-1}	$C_{m_{\dot{\alpha}}}$, rad^{-1}	C_{Y_p}, rad^{-1}	C_{l_p}, rad^{-1}	C_{n_p}, rad^{-1}	C_{Y_r}, rad^{-1}	C_{l_r}, rad^{-1}	C_{n_r}, rad^{-1}
-8	-25.8	-10.3	-0.1135	-0.4329	-0.1215	0.0160	0.4219	-0.1106
-4	↓	↓	-.1143	-.4527	-.1455	.0080	.4030	-.0908
0			-.1146	-.4690	-.1719	0	.3782	-.0745
4			-.1143	-.4814	-.2005	-.0080	.3481	-.0621
8			-.1135	-.4898	-.2303	-.0160	.3132	-.0537
12			-.1121	-.4939	-.2610	-.0238	.2742	-.0496
16			-.1102	-.4937	-.2921	-.0316	.2319	-.0498

TABLE III.- AERODYNAMIC DATA USED IN SIMULATION OF REFERENCE AIRPLANE

α, deg	$C_{m_{\delta_h}}$, deg^{-1}	C_X	C_Z	C_m	C_X	C_Z	C_m
		$\delta_f = 25°$			$\delta_f = 40°$		
-8	-0.0410	-0.0827	-0.0641	0.0308	-0.1500	-0.3273	-0.0177
-4	↓	-.0940	-.4846	-.0788	-.1647	-.7503	-.1273
0		-.0820	-.9200	-.1884	-.1470	-1.1800	-.2369
4		-.0299	-1.3353	-.2980	-.0879	-1.6100	-.3465
8		.0524	-1.7598	-.4076	.0012	-2.0346	-.4561
12		.1528	-2.1860	-.5172	.1081	-2.4613	-.5657
16		.2833	-2.6132	-.6268	.2665	-2.8884	-.6753

α, deg	$C_{X_{\delta_e}}$, deg^{-1}	$C_{Z_{\delta_e}}$, deg^{-1}	$C_{m_{\delta_e}}$, deg^{-1}	$\Delta C_{X_{lg}}$	$\Delta C_{Z_{lg}}$	$\Delta C_{m_{lg}}$
-8	-0.00079	-0.00560	-0.02356	-0.0301	0.0042	-0.0175
-4	-.00046	-.00564	↓	-.0252	.0018	-.0146
0	0	-.00565		-.0215	0	-.0125
4	.00046	-.00564		-.0210	-.0015	-.0122
8	.00079	-.00560		-.0219	-.0031	-.0127
12	.00118	-.00553		-.0163	-.0035	-.0095
16	.00156	-.00544		0	0	0

TABLE III.- Continued

α, deg	Numerical values at h, ft, of -								
	19	40	60	80	100	130	160	190	219.2
				$C_{X_{ge}}$					
-8	0.00376	0.00219	0.00131	0.00084	0.00058	0.00035	0.00020	0.00009	0
-4	.00320	.00186	.00111	.00071	.00049	.00030	.00017	.00008	↓
0	.00871	.00507	.00303	.00194	.00133	.00082	.00047	.00021	
4	.02027	.01181	.00706	.00452	.00309	.00192	.00109	.00049	
8	.03781	.02203	.01317	.00842	.00576	.00358	.00204	.00091	
12	.06121	.03567	.02131	.01363	.00932	.00579	.00330	.00147	
16	.09026	.05260	.03143	.02011	.01375	.00855	.00486	.00217	↓
				$C_{Z_{ge}}$					
-8	-0.03583	-0.02088	-0.01247	-0.00798	-0.00545	-0.00339	-0.00193	-0.00086	0
-4	-.07906	-.04607	-.02753	-.01761	-.01203	-.00749	-.00425	-.00190	↓
0	-.12233	-.07130	-.04261	-.02725	-.01862	-.01159	-.00659	-.00294	
4	-.16502	-.09618	-.05747	-.03676	-.02513	-.01563	-.00889	-.00397	
8	-.20646	-.12033	-.07191	-.04600	-.03143	-.01956	-.01111	-.00495	
12	-.24606	-.14341	-.08570	-.05481	-.03746	-.02331	-.01324	-.00590	
16	-.28319	-.16505	-.09863	-.06308	-.04384	-.02683	-.01524	-.00680	↓
				$C_{m_{ge}}$					
-8	-0.00886	-0.00517	-0.00309	-0.00197	-0.00135	-0.00084	-0.00048	-0.00021	0
-4	-.01997	-.01164	-.00696	-.00445	-.00307	-.00189	-.00108	-.00048	↓
0	-.03107	-.01811	-.01082	-.00692	-.00473	-.00294	-.00167	-.00075	
4	-.04217	-.02458	-.01469	-.00940	-.00642	-.00400	-.00227	-.00101	
8	-.05330	-.03107	-.01856	-.01187	-.00811	-.00505	-.00287	-.00128	
12	-.06436	-.03751	-.02242	-.01434	-.00980	-.00610	-.00346	-.00155	
16	-.07547	-.04398	-.02628	-.01681	-.01149	-.00715	-.00406	-.00181	↓

TABLE III.- Concluded

α, deg	$C_{Y_{\delta_a}}$, deg^{-1}	$C_{l_{\delta_a}}$, deg^{-1}	$C_{n_{\delta_a}}$, deg^{-1}	$C_{Y_{\delta_a}}$, deg^{-1}	$C_{l_{\delta_a}}$, deg^{-1}	$C_{n_{\delta_a}}$, deg^{-1}
	$\delta_f = 25°$			$\delta_f = 40°$		
-8	0	0.00176	-0.00017	0	0.00247	0.00002
-4	↓	.00178	-.00004	↓	.00246	.00019
0	↓	.00177	.00008	↓	.00244	.00036
4	↓	.00176	.00020	↓	.00240	.00053
8	↓	.00174	.00033	↓	.00237	.00070
12	↓	.00171	.00045	↓	.00232	.00086
16	↓	.00168	.00057	↓	.00225	.00102

α, deg	$C_{Y_{\delta_r}}$, deg^{-1}	$C_{l_{\delta_r}}$, deg^{-1}	$C_{n_{\delta_r}}$, deg^{-1}	C_{Y_β}, deg^{-1}	C_{l_β}, deg^{-1}	C_{n_β}, deg^{-1}
-8	0.00360	0.00028	-0.00187	-0.0129	-0.0021	0.0029
-4	↓	↓	-.00187	↓	-.0023	.0028
0	↓	↓	-.00185	↓	-.0025	.0026
4	↓	↓	-.00183	↓	-.0026	.0024
8	↓	↓	-.00179	↓	-.0028	.0022
12	↓	↓	-.00175	↓	-.0030	.0020
16	↓	↓	-.00170	↓	-.0031	.0018

α, deg	C_{m_q}, rad^{-1}	$C_{m_{\dot{\alpha}}}$, rad^{-1}	C_{Y_p}, rad^{-1}	C_{l_p}, rad^{-1}	C_{n_p}, rad^{-1}	C_{Y_r}, rad^{-1}	C_{l_r}, rad^{-1} (a)	C_{n_r}, rad^{-1}
-8	-24.1	-7.9	0	-0.3791	-0.0893	0	0.7273	-0.2559
-4	↓	↓	↓	-.3953	-.0991	↓	.7060	-.2397
0	↓	↓	↓	-.4100	-.1110	↓	.6798	-.2250
4	↓	↓	↓	-.4229	-.1248	↓	.6494	-.2120
8	↓	↓	↓	-.4337	-.1403	↓	.6153	-.2013
12	↓	↓	↓	-.4423	-.1572	↓	.5782	-.1927
16	↓	↓	↓	-.4484	-.1751	↓	.5388	-.1866

[a]Modified to match flight-test spiral stability.

TABLE IV.- PILOT RATING SYSTEM

CONTROLLABLE Capable of being controlled or managed in context of mission, with available pilot attention.	ACCEPTABLE May have deficiencies which warrant improvement, but adequate for mission. Pilot compensation, if required to achieve acceptable performance, is feasible.	SATISFACTORY Meets all requirements and expectations; good enough without improvement. Clearly adequate for mission.	Excellent, highly desirable.	1
			Good, pleasant, well behaved.	2
			Fair. Some mildly unpleasant characteristics. Good enough for mission without improvement.	3
		UNSATISFACTORY Reluctantly acceptable. Deficiencies which warrant improvement. Performance adequate for mission with feasible pilot compensation.	Some minor but annoying deficiencies. Improvement is requested. Effect on performance is easily compensated for by pilot.	4
			Moderately objectionable deficiencies. Improvement is needed. Reasonable performance requires considerable pilot compensation.	5
			Very objectionable deficiencies. Major improvements are needed. Requires best available pilot compensation to achieve acceptable performance.	6
	UNACCEPTABLE Deficiencies which require improvement. Inadequate performance for mission even with maximum feasible pilot compensation.		Major deficiencies which require improvement for acceptance. Controllable. Performance inadequate for mission, or pilot compensation required for minimum acceptable performance in mission is too high.	7
			Controllable with difficulty. Requires substantial pilot skill and attention to retain control and continue mission.	8
			Marginally controllable in mission. Requires maximum available pilot skill and attention to retain control.	9
UNCONTROLLABLE Control will be lost during some portion of mission.			Uncontrollable in mission.	10

TABLE V.- TURBULENCE EFFECT RATING SCALE

Increase of pilot effort with turbulence	Deterioration of task performance with turbulence	Rating
No significant increase	No significant deterioration	A
More effort required	No significant deterioration	B
	Minor	C
	Moderate	D
Best efforts required	Moderate	E
	Major (but evaluation tasks can still be accomplished)	F
	Large (some tasks cannot be performed)	G
Unable to perform tasks		H

TABLE VI.- DYNAMIC STABILITY CHARACTERISTICS OF SIMULATED LARGE SUBSONIC TRANSPORT AIRPLANES

(a) Twin-fuselage cargo transport; $\eta_b = 0.5$

Parameter	V_{app}/δ_f = 138/30		V_{ℓ}/δ_f = 126/50		Satisfactory criterion	Acceptable criterion
	Without augmentation	SCAS (a)	Without augmentation	SCAS (a)		
Short-period mode						
ω_{sp}, rad/sec	0.705	1.598	0.629	1.439	See fig. 8(a)	See fig. 8(a)
P_{sp}, sec		7.33		7.25		
ζ_{sp}	1.234	0.844	1.252	0.799	0.35 to 1.30	0.25 to 2.00
L_α/ω_{sp}	0.679	0.300	0.695	0.304	See fig. 8(b)	See fig. 8(b)
n/α, g units/rad	3.46	3.46	2.89	2.89	See fig. 8(a)	See fig. 8(a)
Long-period (aperiodic) mode						
t_2, sec						>6
Long-period mode						
ω_{ph}, rad/sec	0.086	0.235	0.096	0.255		
P_{ph}, sec	78.73		73.02			
ζ_{ph}	0.359	1.210	0.440	1.070	>0.04	>0
Roll-spiral mode						
τ_R, sec	2.01	1.22	2.15	1.33	<1.4	<3.0
t_{s2}, sec	31.14		30.31		>12	>8
ω_{rs}, rad/sec		1.430		1.294		
ζ_{rs}		0.485		0.449		
$\zeta_{rs}\omega_{rs}$, rad/sec		0.694		0.581	>0.5	>0.3
P_{rs}, sec		5.02		5.44		
Dutch roll mode						
ω_d, rad/sec	0.385	0.269	0.359	0.245	>0.4	>0.4
ζ_d	0.025	0.240	0.012	0.244	>0.08	>0.02
$\zeta_d\omega_d$, rad/sec	0.010	0.065	0.004	0.060	>0.10	>0.05
P_d, sec	16.33	24.05	17.53	26.45		
ϕ/β	0.919	0.116	0.877	0.123		
Roll control parameters						
ω_ϕ/ω_d	0.690	0.991	0.676	0.993	0.80 to 1.15	0.65 to 1.35
ζ_ϕ/ζ_d	8.454	1.022	12.543	0.974		

[a]Autothrottle on.

TABLE VI.- Continued

(b) Effect of fuselage location, basic SCAS, and lateral control system for V_{ℓ}/δ_f = 126/50

[SCAS and autothrottle on]

Parameter	Values for η_b/K_a of -				Satisfactory criterion	Acceptable criterion
	0.5/1.00	0.4/1.00	0.3/1.00	0.2/1.00		
Roll-spiral mode						
τ_R, sec	1.33	1.13	0.89	0.71	≤1.4	≤3.0
t_{s2}, sec					≥12	≥8
ω_{rs}, rad/sec	1.294	1.549	1.908	2.491		
ζ_{rs}	0.449	0.518	0.615	0.681		
$\zeta_{rs}\omega_{rs}$, rad/sec	0.581	0.803	1.173	1.697	≥0.5	≥0.3
P_{rs}, sec	5.44	4.74	4.17	3.45		
Dutch roll mode						
ω_d, rad/sec	0.245	0.275	0.309	0.343	≥0.4	≥0.4
ζ_d	0.244	0.247	0.253	0.259	≥0.08	≥0.02
$\zeta_d\omega_d$, rad/sec	0.060	0.068	0.078	0.089	≥0.10	≥0.05
P_d, sec	26.45	23.56	21.03	18.98		
ϕ/β	0.123	0.120	0.088	0.109		
Roll control parameters						
ω_ϕ/ω_d	0.993	0.995	0.998	1.001	0.80 to 1.15	0.65 to 1.35
ζ_ϕ/ζ_d	0.974	0.936	0.902	0.882		

TABLE VI.- Continued

(c) Effect of fuselage location, modified SCAS, and lateral control system for V_{ℓ}/δ_f = 126/50

[SCAS and autothrottle on]

Parameter	Values for η_b/K_a of -				Satisfactory criterion	Acceptable criterion
	0.5/1.00	0.4/1.38	0.3/1.74	0.2/2.17		
Roll-spiral mode						
τ_R, sec		1.06	0.70	0.50	<1.4	<3.0
t_{s2}, sec					>12	>8
ω_{rs}, rad/sec		1.744	2.447	4.317		
ζ_{rs}		0.402	0.488	0.632		
$\zeta_{rs}\omega_{rs}$, rad/sec		0.701	1.194	2.729	>0.5	>0.3
P_{rs}, sec		3.94	2.94	1.88		
Dutch roll mode						
ω_d, rad/sec		0.275	0.308	0.379	>0.4	>0.4
ζ_d		0.244	0.244	0.248	>0.08	>0.02
$\zeta_d\omega_d$, rad/sec		0.067	0.075	0.094	>0.10	>0.05
P_d, sec		23.59	21.02	17.09		
ϕ/β		0.093	0.067	0.075		
Roll control parameters						
ω_ϕ/ω_d		0.997	1.000	1.001	0.80 to 1.15	0.65 to 1.35
ζ_ϕ/ζ_d		0.949	0.936	0.937		

TABLE VI.- Concluded

(d) Reference transport

Parameter	V_{app}/δ_f = 135/25		V_{ℓ}/δ_f = 128/40		Satisfactory criterion	Acceptable criterion
	Without augmentation	SAS (a)	Without augmentation	SAS (a)		
Short-period mode						
ω_{sp}, rad/sec	0.675	0.754	0.645	0.706	See fig. 8(a)	See fig. 8(a)
P_{sp}, sec	18.80	23.79	19.73	25.99		
ζ_{sp}	0.869	0.937	0.870	0.940	0.35 to 1.30	0.25 to 2.00
L_{α}/ω_{sp}	0.829	0.742	0.823	0.752	See fig. 8(b)	See fig. 8(b)
n/α, g units/rad	3.96	3.96	3.56	3.56	See fig. 8(a)	See fig. 8(a)
Long-period (aperiodic) mode						
t_2, sec		[b] -35.69		[b] -35.82		>6
Long-period mode						
ω_{ph}, rad/sec	0.122		0.129			
P_{ph}, sec	51.39		48.72			
ζ_{ph}	0.045		0.072		>0.04	>0
Roll-spiral mode						
τ_R, sec	1.75	2.31	1.79	3.35	<1.4	<3.0
t_{s2}, sec	10.75	[b] -28.20	10.37	[b] -3.41	>12	>8
ω_{rs}, rad/sec						
ζ_{rs}						
$\zeta_{rs}\omega_{rs}$, rad/sec					>0.5	>0.3
P_{rs}, sec						
Dutch roll mode						
ω_d, rad/sec	0.579	0.432	0.553	0.395	>0.4	>0.4
ζ_d	0.135	0.544	0.125	0.445	>0.08	>0.02
$\zeta_d\omega_d$, rad/sec	0.078	0.235	0.069	0.176	>0.10	>0.05
P_d, sec	10.95	17.33	11.44	17.77		
ϕ/β	1.053	0.850	1.187	0.861		
Roll control parameters						
ω_{ϕ}/ω_d	0.824	1.148	0.857	1.243	0.80 to 1.15	0.65 to 1.35
ζ_{ϕ}/ζ_d	1.951	0.818	2.332	1.022		

[a] Autothrottle on.

[b] Minus sign signifies time to half amplitude.

TABLE VII.- CONTROL RESPONSE CHARACTERISTICS OF SIMULATED LARGE SUBSONIC CRUISE TRANSPORT AIRPLANES

(a) Twin-fuselage cargo transport; $\eta_b = 0.5$

Parameter	$V_{app}/\delta_f = 138/30$		$V_{\ell}/\delta_f = 126/50$		Satisfactory criterion	Acceptable criterion
	Without augmentation	SCAS (a)	Without augmentation	SCAS (a)		
Longitudinal						
$\ddot{\theta}_{max}$, rad/sec^2	[b]-0.069	[b]-0.069	[b]-0.059	[b]-0.059	[b]-0.055	[b]-0.035
$\dot{\theta}/\dot{\theta}_{ss}$					See figure 17[c]	
$\Delta a_n/\ddot{\theta}$, $\frac{\text{g units}}{\text{deg/sec}^2}$ ...						See figure 11[c]
t_1, sec	0.05	0.10	0.05	0.10	$\leq$0.200	$\leq$0.283
Δt, sec	1.53	1.00	1.58	0.88	[c]0.041 to 0.909	[c]0.015 to 2.932
$\Delta\dot{\theta}_2/\Delta\dot{\theta}_1$	0	0.13	0	0.13	$\leq$0.30	$\leq$0.60
Lateral						
$\ddot{\phi}_{max}$, rad/sec^2	0.036	0.035	0.031	0.030	See figure 30	See figure 30
$\dot{\phi}_{max}$, deg/sec	4.40	7.78	3.98	6.91		See figure 31
p_2/p_1	0.154	0.930	0.157	0.937	$\geq$0.60	$\geq$0.25
ϕ_{osc}/ϕ_{av}	0.608	0.070	0.692	0.090	See figure 32	See figure 32
$t_{\phi=30}$, sec	10.4	7.0	12.2	7.8	$\leq$2.5	$\leq$4.0
t_1, sec	0.26	0.26	0.25	0.25	$\leq$0.283	$\leq$0.400
Δt, sec		1.42		1.58		

[a]Autothrottle on.
[b]Minimum demonstrated speed = $1.06V_s$.
[c]Landing configuration.

TABLE VII.- Continued

(b) Effect of fuselage location, basic SCAS, and lateral control system for V_ℓ/δ_f = 126/50

[SCAS and autothrottle on]

Parameter	Values for η_b/K_a of -				Satisfactory criterion	Acceptable criterion
	0.5/1.00	0.4/1.00	0.3/1.00	0.2/1.00		
Lateral						
$\ddot{\phi}_{max}$, rad/sec^2	0.030	0.039	0.049	0.061	See figure 30	See figure 30
$\dot{\phi}_{max}$, deg/sec	6.91	7.37	7.74	7.90		See figure 31
p_2/p_1	0.937	0.970	0.991	0.995	$\geq$0.60	$\geq$0.25
ϕ_{osc}/ϕ_{av}	0.090	0.071	0.050	0.041	See figure 32	See figure 32
$t_{\phi=30}$, sec	7.8	7.1	6.5	6.1	$\leq$2.5	$\leq$4.0
t_1, sec	0.25	0.20	0.23	0.22	$\leq$0.283	$\leq$0.400
Δt, sec	1.58	1.35	0.94	0.73		

TABLE VII.- Continued

(c) Effect of fuselage location, modified SCAS, and lateral control system for V_{ℓ}/δ_f = 126/50

[SCAS and autothrottle on]

Parameter	Values for η_b/K_a of -				Satisfactory criterion	Acceptable criterion
	0.5/1.00	0.4/1.38	0.3/1.74	0.2/2.17		
Lateral						
$\ddot{\phi}_{max}$, rad/sec^2		0.053	0.085	0.131	See figure 30	See figure 30
$\dot{\phi}_{max}$, deg/sec		8.89	10.64	12.58		See figure 31
p_2/p_1		0.963	0.989	1.000	$\geq$0.60	$\geq$0.25
ϕ_{osc}/ϕ_{av}		0.060	0.039	0.020	See figure 32	See figure 32
$t_{\phi=30}$, sec		5.8	4.7	3.8	$\leq$2.5	$\leq$4.0
t_1, sec		0.17	0.25	0.15	$\leq$0.283	$\leq$0.400
Δt, sec		1.23	0.75	0.56		

TABLE VII.- Concluded

(d) Reference transport

Parameter	V_{app}/δ_f = 135/25		V_{ℓ}/δ_f = 128/40		Satisfactory criterion	Acceptable criterion
	Without augmentation	SAS (a)	Without augmentation	SAS (a)		
Longitudinal						
$\ddot{\theta}_{max}$, rad/sec^2	[b]-0.051	[b]-0.051	[b]-0.046	[b]-0.046	[b]-0.055	[b]-0.035
$\dot{\theta}/\dot{\theta}_{ss}$					See figure 17[c]	
$\Delta a_n/\ddot{\theta}$, $\frac{\text{g units}}{\text{deg/sec}^2}$ ...						See figure 11[c]
t_1, sec	0.05	0.03	0.05	0.03	⩽0.200	⩽0.283
Δt, sec	1.58	1.42	1.71	1.35	[c]0.041 to 0.901	[c]0.014 to 2.905
$\Delta\dot{\theta}_2/\Delta\dot{\theta}_1$	0	0.14	0	0.18	⩽0.30	⩽0.60
Lateral						
$\ddot{\phi}_{max}$, rad/sec^2	0.121	0.120	0.155	0.153	See figure 30	See figure 30
$\dot{\phi}_{max}$, deg/sec	15.56	17.25	20.86	22.52		See figure 31
p_2/p_1	0.865	0.854	0.930	0.918	⩾0.60	⩾0.25
ϕ_{osc}/ϕ_{av}					See figure 32	See figure 32
$t_{\phi=30}$, sec	3.6	3.6	3.1	3.1	⩽2.5	⩽4.0
t_1, sec	0.15	0.15	0.16	0.16	⩽0.283	⩽0.400
Δt, sec		2.90		2.51		

[a]Autothrottle on.
[b]Minimum demonstrated speed = $1.06V_s$.
[c]Landing configuration.

TABLE VIII.- LATERAL-DIRECTIONAL SCAS GAINS

Roll axis

	η_b	K_a	$K_{p,c}$	$K_{p,I}$	K_p	$K_{\phi,2}$	$K_{\phi,TC}$	K_{WL}
Basic roll control	0.5	1.00	0.35	9.0	15.0	20.0	-50.0	1.0
	.4	↓	↓	9.0	↓	↓	↓	↓
	.3	↓	↓	9.0	↓	↓	↓	↓
	.2	↓	↓	12.0	↓	↓	↓	↓
Increased roll control	0.4	1.38	0.35	7.0	10.0	20.0	-50.0	1.0
	.3	1.74	.35	7.0	10.0	20.0	-50.0	1.0
	.2	2.17	.35	7.0	10.0	20.0	-50.0	1.0

Yaw axis

	η_b	K_a	K_{δ_p}	$K_{\phi,R}$	$K_{p,Y}$
Basic roll control	0.5	1.00	-14.0	-0.18	-6.0
	.4	↓	↓	↓	-5.5
	.3	↓	↓	↓	-5.0
	.2	↓	↓	↓	-4.5
Increased roll control	0.4	1.38	-14.0	-0.18	-5.5
	.3	1.74	-14.0	-0.18	-5.0
	.2	2.17	-14.0	-0.18	-4.5

TABLE IX.- PILOT OPINION OF VARIOUS CONFIGURATIONS OF SIMULATED TWIN-FUSELAGE TRANSPORT AND REFERENCE TRANSPORT FOR VARIOUS LANDING TASKS

Airplane	Fuselage location, η_b	Aileron control multiplier, K_a	Landing task				Average PR	$t_{\phi=30'}$ sec
			Ceiling, ft	Lateral offset, ft	Crosswind, knots			
					Steady	Shear (a)		
Twin fuselage	0.5	1.00	Unlimited	0	0	0	5.0	7.8
Twin fuselage	.4	↓	↓	↓	↓	↓	4.5	7.1
Twin fuselage	.3	↓	↓	↓	↓	↓	4.0	6.5
Twin fuselage	.2	↓	↓	↓	↓	↓	3.5	6.1
Reference	.0	↓	↓	↓	↓	↓	4.0	3.1
Twin fuselage	.4	1.38	Unlimited	0	0	0	4.0	5.8
Twin fuselage	.3	1.74	↓	↓	↓	↓	3.0	4.7
Twin fuselage	.2	2.17	↓	↓	↓	↓	2.5	3.8
Reference	.0	1.00	↓	↓	↓	↓	4.0	3.1
Twin fuselage	.4	1.38	300	0	0	16/200	5.0	5.8
Twin fuselage	.3	1.74	↓	↓	↓	↓	3.5	4.7
Twin fuselage	.2	2.17	↓	↓	↓	↓	3.0	3.8
Reference	.0	1.00	↓	↓	↓	↓	4.5	3.1
Twin fuselage	.4	1.38	300	-200	0	16/200	5.5	5.8
Twin fuselage	.3	1.74	↓	↓	↓	↓	4.0	4.7
Twin fuselage	.2	2.17	↓	↓	↓	↓	3.5	3.8
Reference	.0	1.00	↓	↓	↓	↓	4.5	3.1
Twin fuselage	.4	1.38	300	-200	15	0	6.0	5.8
Twin fuselage	.3	1.74	↓	↓	↓	↓	4.0	4.7
Twin fuselage	.2	2.17	↓	↓	↓	↓	3.5	3.8
Reference	.0	1.00	↓	↓	↓	↓	4.5	3.1

[a]0 knots at 200 ft increasing by 8 knots per 100 feet of altitude to 16 knots at touchdown.

TABLE X.- VARIABLES AT TOUCHDOWN OF SIMULATED TWIN-FUSELAGE TRANSPORT

Variable	Average value	Standard deviation, $\pm\sigma$	$\pm 2\sigma$	Requirements of reference 10
x'_{td}, ft	875.53	370.30	740.60	A 2σ total dispersion of less than 1500 ft about some nominal point[a]
y_{td}, ft	-.89	15.94	31.88	A 2σ dispersion of $\pm$27 ft from runway centerline[a]
$-\dot{h}_{td}$, ft/sec	3.47	1.23	2.46	Limit of 5 ft/sec for passenger comfort
$\dot{y}_{td}$, ft/sec	1.43	3.59	7.18	$\pm$8 ft/sec
ψ_{td}, deg	.57	1.69	3.38	$\pm 4°$
ϕ_{td}, deg	-.10	1.81	3.62	$\pm 5°$

[a]FAA requirement (ref. 9).

TABLE XI.- ACCELERATIONS MEASURED AT AIRCRAFT CENTER OF GRAVITY IN VERTICAL DIRECTION FOR VARIOUS FLIGHT CONDITIONS

[Compiled from ref. 13]

Condition	Taxi	Take-off roll	Ascent	Smooth cruise	Rough cruise	Descent	Touchdown roll
727-100							
$(\Delta a_n)_{rms}/\sigma$	0.025/0.008	0.049/0.008	0.059/0.009	0.006/0.001	0.042/0.006	0.062/0.010	0.059/0.004
$(\Delta a_n)_{max}/\sigma$	0.129/0.050	0.178/0.010	0.240/0.034	0.019/0.004	0.225/0.046	0.422/0.091	0.460/0.136
DC-9-10							
$(\Delta a_n)_{rms}/\sigma$	0.030/0.010	0.055/0.014	0.077/0.016	0.006/0.001	0.042/0.012	0.064/0.016	0.066/0.016
$(\Delta a_n)_{max}/\sigma$	0.159/0.072	0.254/0.065	0.252/0.085	0.023/0.003	0.220/0.051	0.307/0.084	0.500/0.077

TABLE XII.- PEAK ACCELERATIONS MEASURED DURING LANDING-APPROACH LATERAL OFFSET MANEUVERS WITH VARIOUS TWIN-FUSELAGE CONFIGURATIONS

η_b	$(a_y)_{cg}/\sigma$	$(a_y)_{ps}/\sigma$	$(a_y)_{ps}/p_{max}$ (a)	$(\Delta a_n)_{cg}/\sigma$	$(\Delta a_n)_{ps}/\sigma$
0.5	0.061/0.007	0.031/0.004	0.011	0.114/0.024	0.140/0.014
0.4	0.066/0.006	0.048/0.004	0.011	0.099/0.020	0.200/0.027
0.3	0.073/0.007	0.046/0.002	0.009	0.098/0.038	0.203/0.008
0.2	0.053/0.009	0.043/0.005	0.010	0.048/0.008	0.188/0.013

[a]Reference 6 criterion states that $a_y/p_{max} \leq 0.035$ is acceptable.

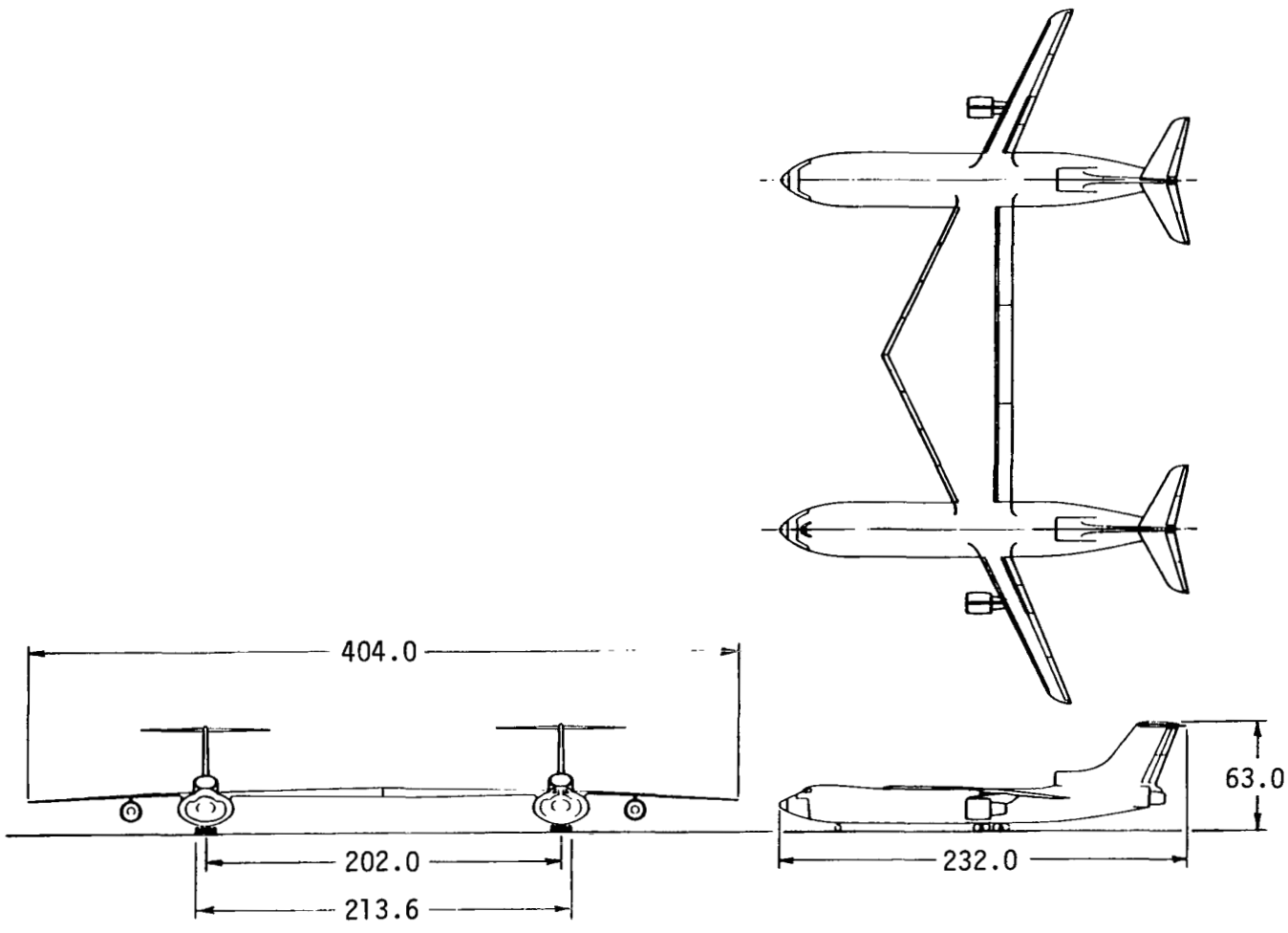

Figure 1.- Three-view sketch of simulated twin-fuselage transport. All linear dimensions are in feet.

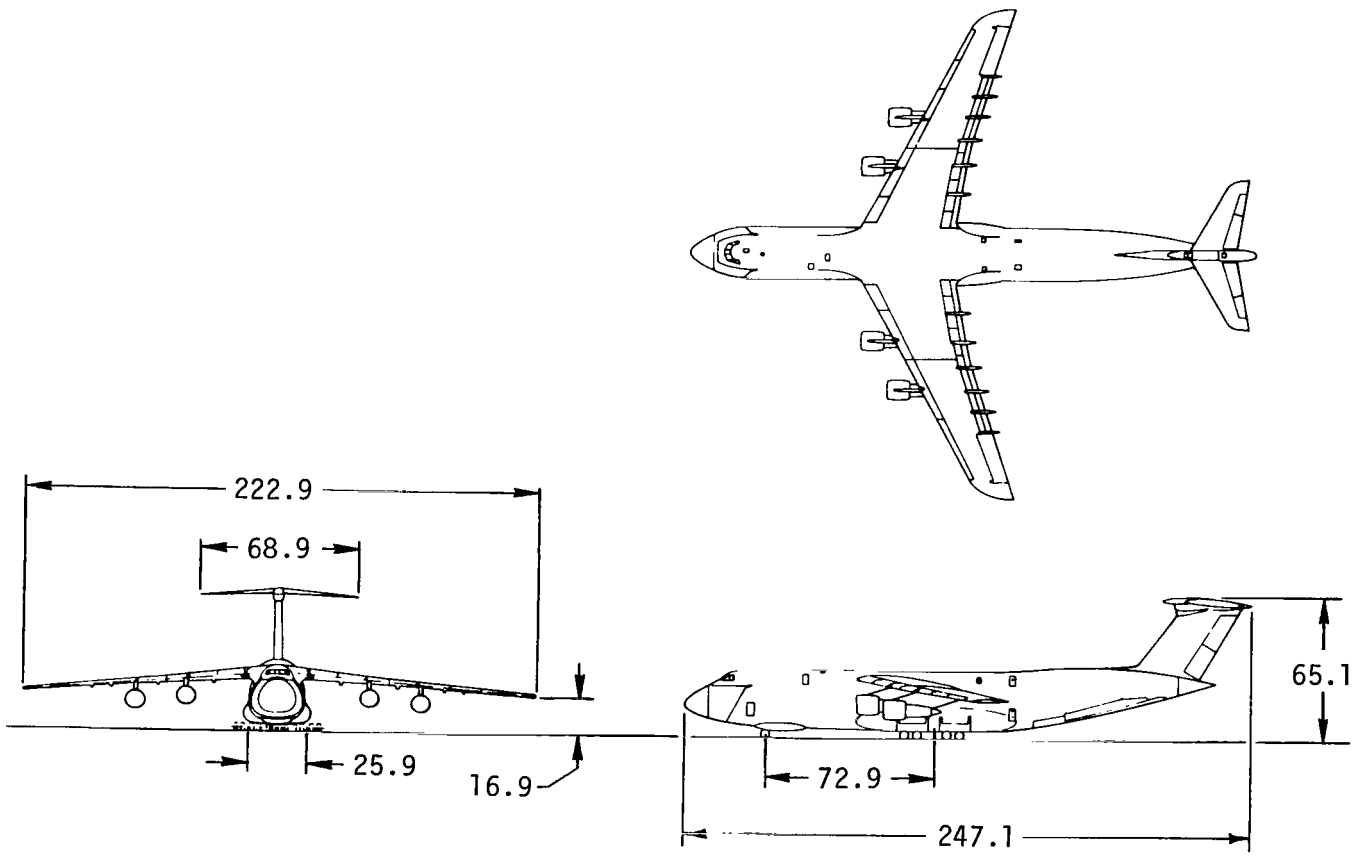

Figure 2.- Three-view sketch of simulated reference transport. All linear dimensions are in feet.

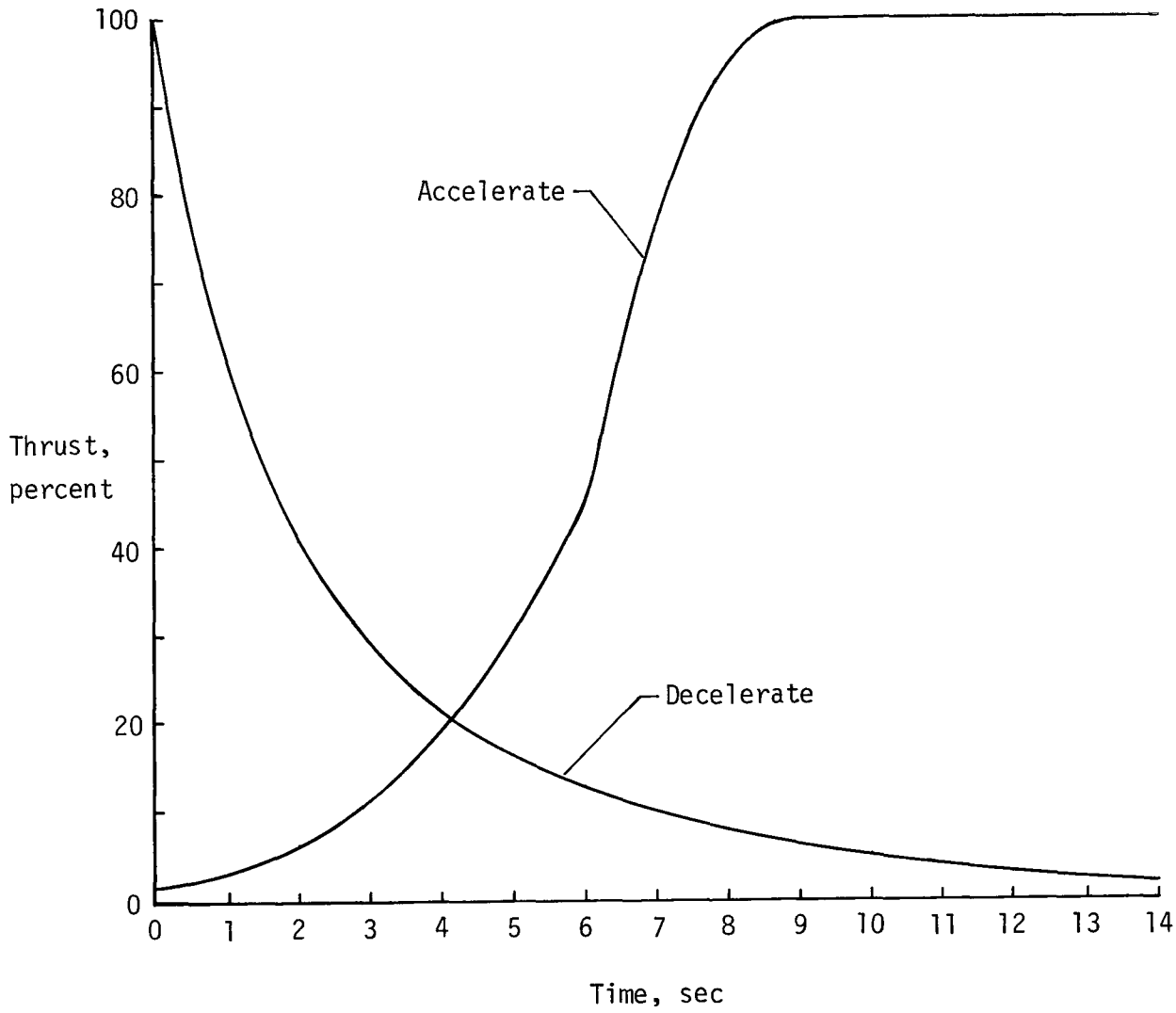

Figure 3.- Example of engine thrust response characteristics used in simulation of twin-fuselage transport airplane.

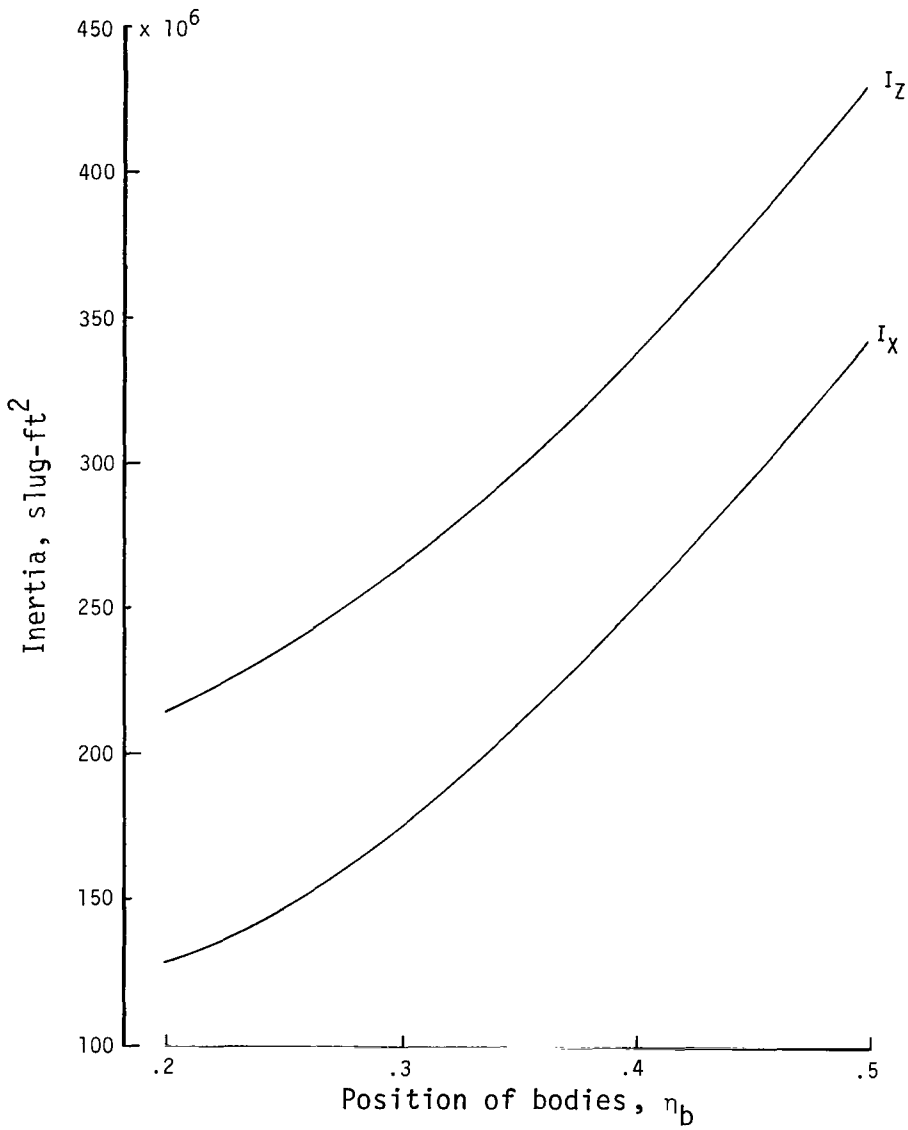

(a) Variation of roll and yaw inertias.

Figure 4.- Effect of spanwise location of fuselages on aircraft inertias and aileron control effectiveness.

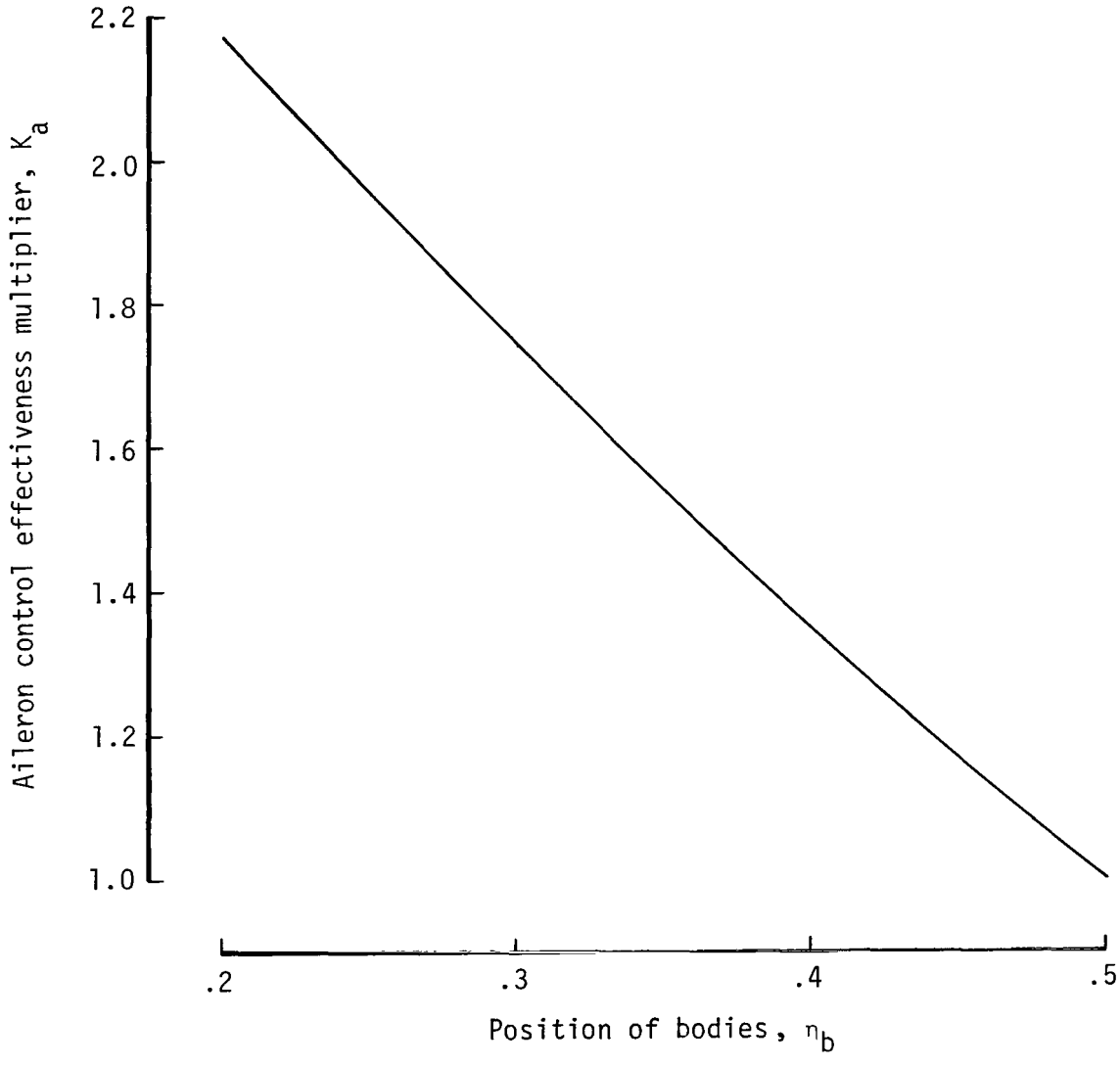

(b) Maximum variation of aileron control effectiveness multiplier K_a.

Figure 4.- Concluded.

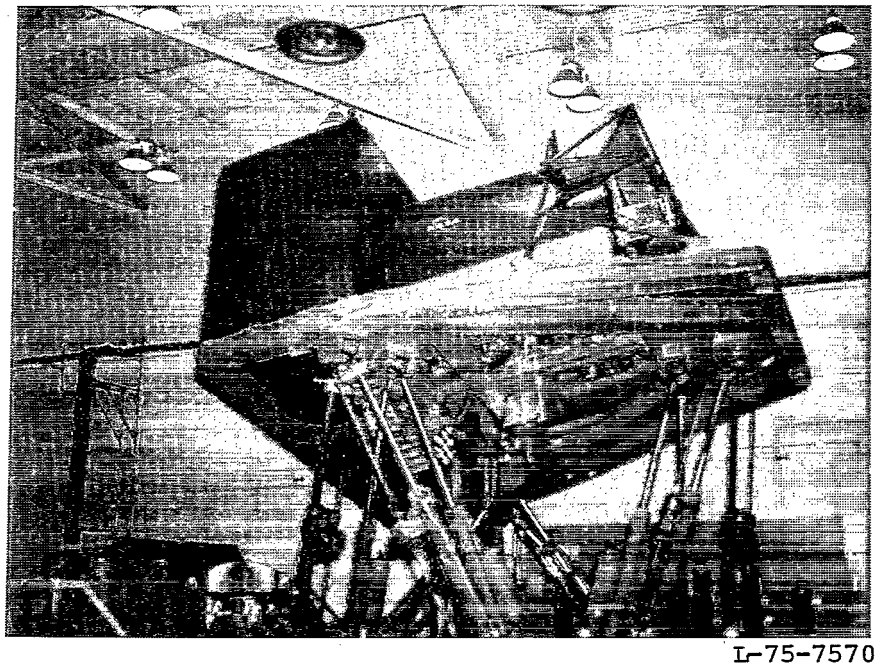

L-75-7570

(a) Langley Visual/Motion Simulator.

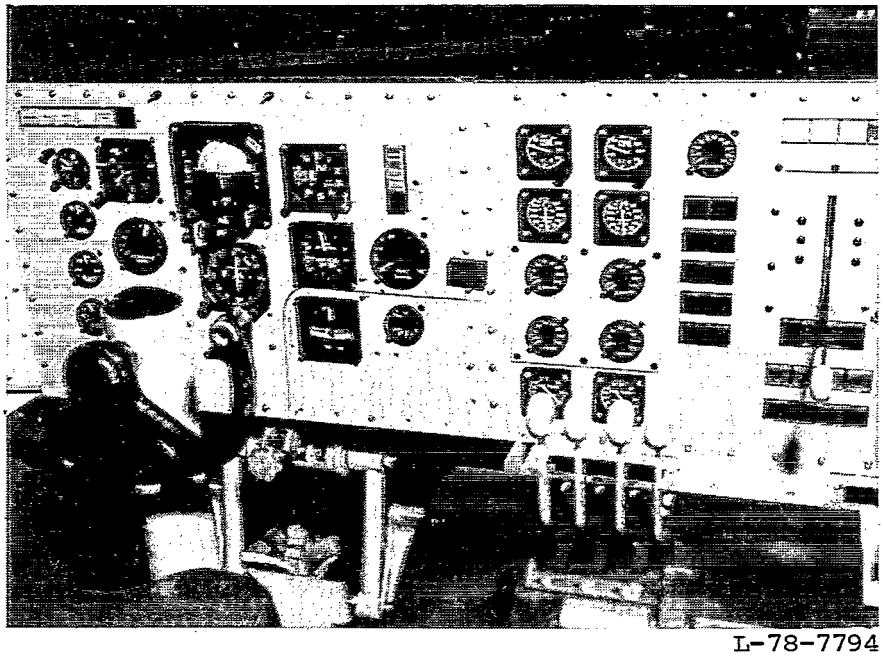

L-78-7794

(b) Instrument panel.

Figure 5.- Langley Visual/Motion Simulator and instrument panel display.

CONVENTIONAL AIRCRAFT

Single fuselage on axis of symmetry

TWIN-FUSELAGE AIRCRAFT

Fuselage located at 0.5 wing semispan

Fuselage located at 0.2 wing semispan

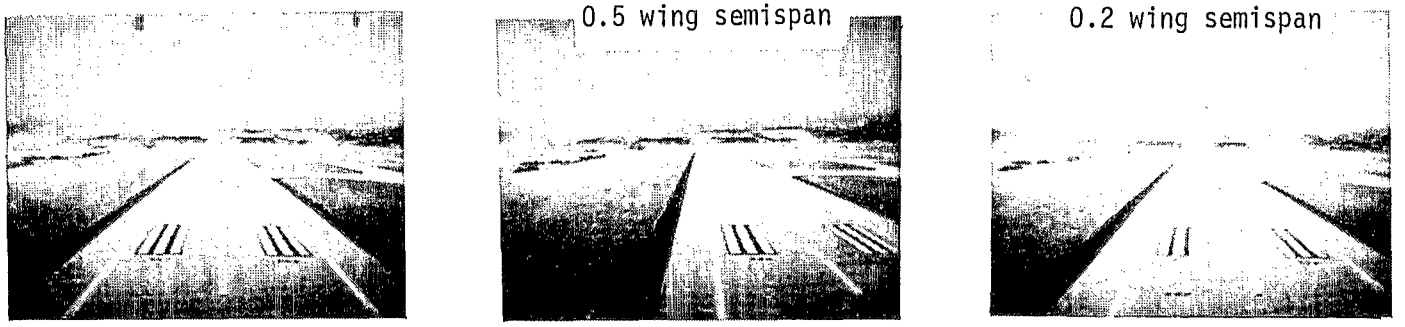

(a) Lateral offset from runway, 0; height of landing gear, 50 ft.

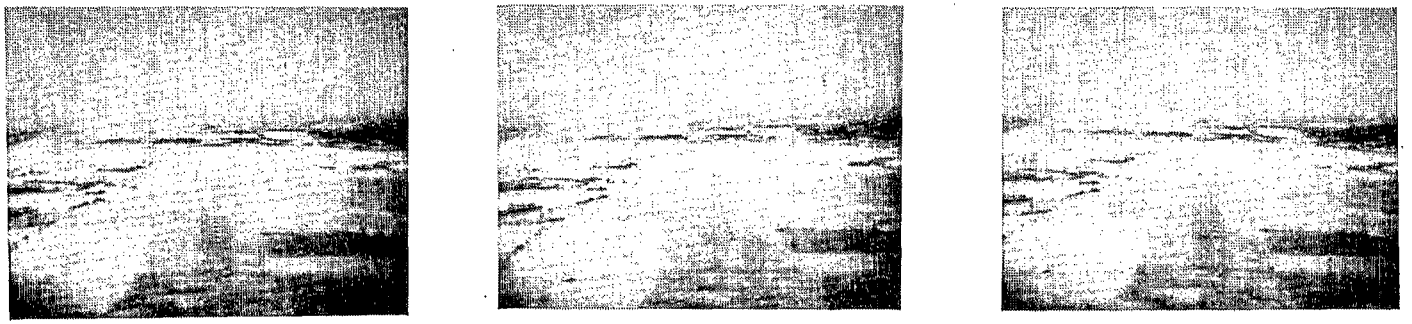

(b) Lateral offset from runway, 0; height of landing gear, 300 ft.

(c) Lateral offset from runway, -200 ft; height of landing gear, 300 ft.

L-83-107

Figure 6.- View of airport scene as observed by pilot.

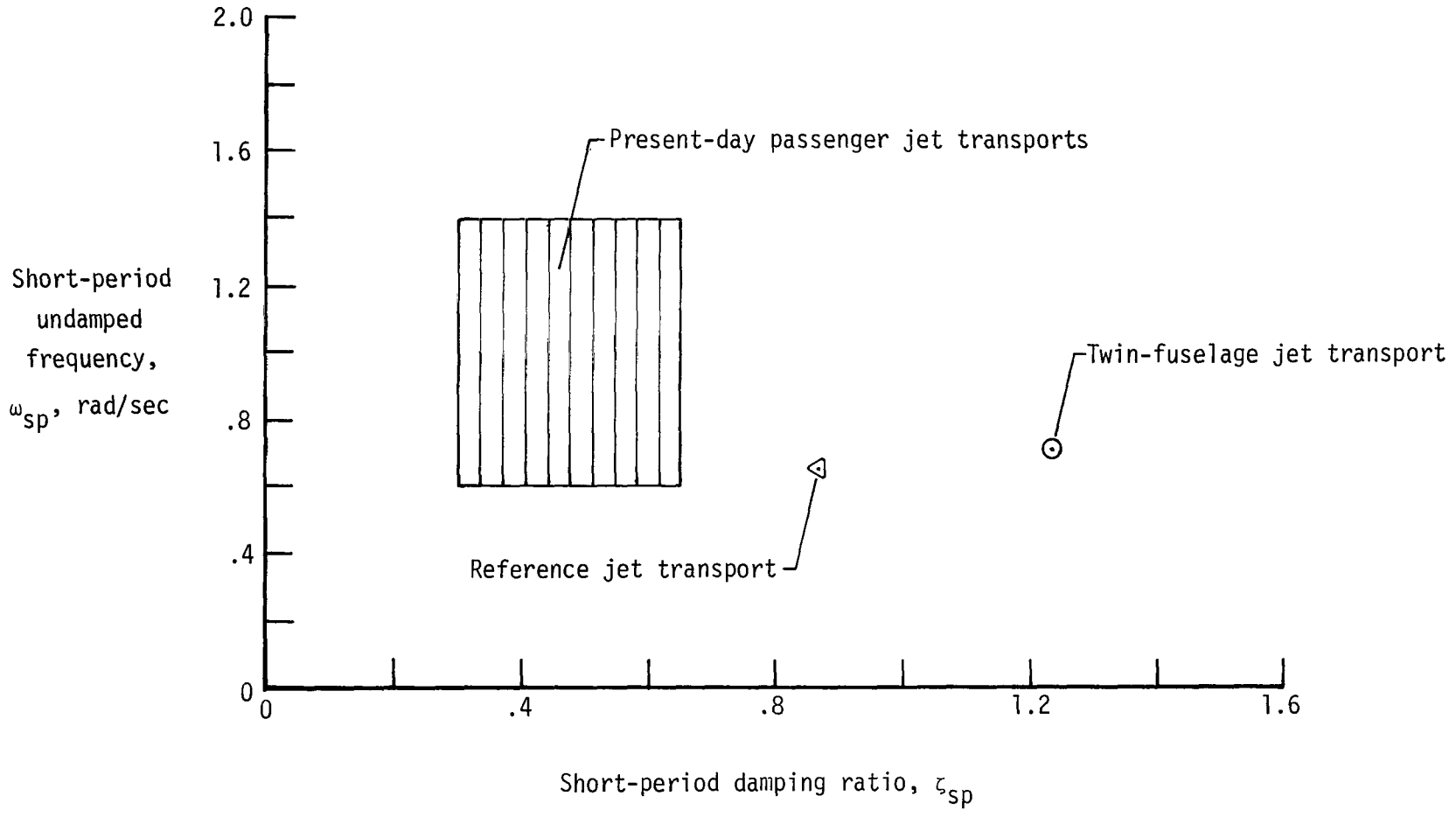

Figure 7.- Comparison of short-period frequency and damping ratio of unaugmented twin-fuselage and reference transport configurations with some present-day passenger jet transports.

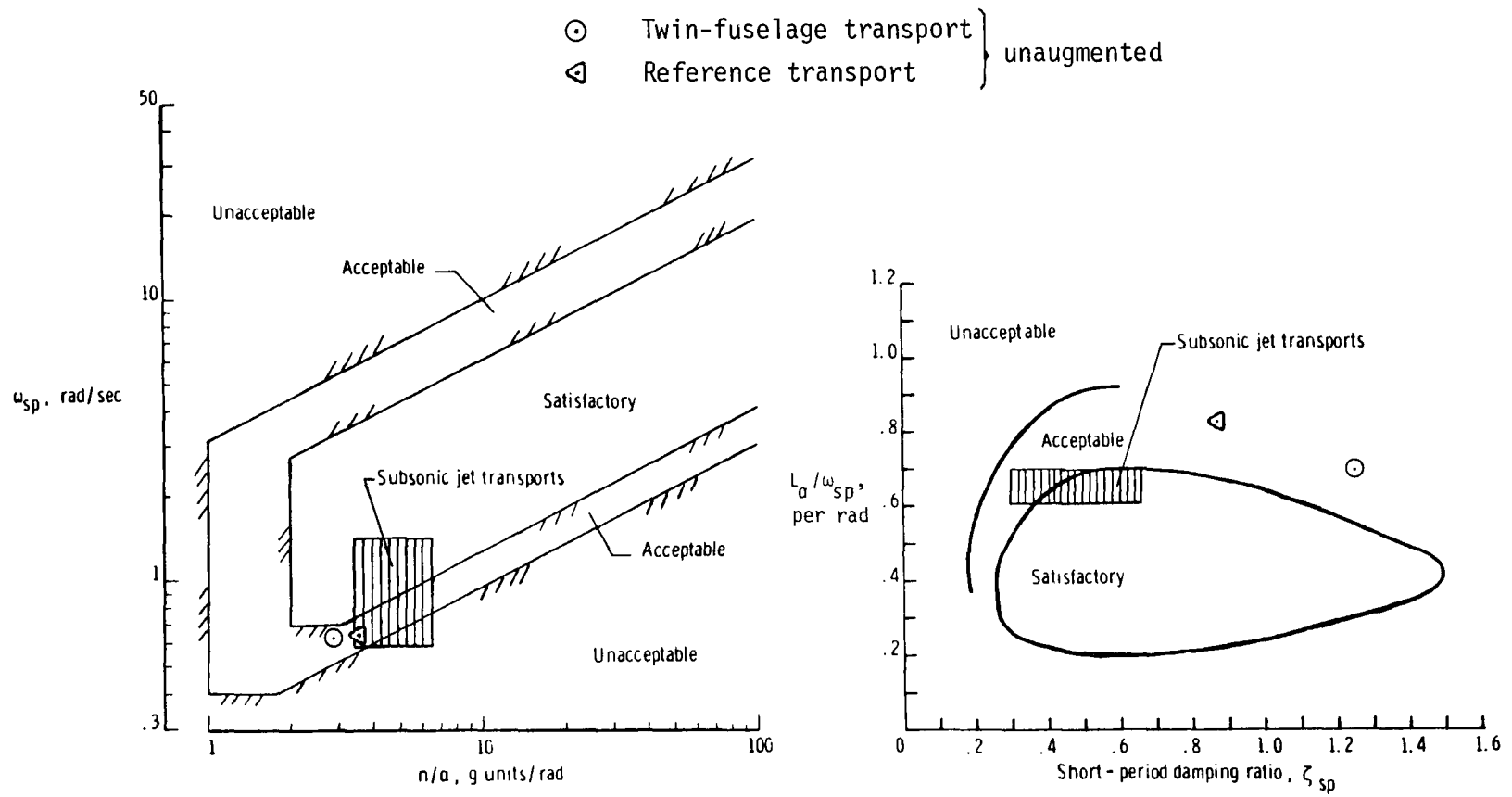

(a) Criterion from reference 4.

(b) Criterion from reference 5.

Figure 8.- Comparison of unaugmented longitudinal characteristics of simulated twin-fuselage and reference transport concepts with various handling qualities criteria.

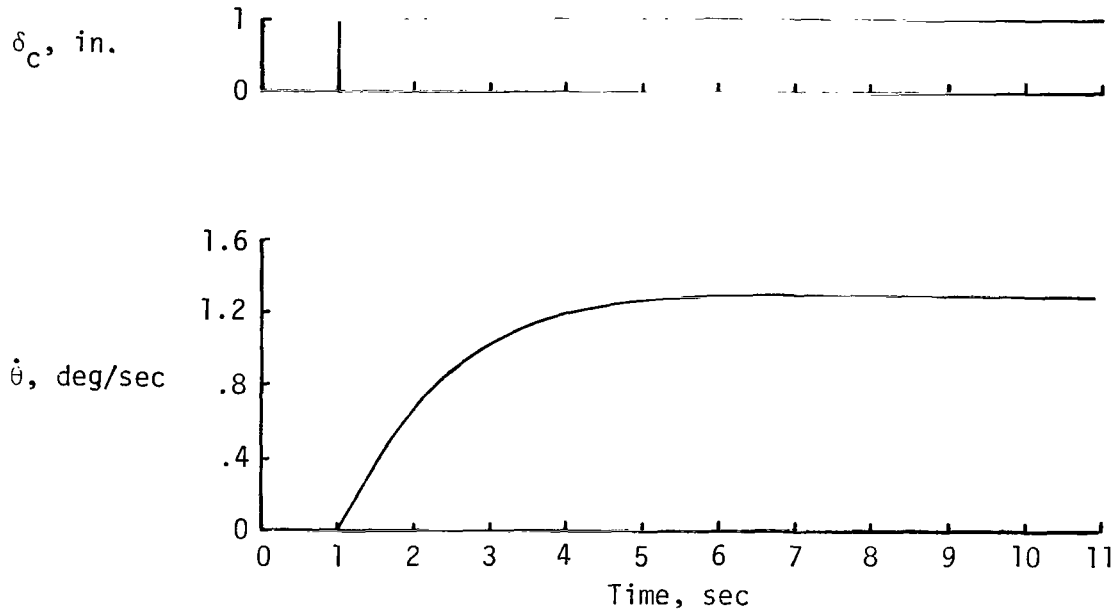

(a) Column step input.

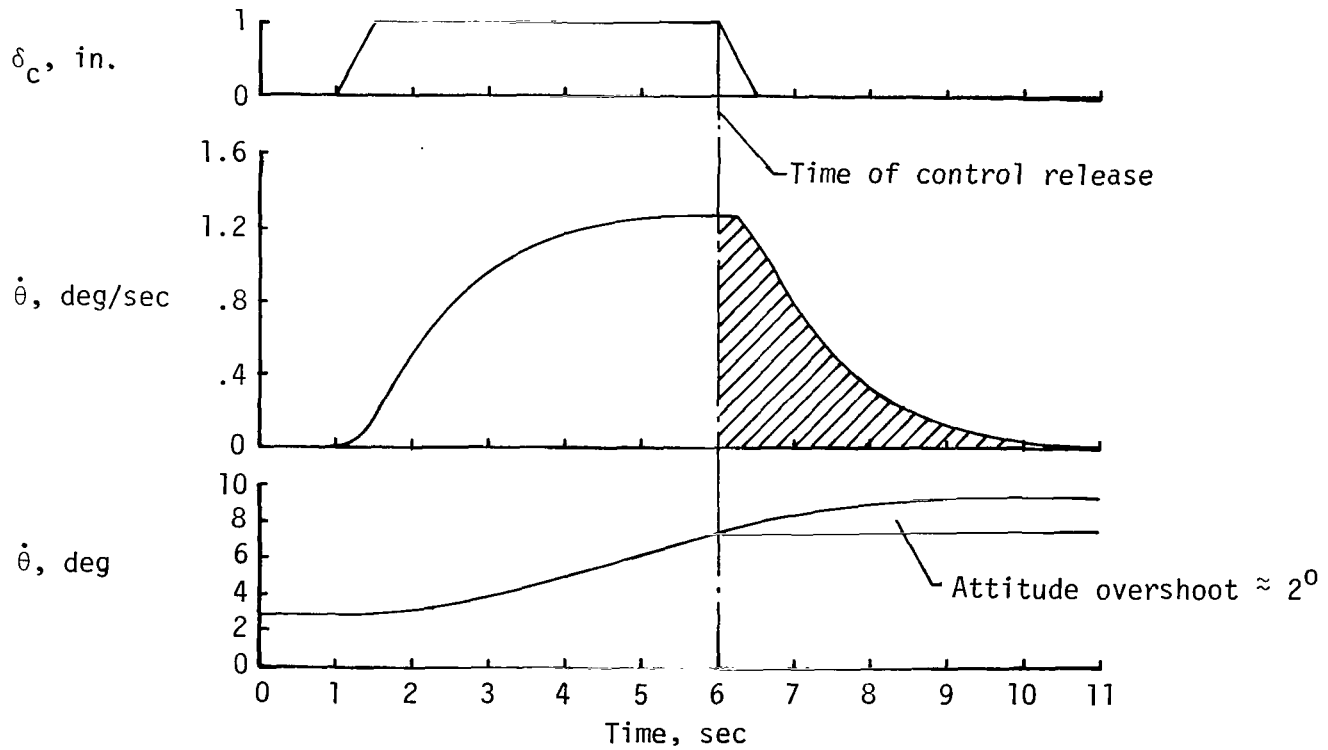

(b) Column pulse input.

Figure 9.- Indication of pitch response to various column inputs.

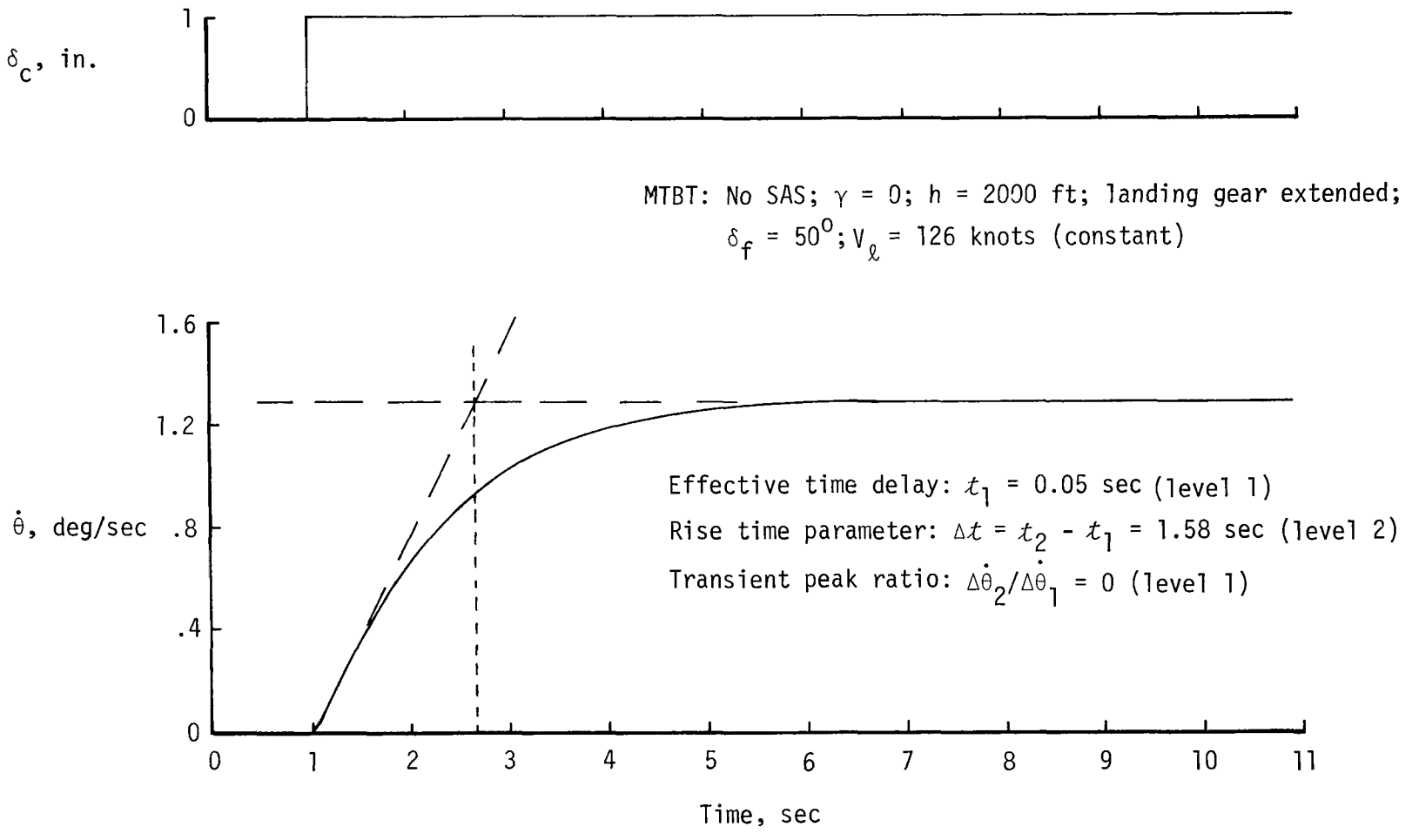

Figure 10.- Pitch-rate response to a column step input on unaugmented twin-fuselage transport airplane.

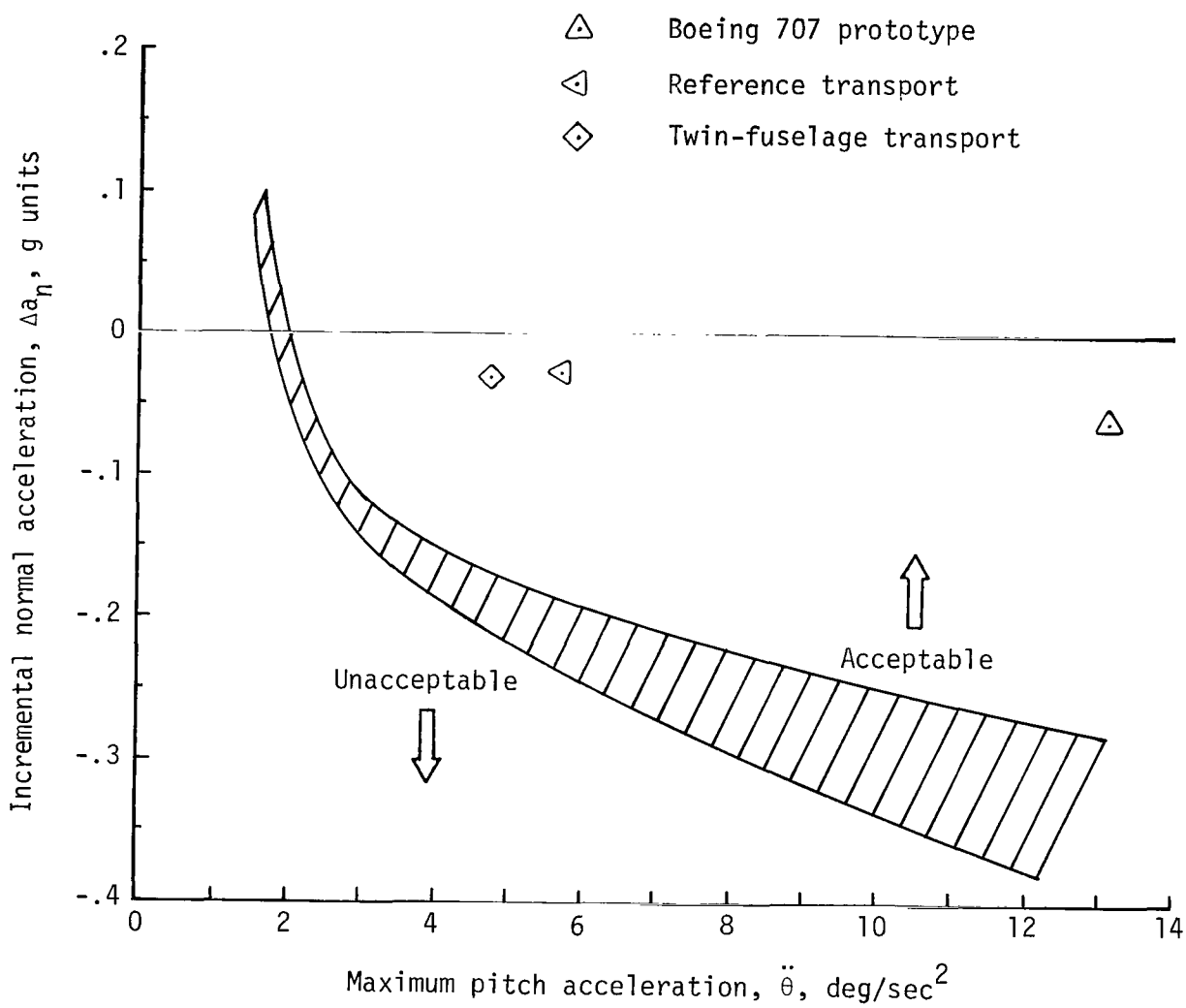

Figure 11.- Comparison of longitudinal control characteristics of simulated transport concepts with control requirements of reference 7.

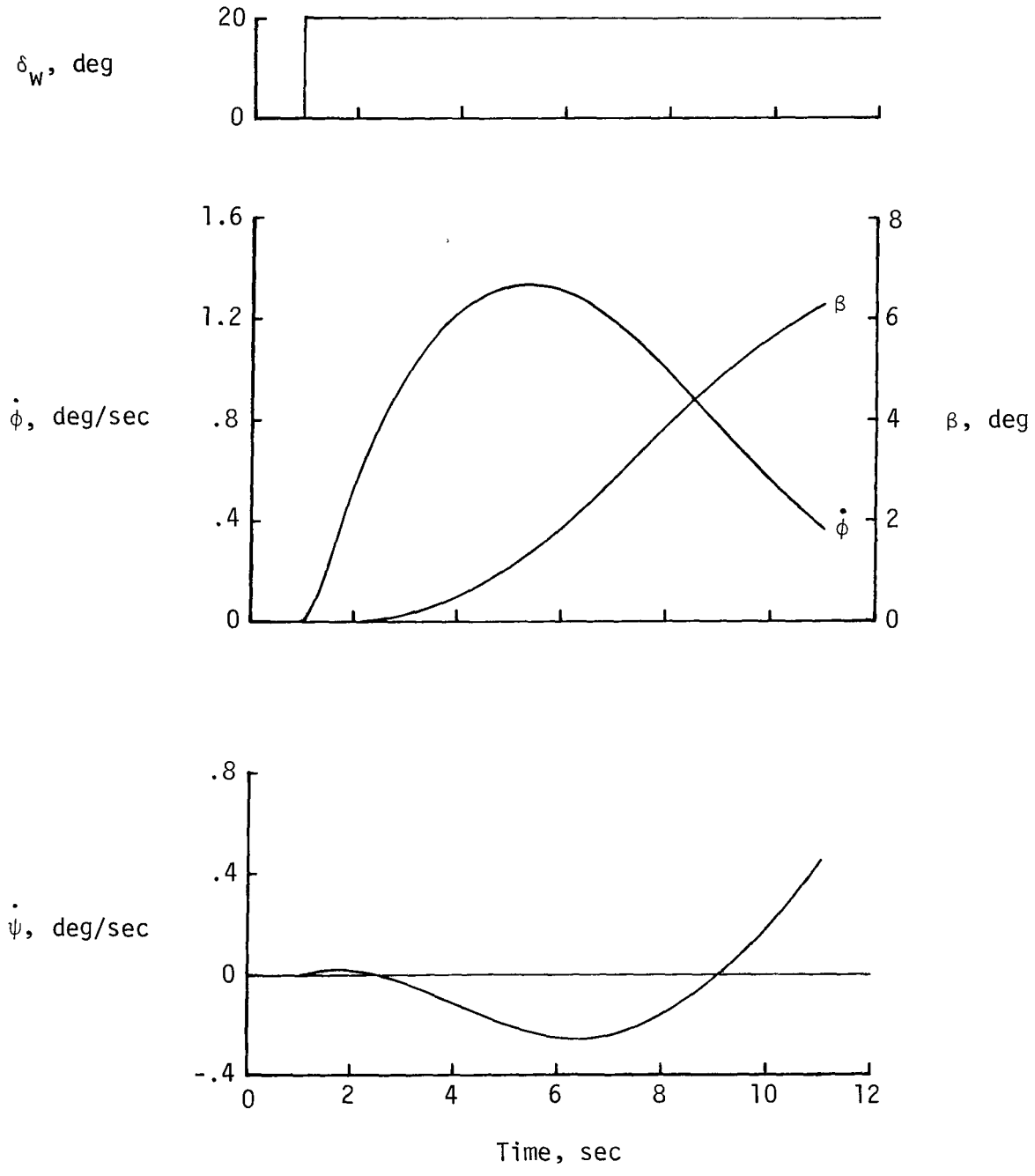

Figure 12.- Lateral-directional response to a step wheel input on unaugmented twin-fuselage transport airplane.

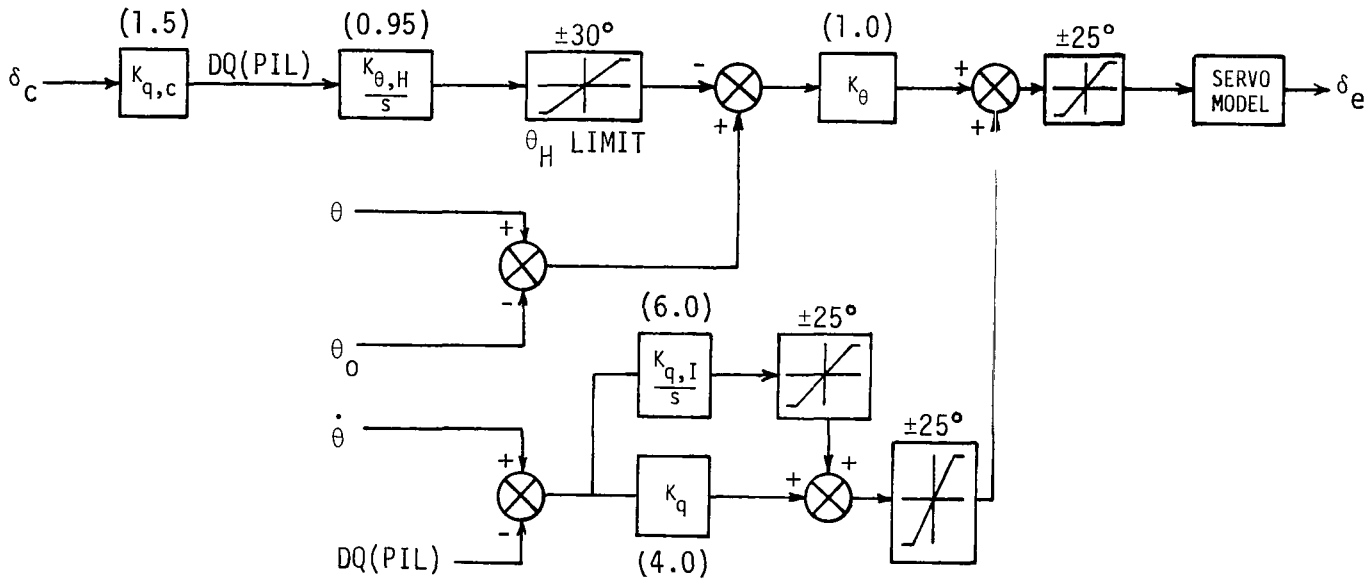

(a) Longitudinal (pitch) control system.

Figure 13.- Normal operational stability and control augmentation system (SCAS). SCAS gains (table VIII) are indicated in parentheses.

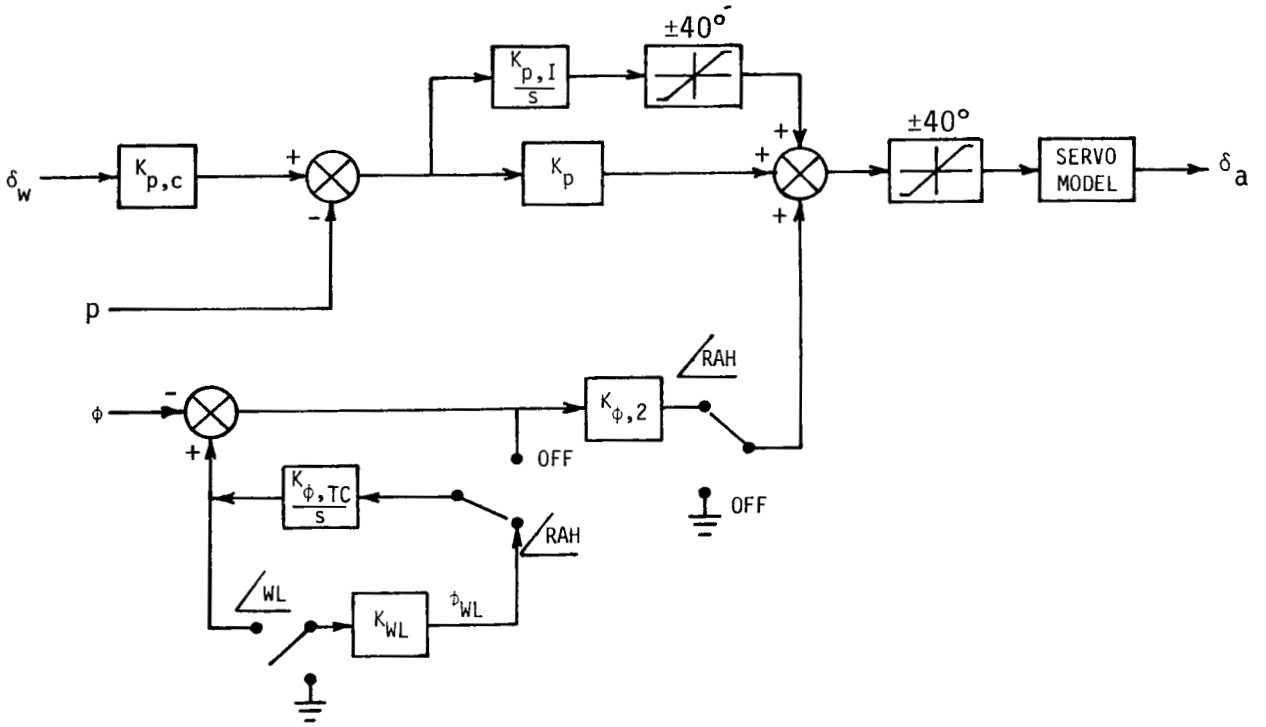

(b) Lateral (roll) control system.

Figure 13.- Continued.

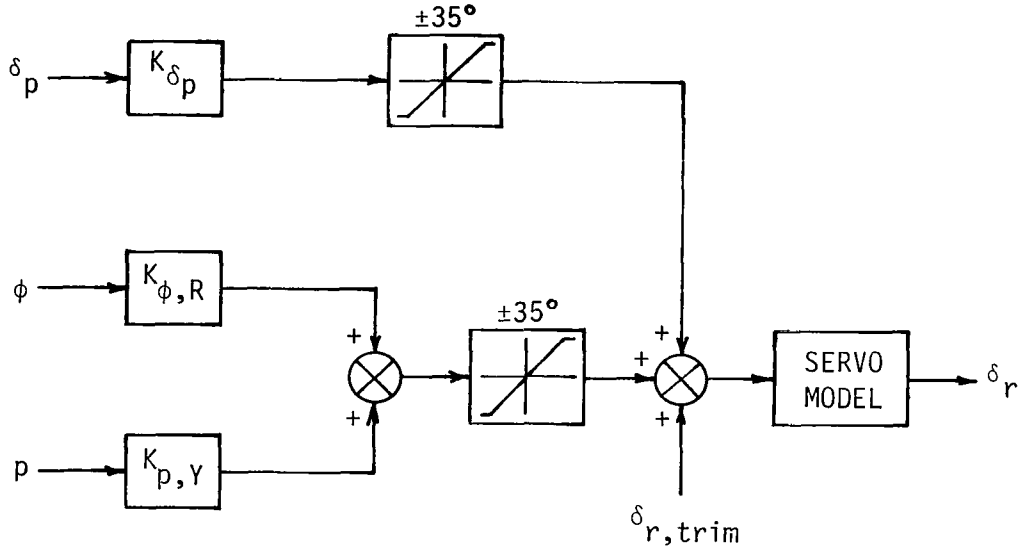

(c) Directional (yaw) control system.

Figure 13.- Concluded.

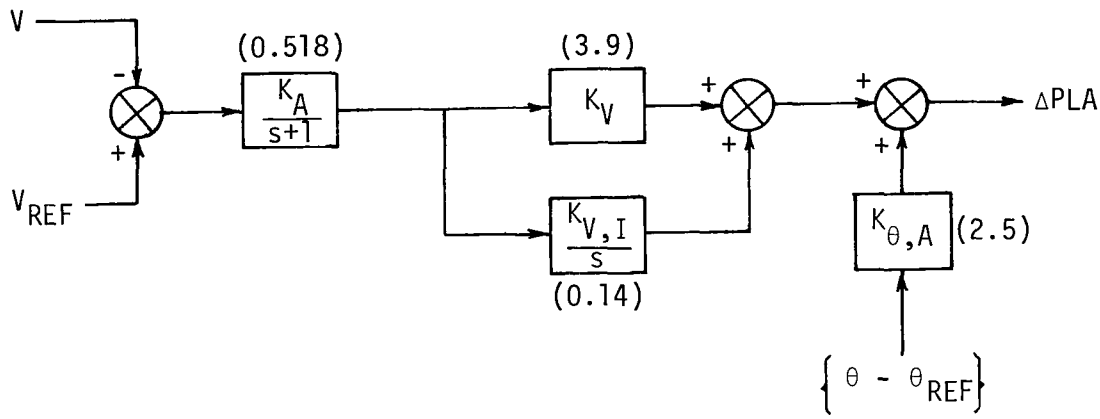

Figure 14.- Block diagram of autothrottle for twin-fuselage configuration. Gains are indicated in parentheses.

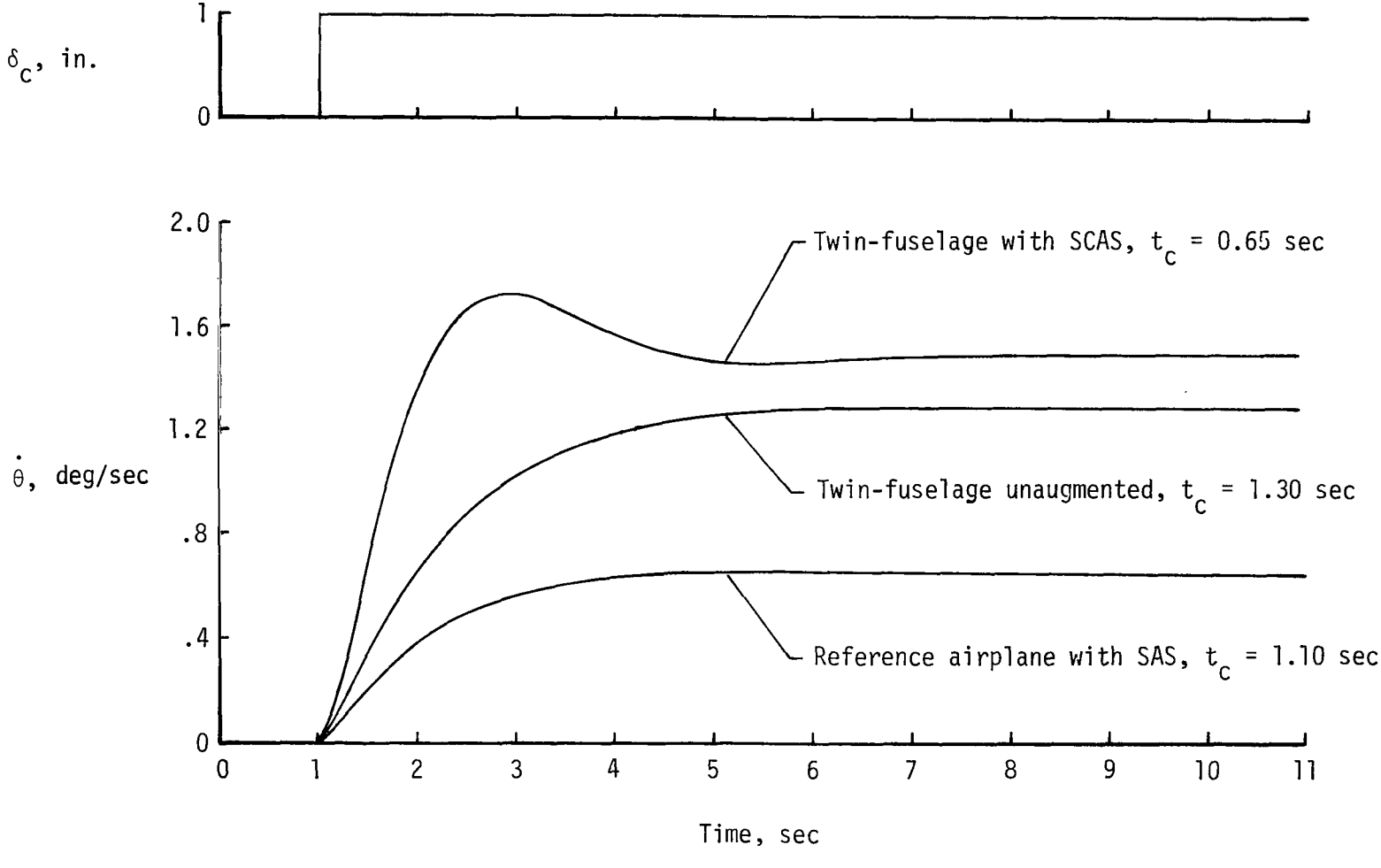

Figure 15.- Comparison of pitch-rate response for unaugmented and augmented twin-fuselage configurations and reference (augmented) transport airplane.

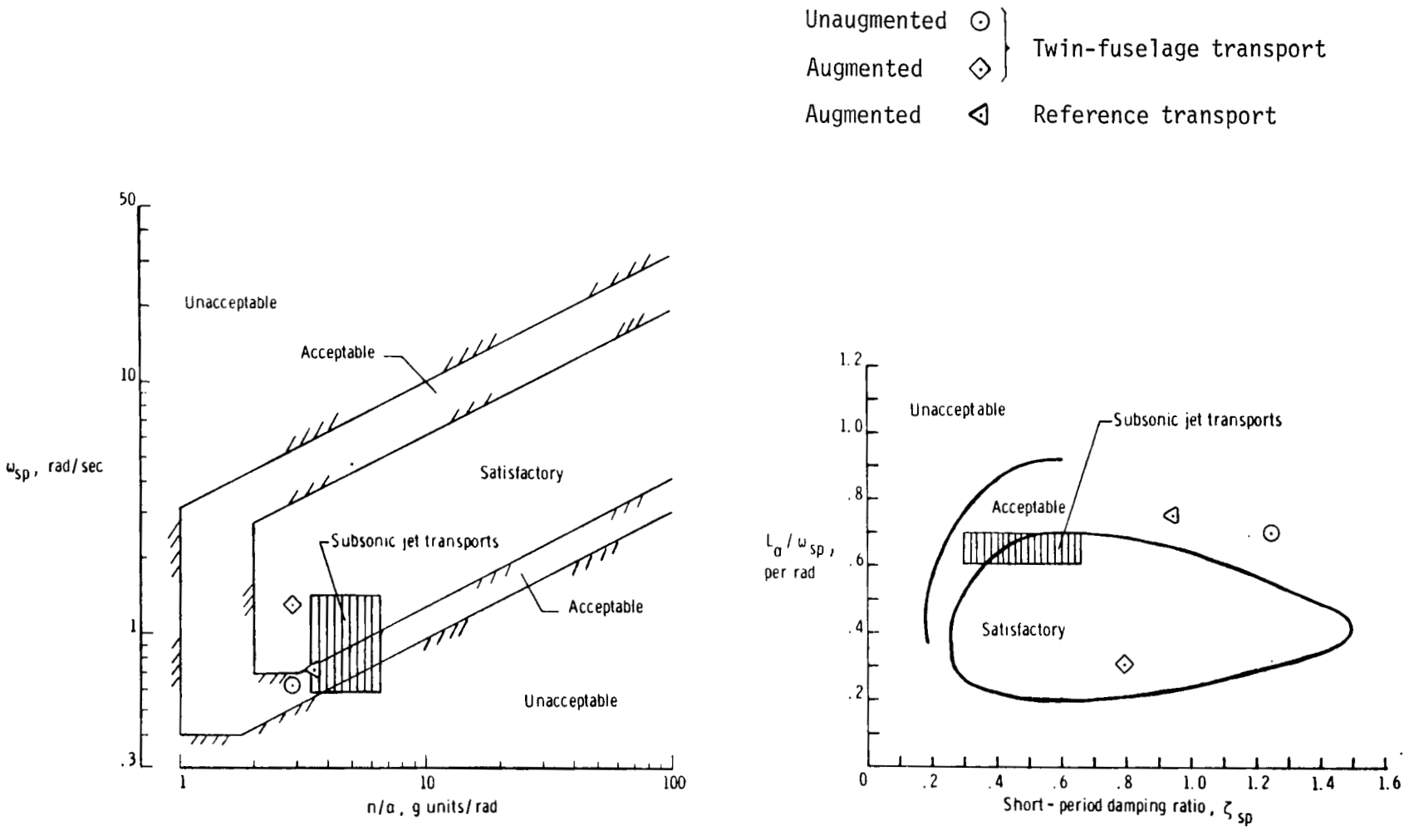

(a) Short-period frequency criterion of reference 4.

(b) Longitudinal handling qualities criterion of reference 5.

Figure 16.- Comparison of unaugmented and augmented twin-fuselage configurations and reference airplane (augmented) with short-period criteria of references 4 and 5.

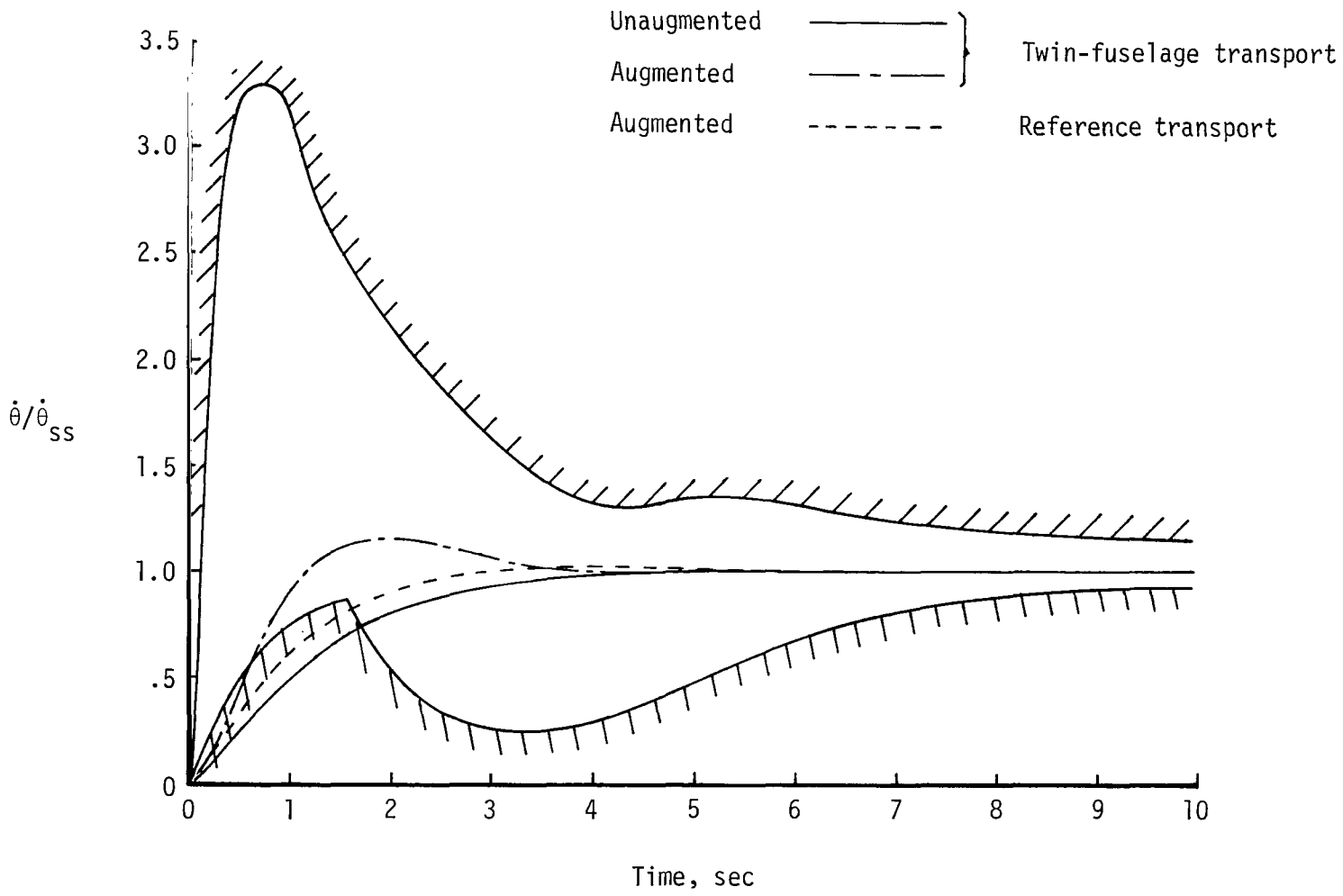

Figure 17.- Low-speed pitch-rate response criterion of reference 8. Boundaries for normal operation (PR ≤ 3.5).

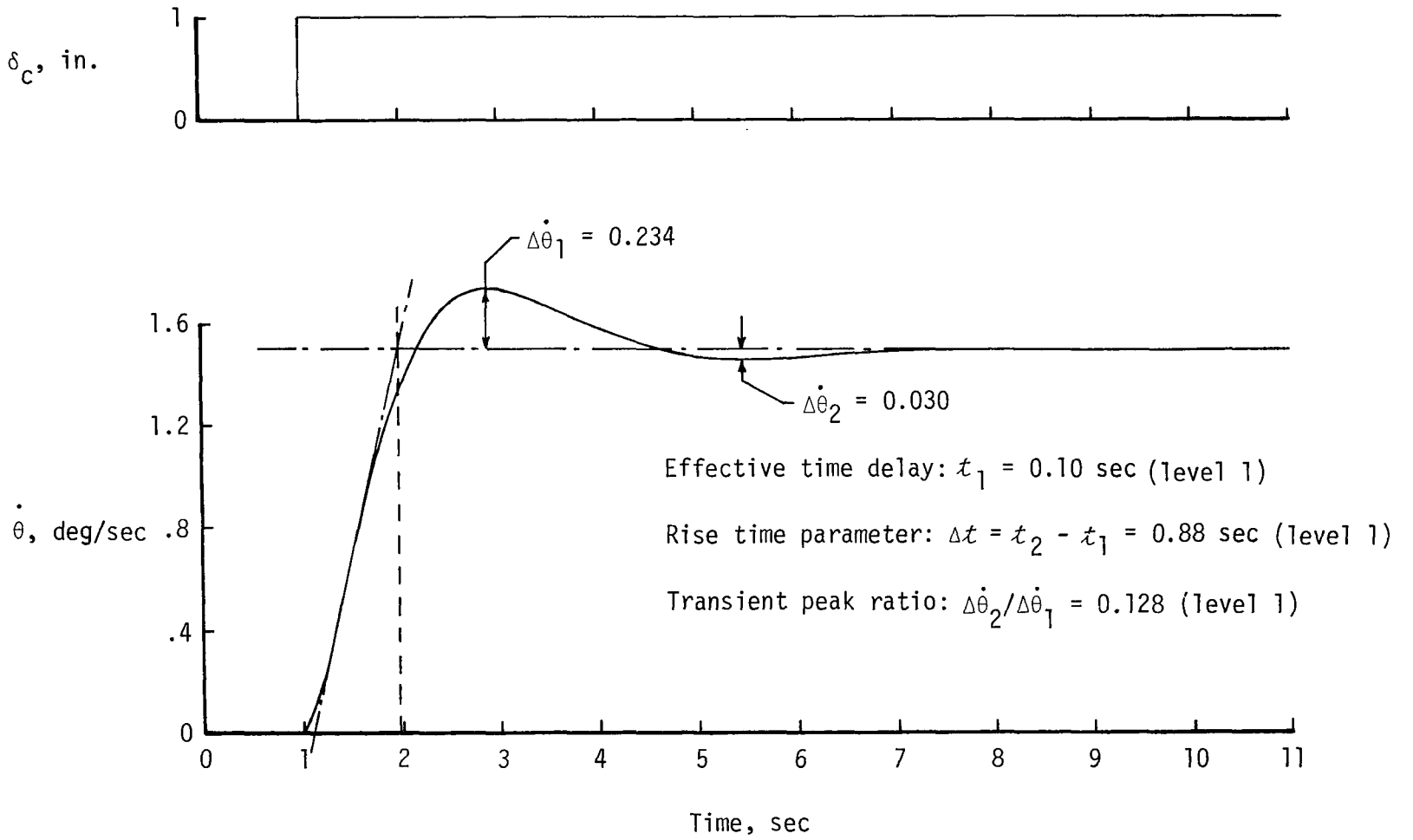

Figure 18.- Pitch-rate response to column step input on augmented twin-fuselage transport. (Criteria from ref. 6.)

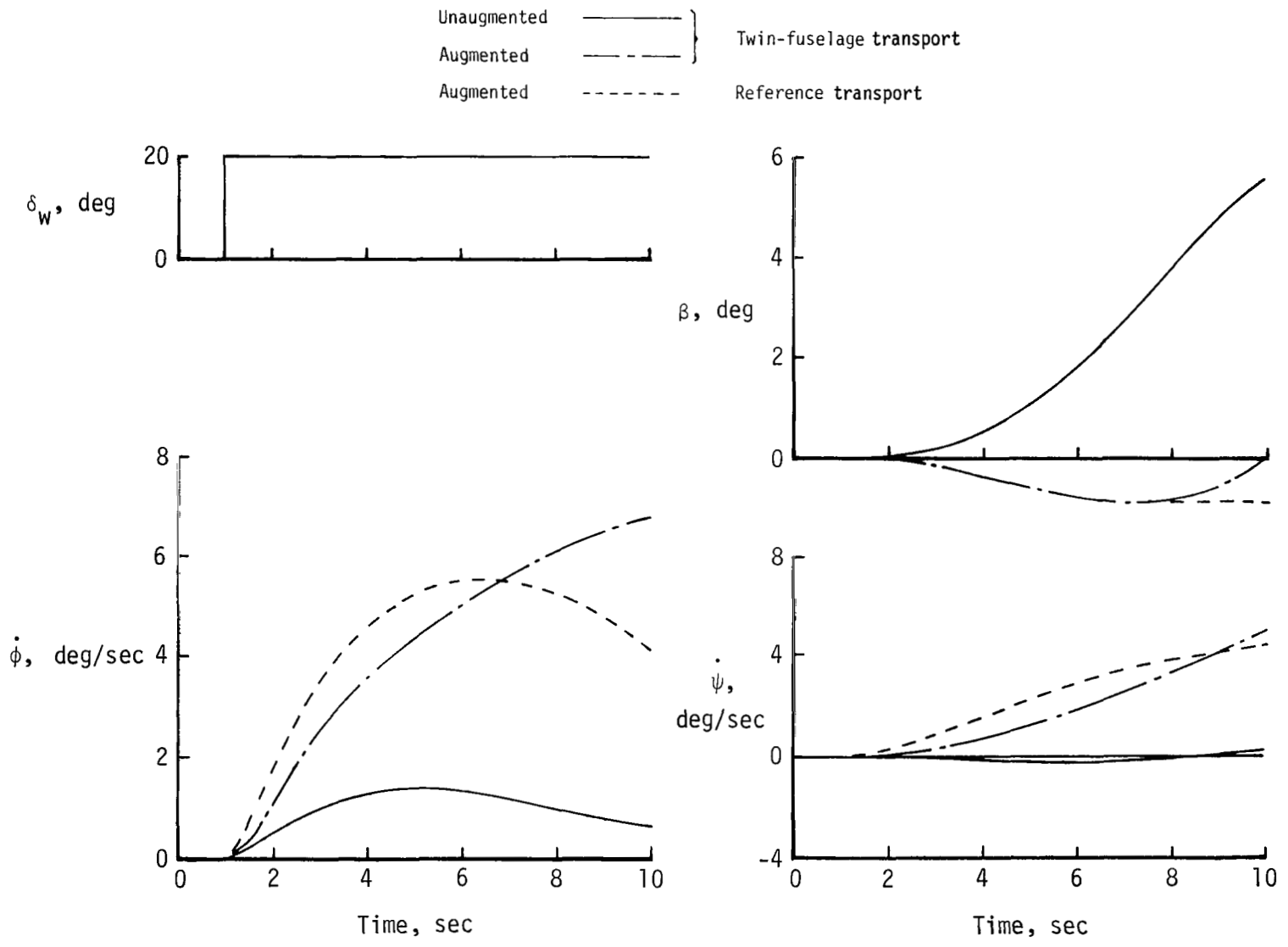

Figure 19.- Lateral-directional response to a step wheel input on unaugmented and augmented twin-fuselage airplane and reference airplane (augmented).

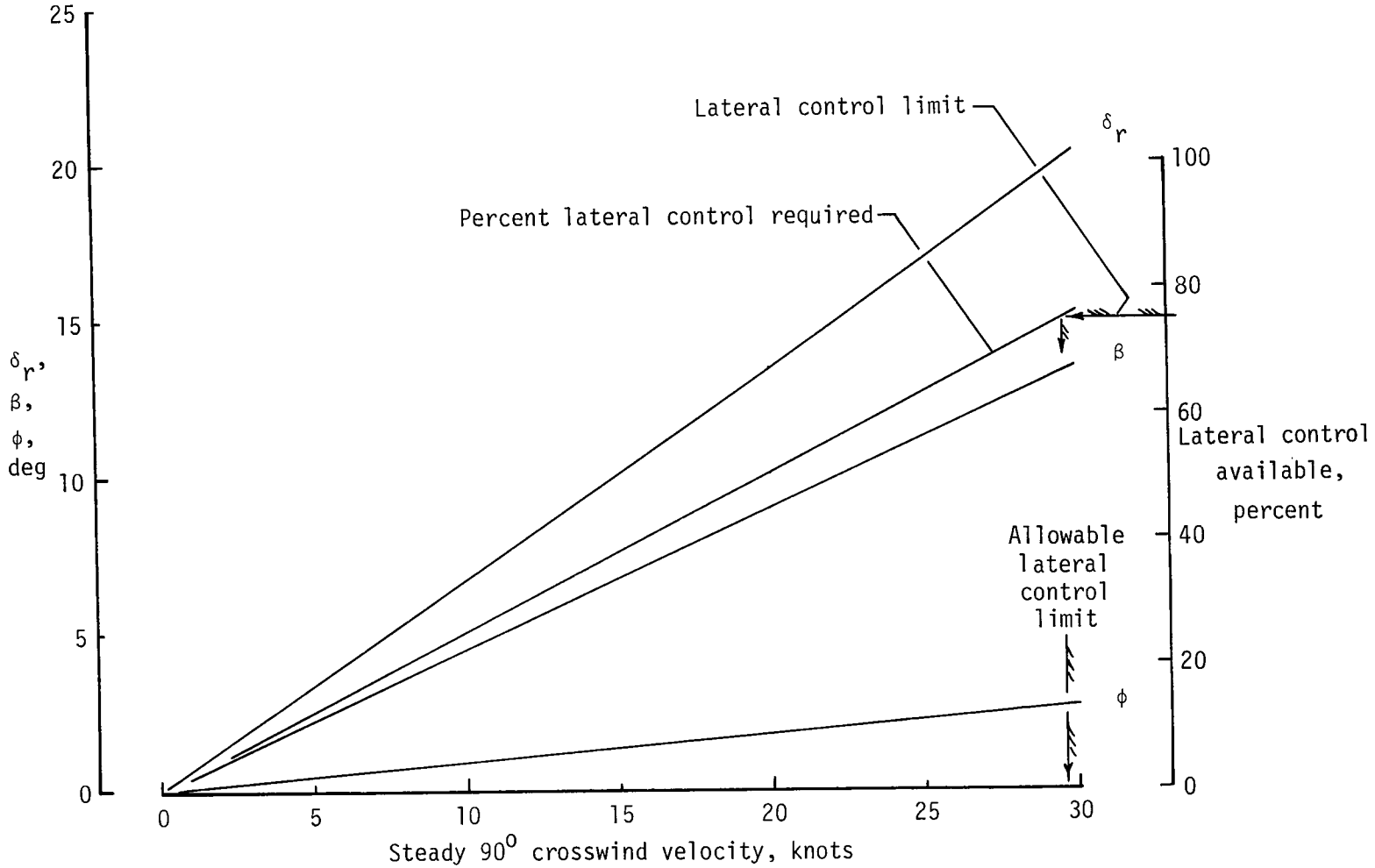

Figure 20.- Indication of crosswind trim capability of simulated twin-fuselage transport.

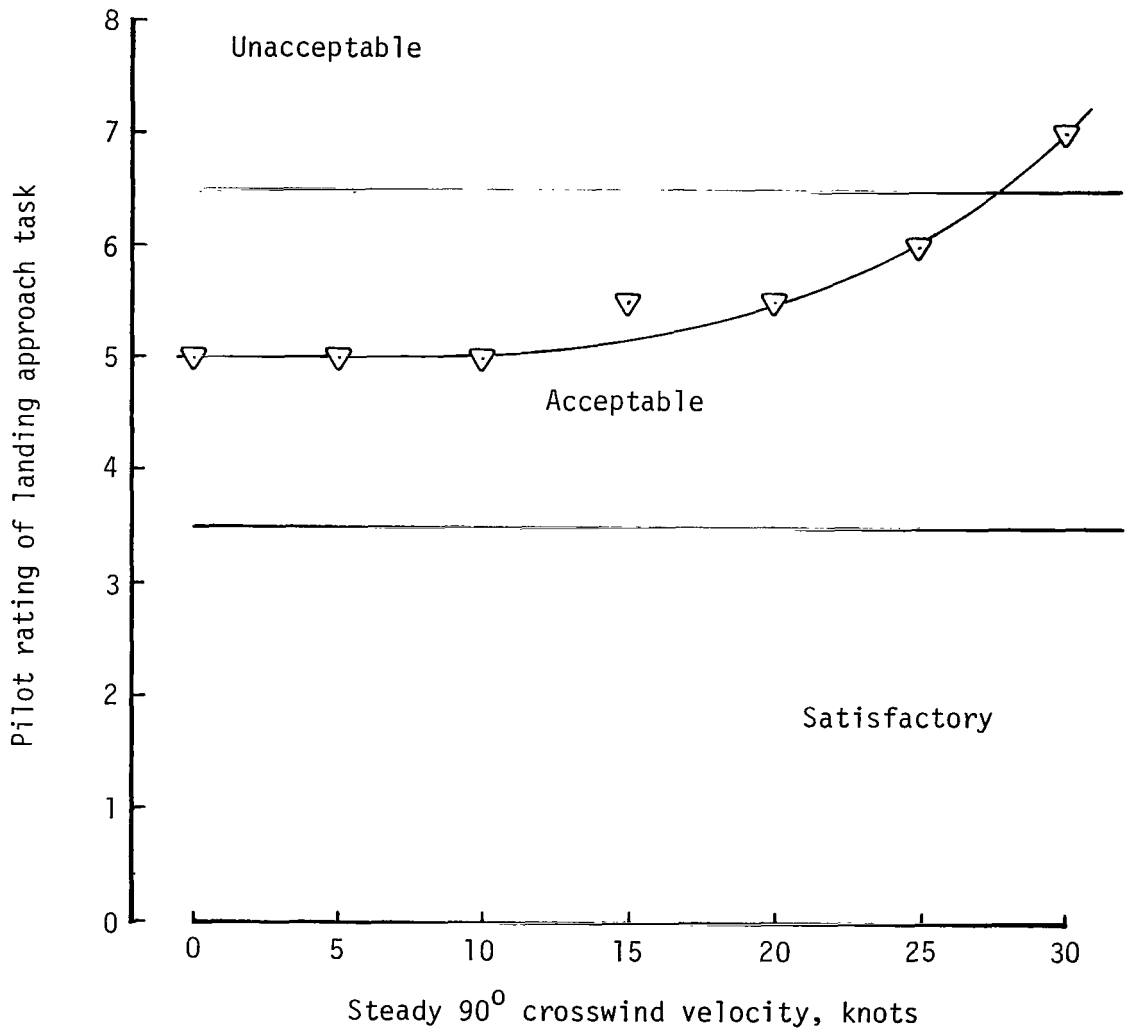

Figure 21.- Indication of pilots' ability to safely land in 90° crosswinds. $\eta_b = 0.5$; $\delta_f = 50°$; $V_\ell = 126$ knots.

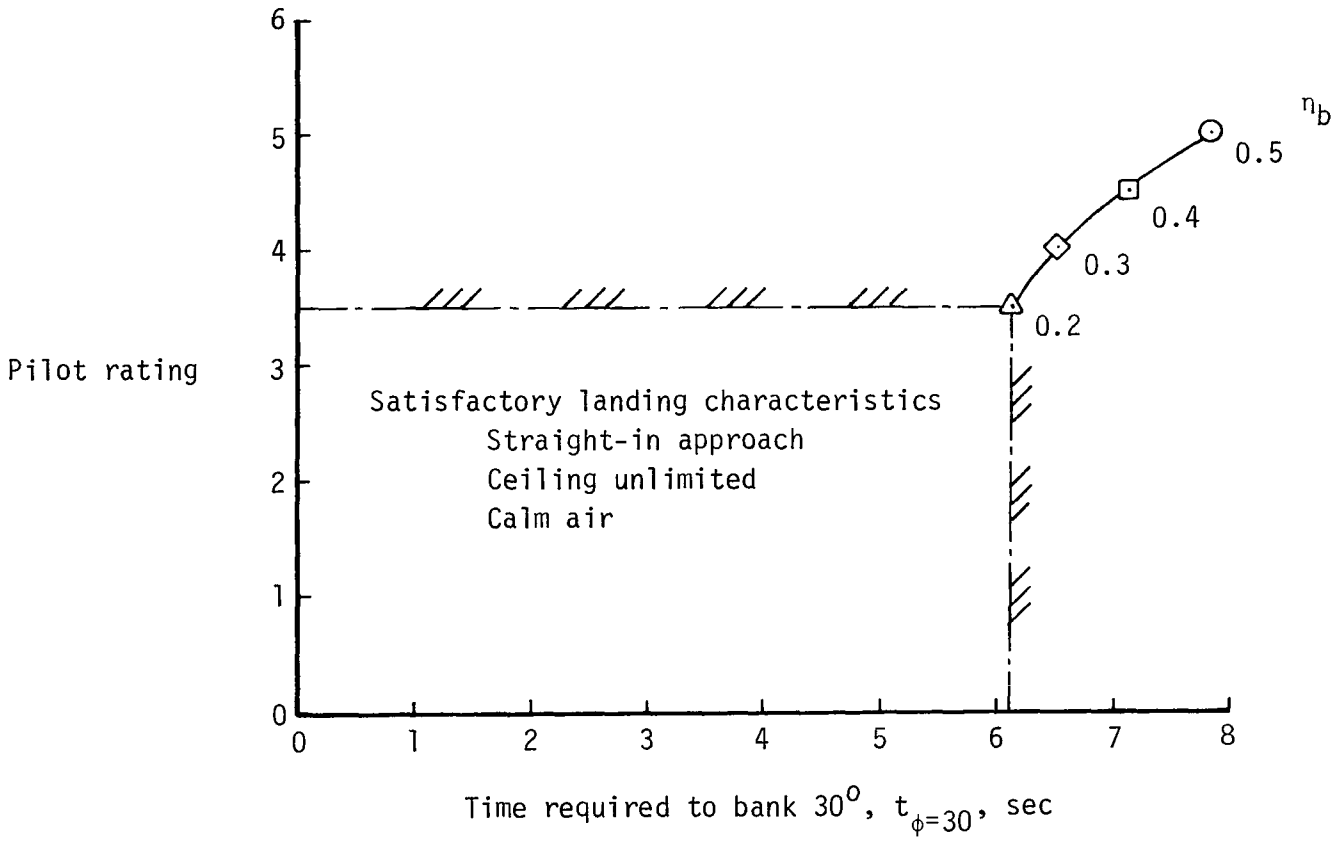

Figure 22.- Indication of average pilot ratings assigned to augmented twin-fuselage concept for various fuselage locations along the wing span with basic ailerons.

Open symbols - landing configuration and speed, and various landing tasks
Solid symbols - approach configuration and speed, and various airwork tasks

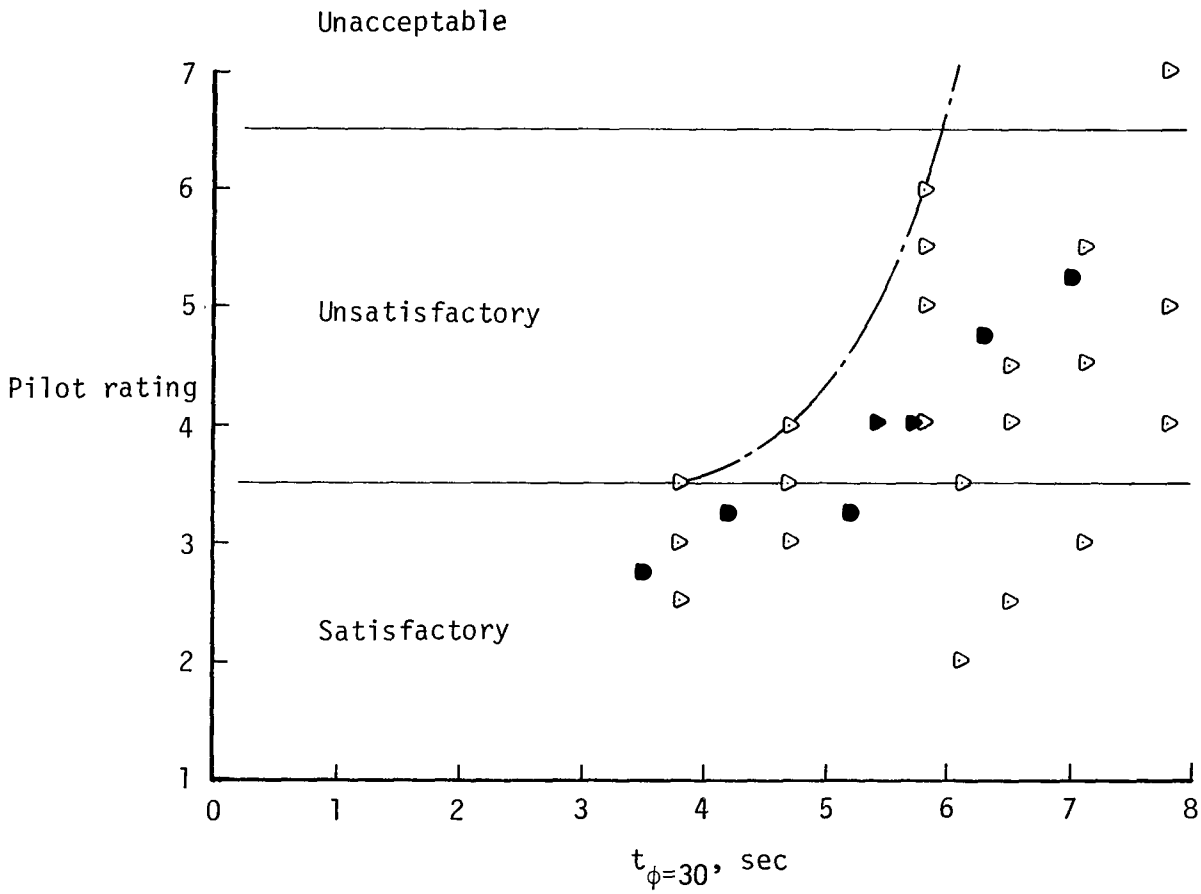

Figure 23.- Summary of roll performance from various approach and landing tasks simulated.

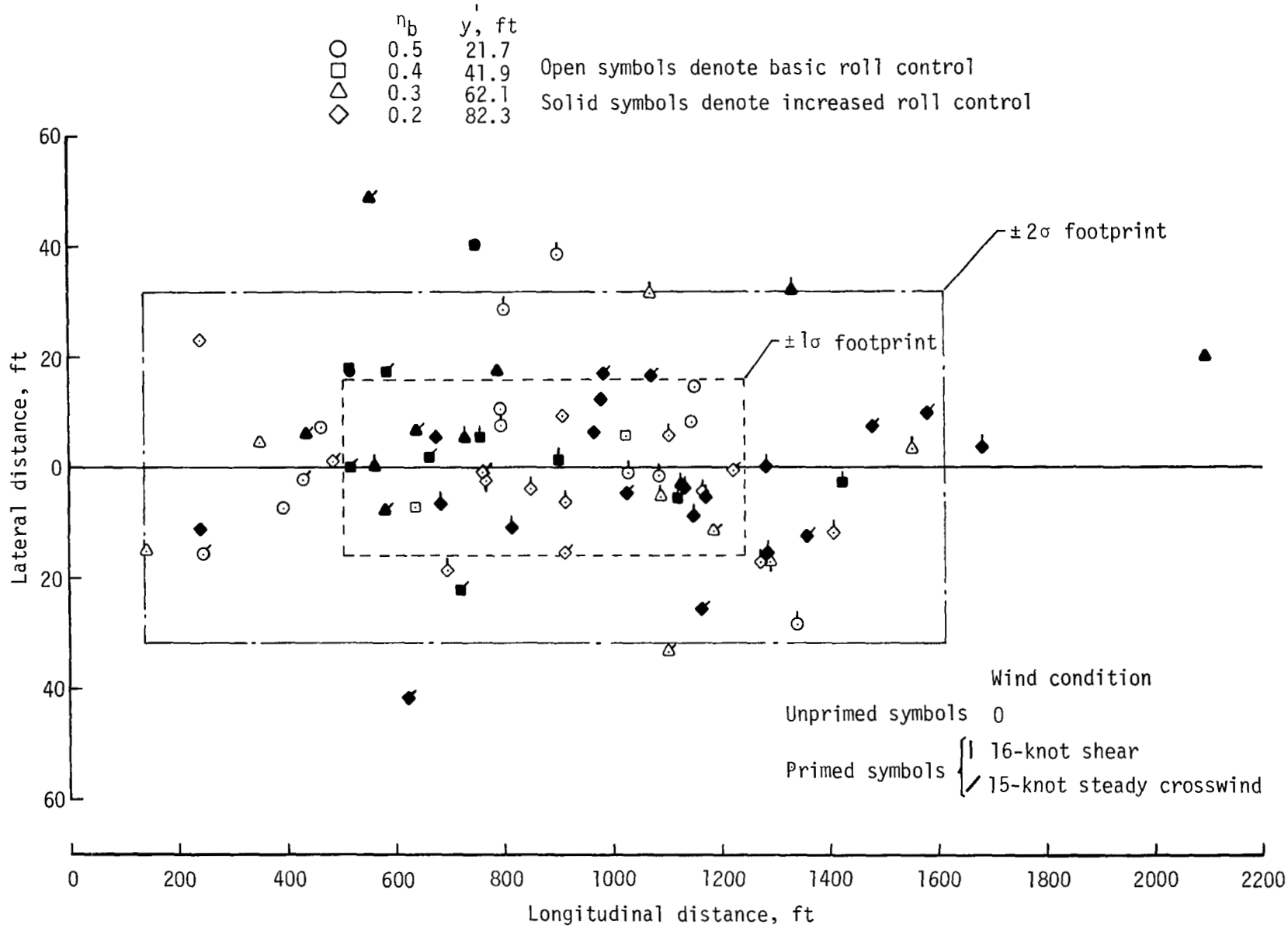

Figure 24.- Lateral and longitudinal dispersion of touchdown points. (Zero index on the longitudinal scale is the point at which the glide slope intercepts the runway.)

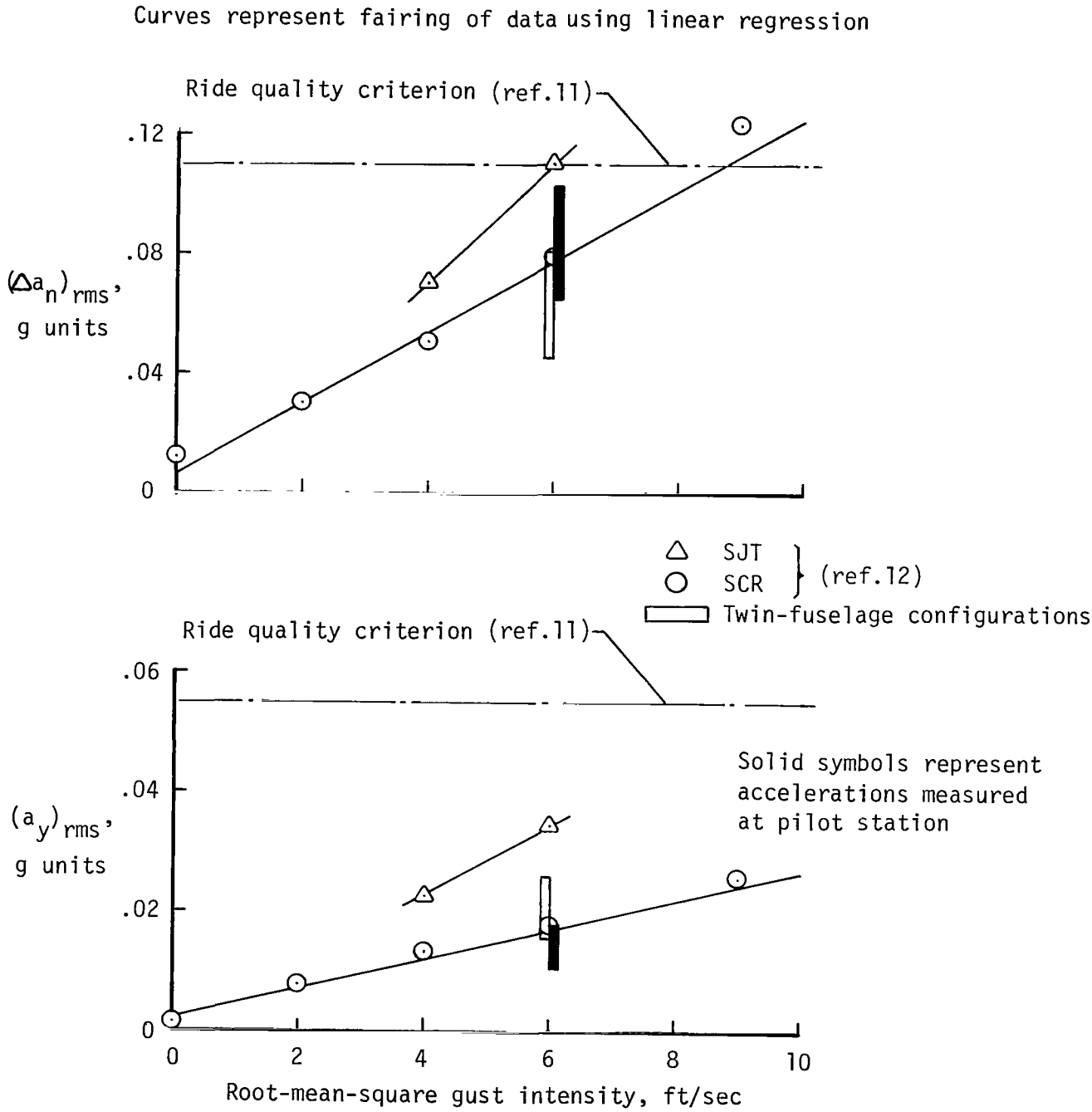

Figure 25.- Acceleration responses during landing approaches in various levels of turbulence. (Accelerations measured at aircraft center of gravity except where noted.)

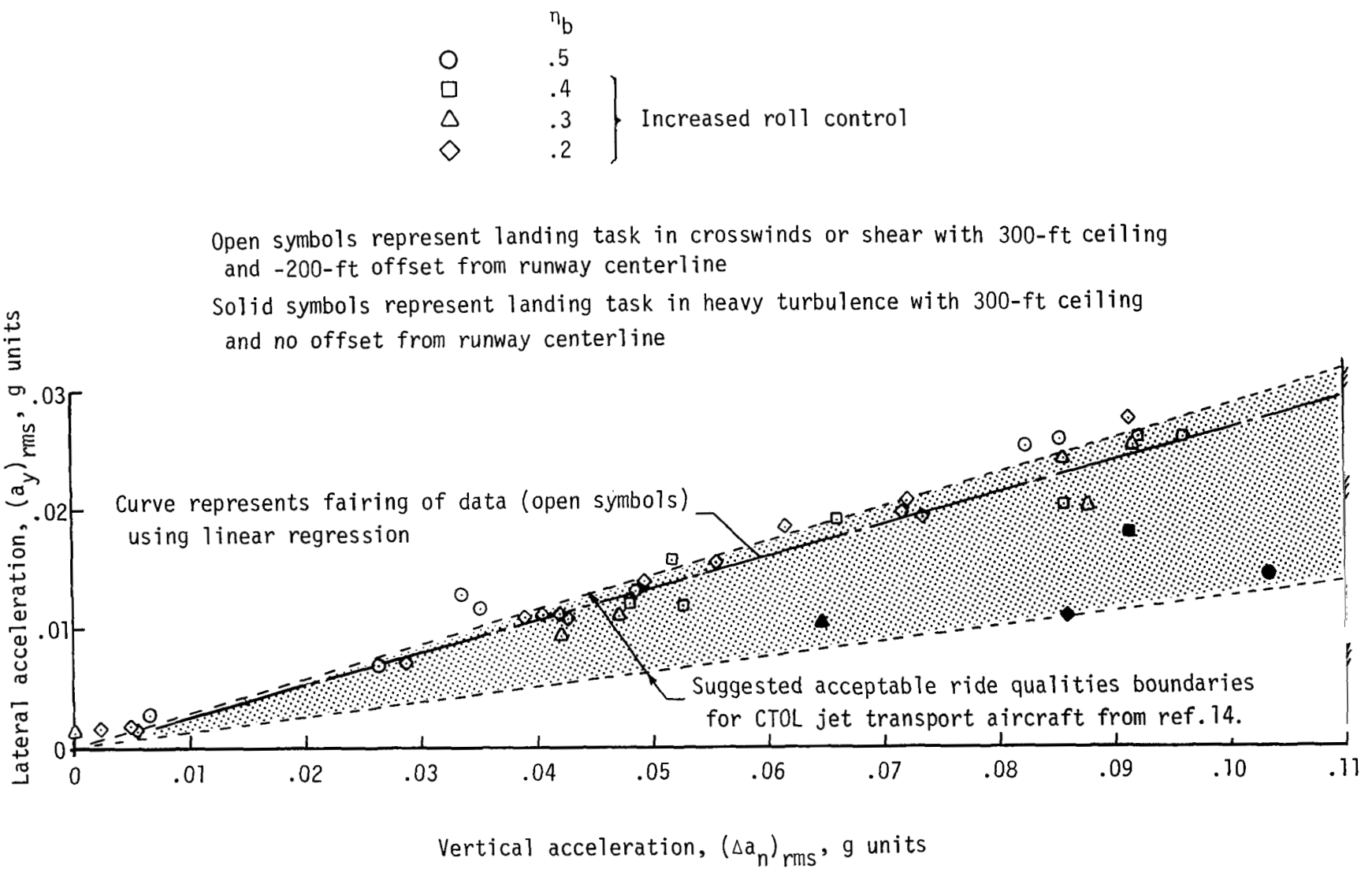

Figure 26.- Acceleration responses, measured at pilot station, during landing task on various twin-fuselage configurations.

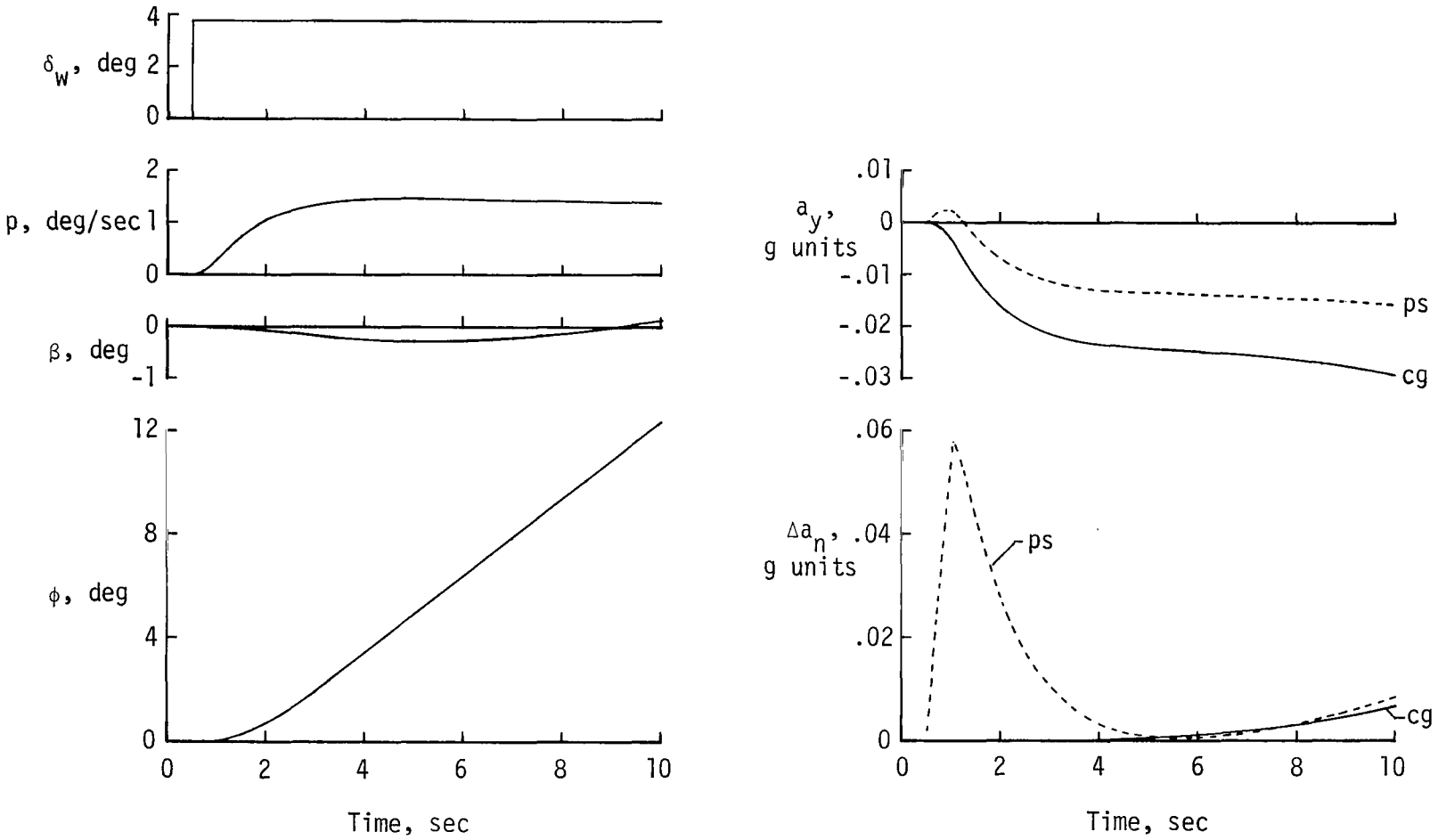

Figure 27.- Calculated lateral and normal acceleration response to a wheel step input. $\eta_b = 0.5$; $V_\ell = 126$ knots; $\delta_f = 50°$; SCAS operative.

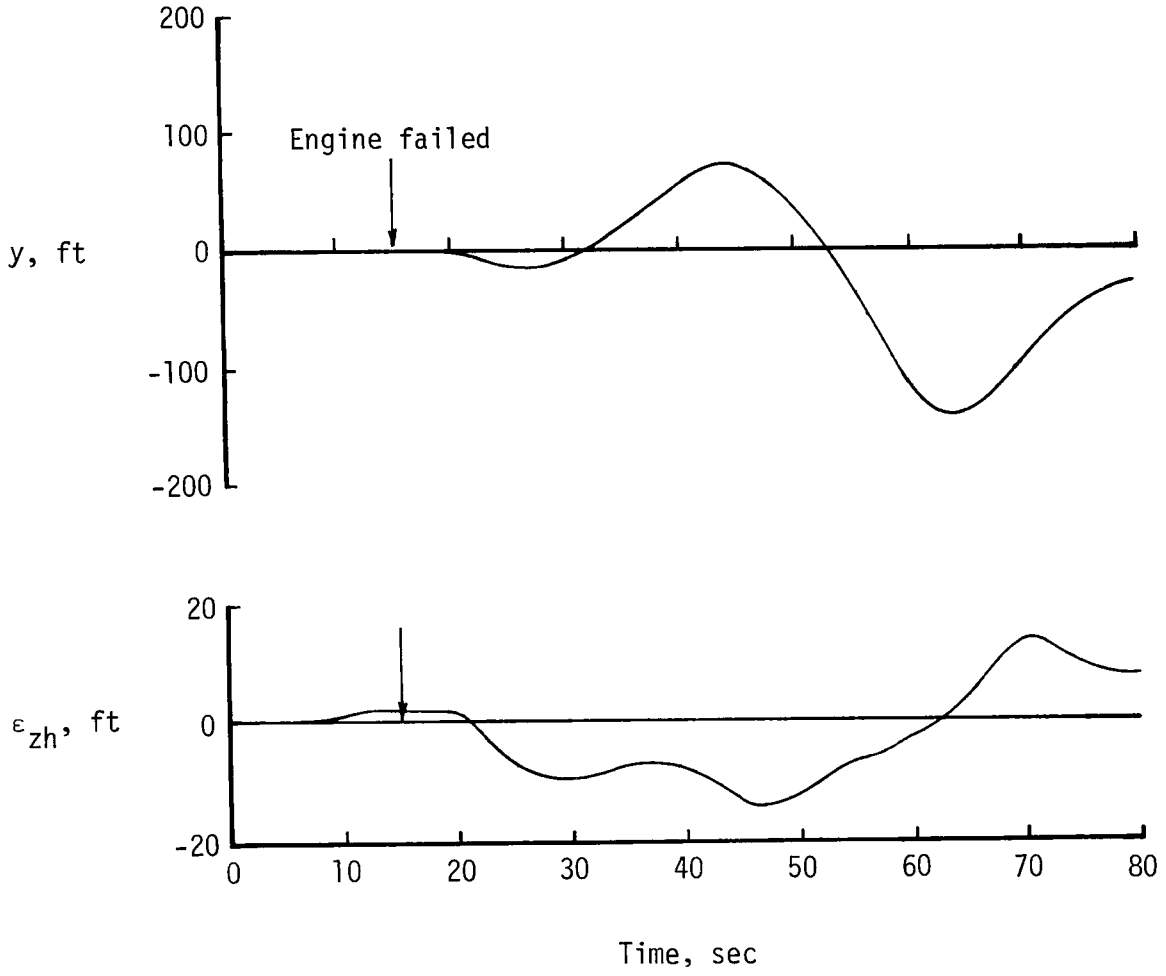

Figure 28.- Indication of lateral and vertical excursions experienced following failure of number 1 engine.

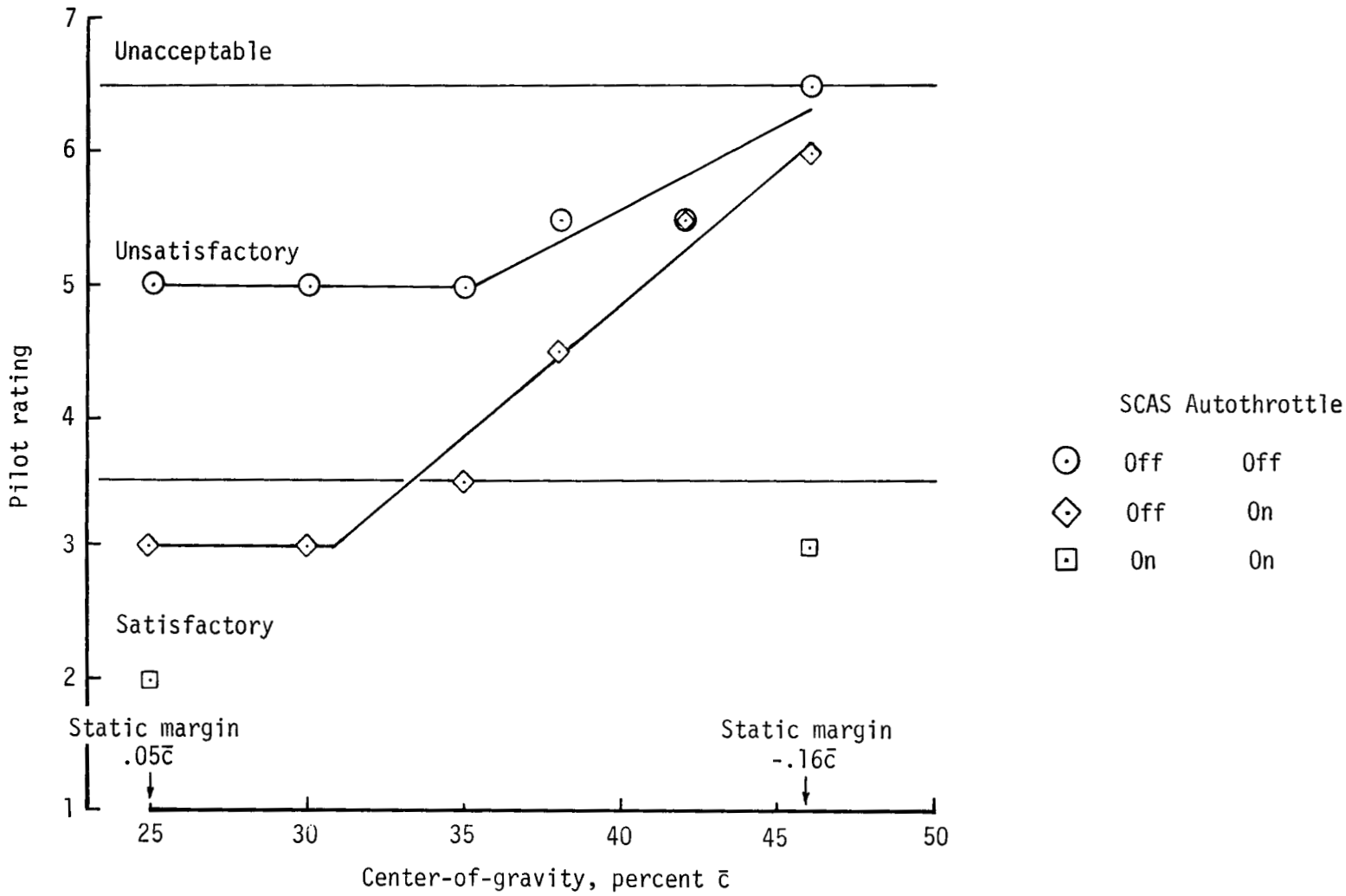

Figure 29.- Indication of effect of center-of-gravity location on pilot rating. (Pilot ratings apply to pitch axis only in calm atmospheric conditions. Glide slope offsets were used for evaluation task.)

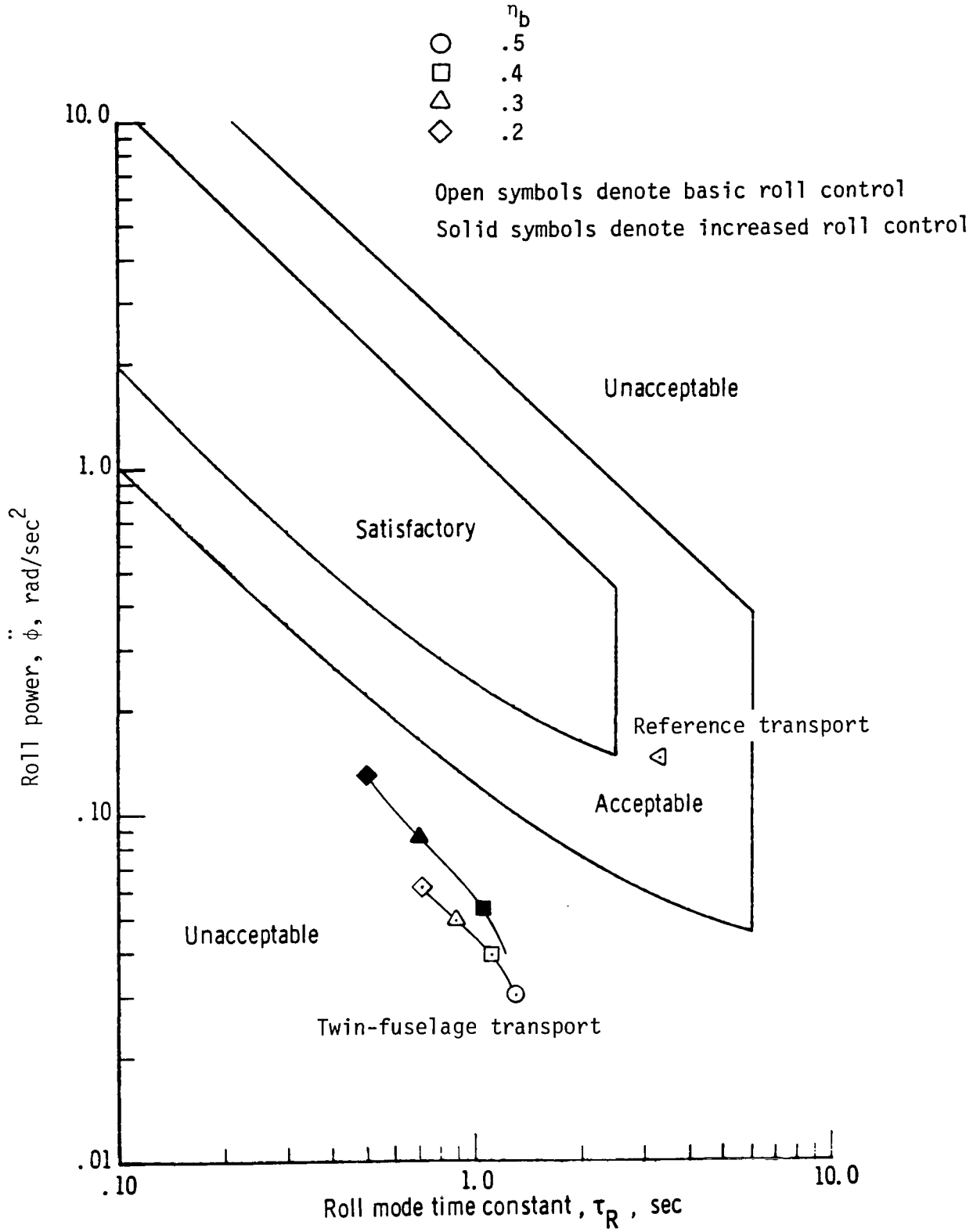

Figure 30.- Roll-acceleration response boundaries for large aircraft. (Boundaries from ref. 16.)

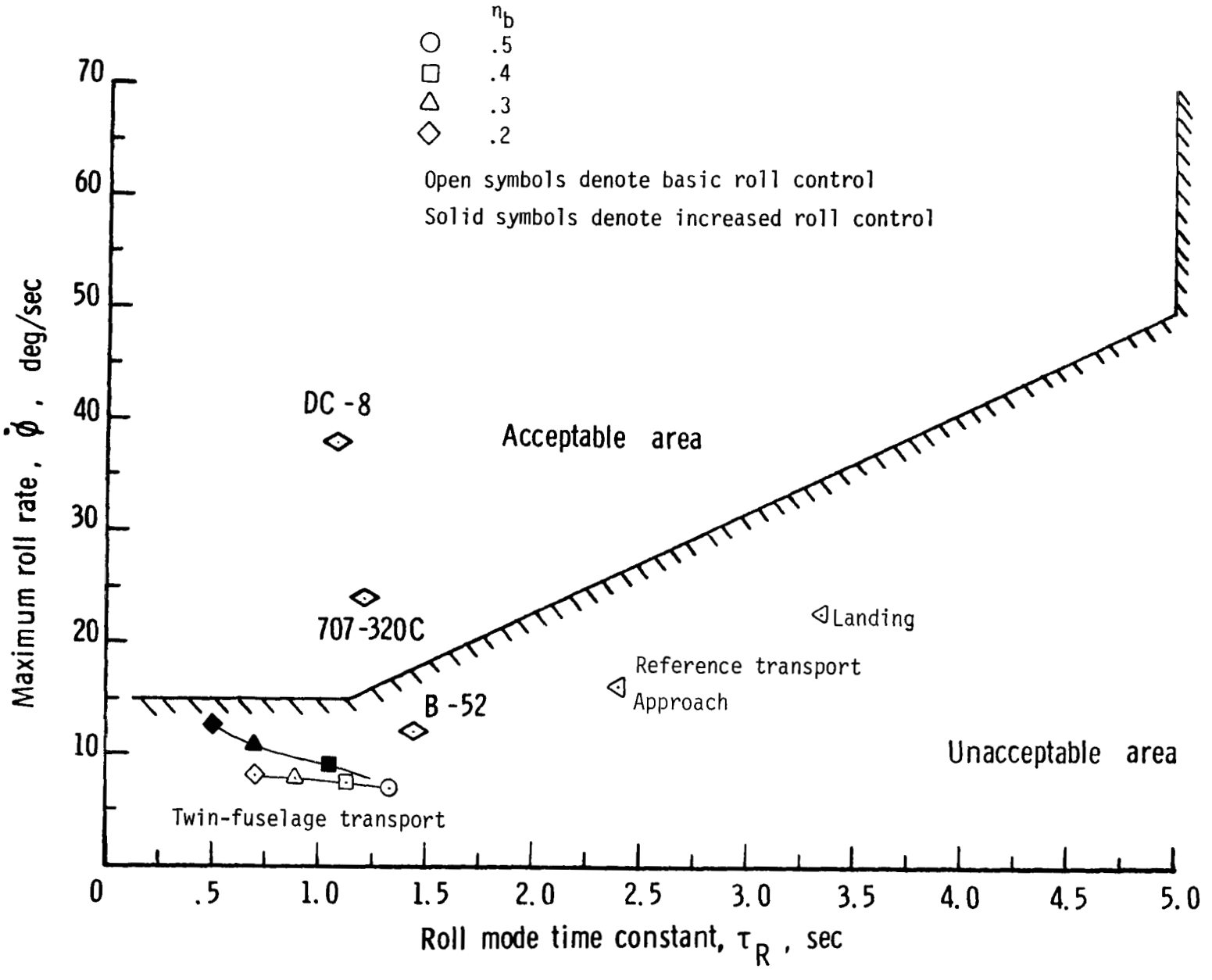

Figure 31.- Roll-rate capability criterion for transport aircraft. (Boundaries from ref. 17.)

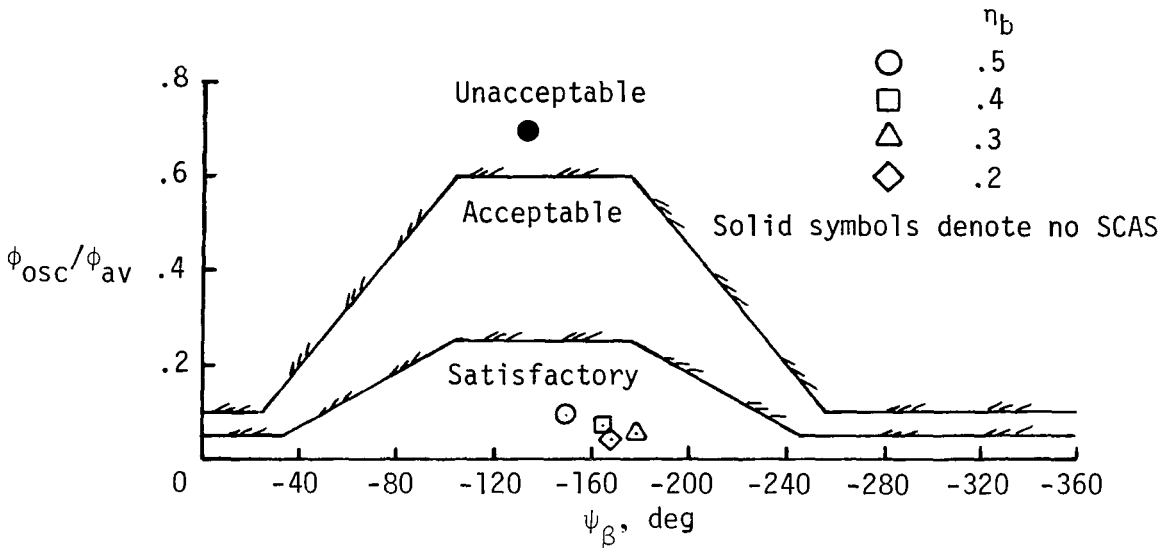

(a) Basic roll control.

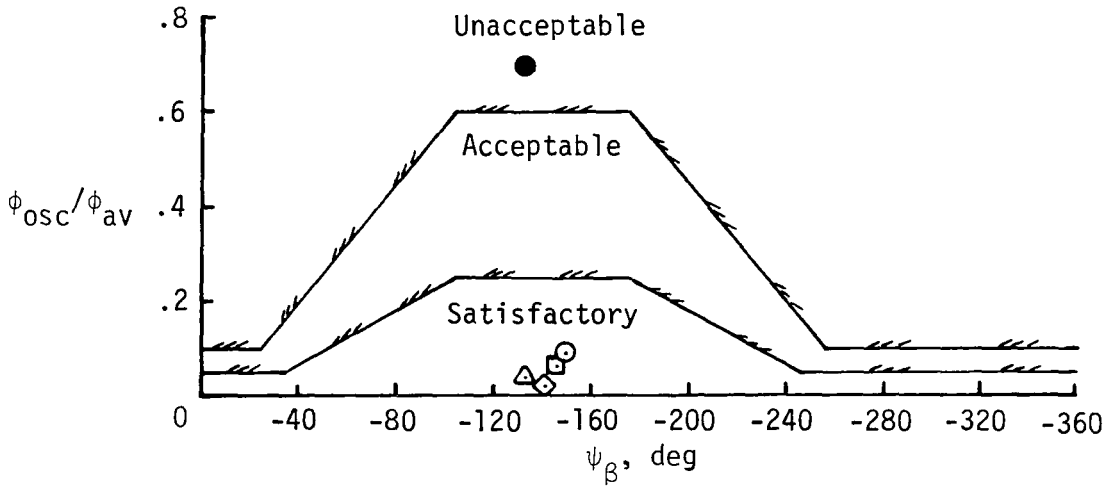

(b) Increased roll control.

Figure 32.- Bank-angle oscillation limitations of reference 16. Final approach; V_ℓ = 126 knots; δ_f = 50°; SCAS on.

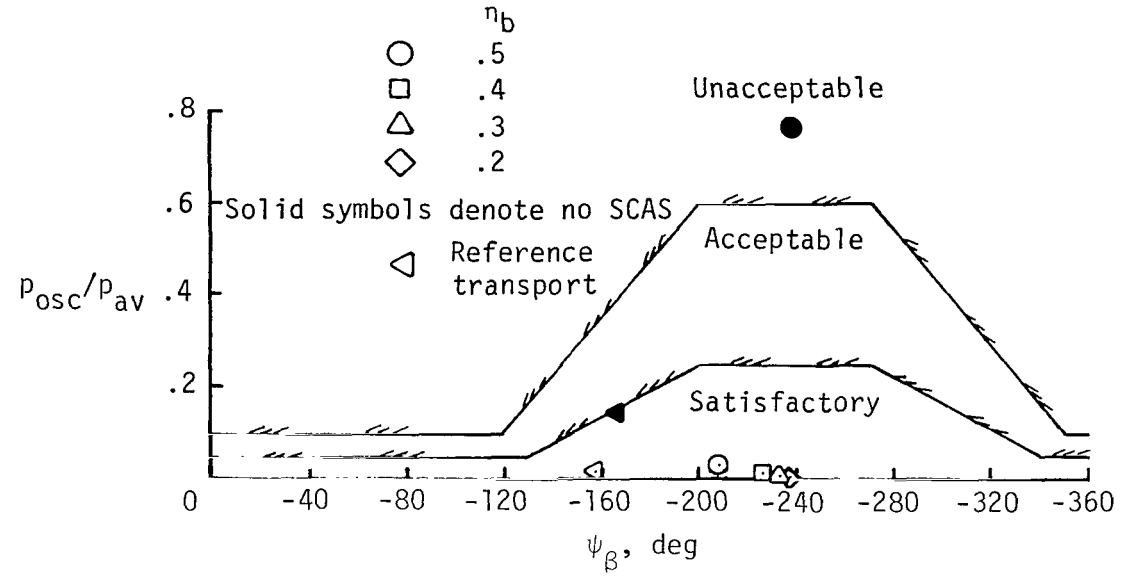

(a) Basic roll control.

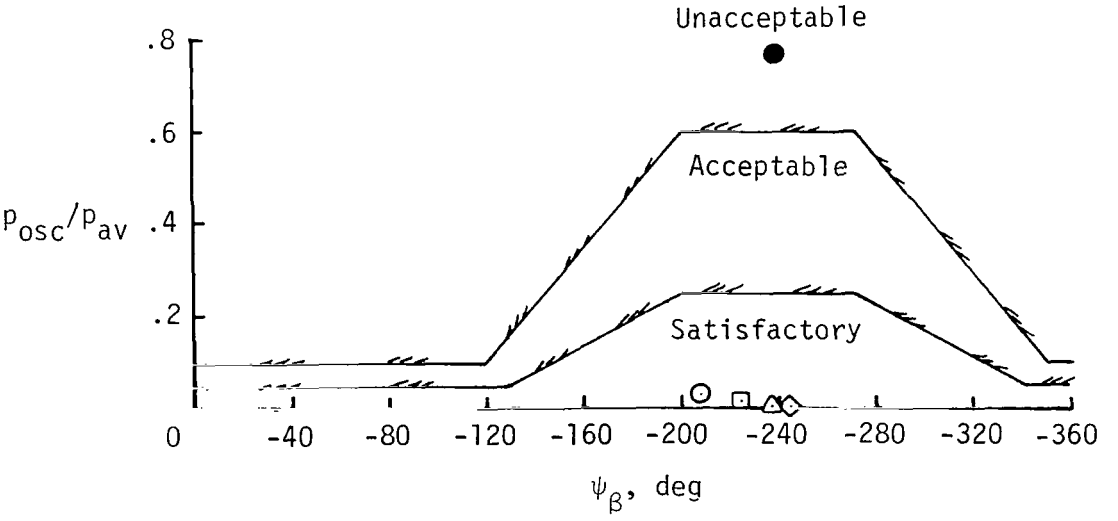

(b) Increased roll control.

Figure 33.- Roll-rate oscillation limitations of reference 16. Final approach; V_ℓ = 126 knots; δ_f = 50°; SCAS on.

Flagged symbols based on achieved roll in 2.5 sec. } Satisfactory,
Unflagged symbols based on achieved roll in 3.2 sec. } full control

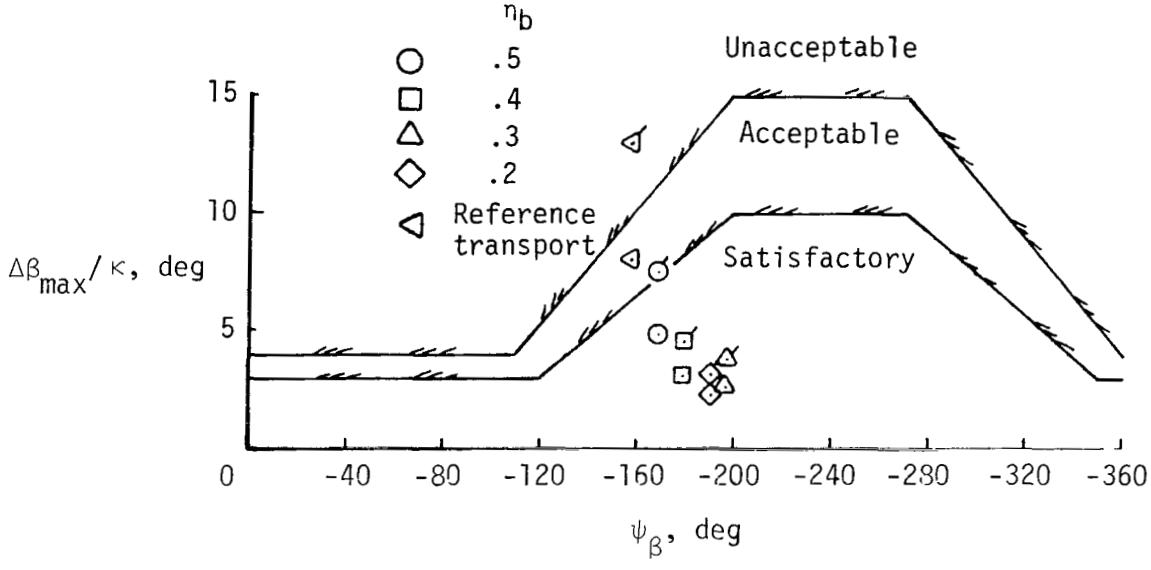

(a) Basic roll control.

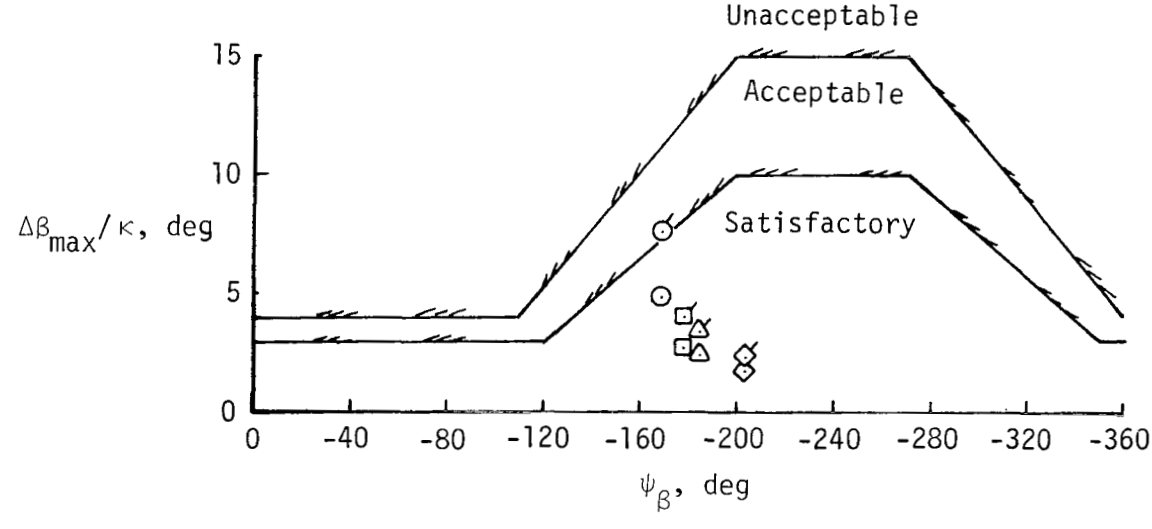

(b) Increased roll control.

Figure 34.- Sideslip excursion limitations of reference 16.
Final approach; V_ℓ = 126 knots; δ_f = 50°; SCAS on.

1. Report No.	2. Government Accession No.	3. Recipient's Catalog No.
NASA TP-2183		

4. Title and Subtitle
SIMULATOR STUDY OF FLIGHT CHARACTERISTICS OF A LARGE TWIN-FUSELAGE CARGO TRANSPORT AIRPLANE DURING APPROACH AND LANDING

5. Report Date
November 1983

6. Performing Organization Code
505-34-03-03

7. Author(s)
William D. Grantham, Perry L. Deal, Gerald L. Keyser, Jr., and Paul M. Smith

8. Performing Organization Report No.
L-15505

9. Performing Organization Name and Address
NASA Langley Research Center
Hampton, VA 23665

10. Work Unit No.

11. Contract or Grant No.

12. Sponsoring Agency Name and Address
National Aeronautics and Space Administration
Washington, DC 20546

13. Type of Report and Period Covered
Technical Paper

14. Sponsoring Agency Code

15. Supplementary Notes
William D. Grantham and Perry L. Deal: Langley Research Center, Hampton, Virginia.
Major Gerald L. Keyser, Jr.: Air Force Systems Command Liaison Office, Langley Research Center, Hampton, Virginia.
Paul M. Smith: Kentron International, Inc., Hampton, Virginia.

16. Abstract
A six-degree-of-freedom, ground-based simulator study has been conducted to evaluate the low-speed flight characteristics of a twin-fuselage cargo transport airplane and to compare these characteristics with those of a large, single-fuselage (reference) transport configuration which was similar to the Lockheed C-5C airplane. The primary piloting task was the approach and landing. The results of this study indicated that in order to achieve "acceptable" low-speed handling qualities on the twin-fuselage concept, considerable stability and control augmentation was required, and although the augmented airplane could be landed safely under adverse conditions, the roll performance of the aircraft had to be improved appreciably before the handling qualities were rated as being "satisfactory." These ground-based simulation results indicated that a value of $t_{\phi=30}$ (time required to bank 30°) less than 6 sec should result in "acceptable" roll response characteristics, and when $t_{\phi=30}$ is less than 3.8 sec, "satisfactory" roll response should be attainable on such large and unusually configured aircraft as the subject twin-fuselage cargo transport concept.

17. Key Words (Suggested by Author(s))	18. Distribution Statement
Large transports Unusually configured aircraft Handling qualities Ride qualities Approach and landing	Unclassified - Unlimited Subject Category 08

19. Security Classif. (of this report)	20. Security Classif. (of this page)	21. No. of Pages	22. Price
Unclassified	Unclassified	85	A05

For sale by the National Technical Information Service, Springfield, Virginia 22161

NASA-Langley, 1983

3 1 1U,A, 831109 S00903DS
DEPT OF THE AIR FORCE
AF WEAPONS LABORATORY
ATTN: TECHNICAL LIBRARY (SUL)
KIRTLAND AFB NM 87117

S